SENSORY PERCEPTUAL METRICS: DESIGN AND APPLICATION OF BIOLOGICALLY BASED METHODS FOR THE ASSESSMENT OF SYSTEMIC CORTICAL ALTERATIONS

Jameson Holden

A dissertation submitted to the faculty of the University of North Carolina at Chapel Hill in partial fulfillment of the requirements for the degree of Doctor of Philosophy in the Department of Biomedical Engineering.

Chapel Hill
2013

Approved By:

Mark Tommerdahl

Robert Dennis

Oleg Favorov

Stephen Folger

Jeffrey Macdonad

ABSTRACT

Jameson Holden: Sensory Perceptual Metrics: Design and Application of Biologically Based Methods for the Assessment of Systemic Cortical Alterations
(Under the direction of Mark A Tommerdahl)

A large number of neurological disorders (neurodegenerative, neurodevelopmental or trauma induced) are difficult to diagnose or assess, thus limiting treatment efficacy. Existing solutions and products attempting to fill this gap are costly, extremely slow, often invasive, and in many cases fail to definitively (and quantitatively) diagnose or assess treatment. Our innovative low-cost sensory testing device and accompanying software package can be used to non-invasively assess the central nervous system (CNS) health status in minutes for numerous patient populations. The somatosensory system is ideally suited for the design of a CNS diagnostic system. First, the organization of the system is such that adjacent skin regions project to adjacent cortical regions (i.e., it is somatotopic). Second, ambient environmental noise in the system can be easily controlled (i.e., it is less likely that a patient will be exposed to distracting tactile input than auditory or visual input). Third, the somatosensory system is the only sensory system that is highly integrated with the pain system, and this is often an important aspect of a patient's diagnosis. The diagnostic system delivers a battery of somatosensory-based tests that are conducted rapidly, much like an eye exam with verbal feedback. Neuro-adaptation, functional connectivity (e.g. cortical synchronization), and feed-forward inhibition are just a few of the cortical mechanisms that can be quantified using somatosensory testing protocols. Many of these protocols leverage tactile illusions which act as confounds on top of a basic somatosensory test, allowing each subject to serve as his or her own control. Design and validation of the perceptual metrics was/is accomplished via correlative studies that

compare non-invasive observations of human sensory percepts with non-human primate neurophysiological studies. Additional validation has been demonstrated through the use of a magnet-compatible version of the device in both functional magnetic resonance imaging (fMRI) and magnetoencephalography (MEG) studies. Based on pilot data (currently an ontological database of roughly 3000 subjects), the system can be used to enable clinicians to have a much better view of a patient's CNS health status.

TABLE OF CONTENTS

LIST OF FIGURES

LIST OF ABBREVIATIONS

MVC	Model View Controller
ADC	Analog to Digital Converter
AFC	Alternative Forced Choice
AWG	American Wire Gauge
BP	Blood Pressure
CAD	Computer-Aided Design
CNC	Computer Numerical Control
CNS	Central Nervous System
CTS	Carpal Tunnel Syndrome
DAC	Digital to Analog Converter
DAL	Database Abstraction Layer
DAQ	Data Acquisition
DC	Direct Current
DL	Difference Limen
DSP	Digital Signal Processor
DXM	Dextromethorphan
FDM	Fusion Deposition Modeling
FFT	Fast Fourier Transform
fMRI	Functional Magnetic Resonance Imaging
FPU	Floating Point Unit
GABA	gamma-Aminobutyric Acid
GAD	Glutamic Acid Decarboxylase
GUI	Graphical User Interface
IBS	Irritable Bowel Syndrome
IC	Integrated Circuit

MCRP	Motor-Related Cortical Potential
MEG	Magnetoencephalography
MRI	Magnetic Resonance Imaging
MSIL	Microsoft Intermediate Language
MVC	Model-View-Controller
NMDA	N-methyl-D-aspartate
OOP	Object-Oriented Programming
PC	Personal Computer
PCA	Principal Component Analysis
PCI	Peripheral Component Interconnect
PID	Proportional-Integral-Derivative
RDBMS	Relational Database Management System
RF	Receptive Field
RMS	Root Mean Square
SPI	Serial-Peripheral Interface
SPS	Samples Per Second
SQL	Structured Query Language
SVM	Support Vector Machine
TBI	Traumatic Brain Injury
TMJD	Temporomandibular Joint Disorder
TOJ	Temporal Order Judgement
USB	Universal Serial Bus
VCA	Voice Coil Actuator
VVS	Vulvar Vestibulitis Syndrome
WCAG	Web Content Accessibility Guidelines
WM	Working Memory
WPF	Windows Presentation Foundation

XAML	Extensible Application Markup Language
XML	Extensible Markup Language

CHAPTER 1: INTRODUCTION

There is currently a significant gap that exists between fundamental neuroscience research and translation of the findings of that research into everyday practice. Experimental findings at the genetic, cellular, molecular and systems level often take a fairly long and often circuitous route to make an impact on a particular neurological disease or disorder. Additionally, there is no standard, reliable, cost-effective paradigm or methodology for assessing the degree to which the central nervous system (CNS) is impacted by any of a given number of neurological disorders. A large number of neurological disorders (neurodegenerative, neurodevelopmental, pharmacological or trauma induced) are difficult to diagnose or assess, thus limiting treatment efficacy. Current existing solutions and products for this need are costly, extremely slow, often invasive, and/or in many cases fail to definitively (and quantitatively) diagnose or assess treatment. Several years ago, Tommerdahl and colleagues proposed to design and fabricate a non-invasive portable sensory based diagnostic system, using state-of-the-art technology to investigate cortical information processing in autism. The device, along with unique protocols that were designed based on in vivo laboratory neurophysiological findings with non-human primates, proved successful in that a number of specific protocols appeared to be very sensitive to detecting differences between autism and controls. Combining the results of several tests and analyzing via SVM (a machine learning analytical tool) yielded close to 90% accuracy in determination of whether or not an individual in that first study had autism. The significance of that finding was that such a system, in which a battery of non-invasive, non-noxious tests can be delivered in 20-25 minutes (each test is 1-3 minutes; delivered in a manner similar to that of an eye exam), proved that it could yield valuable and cost effective, information to a primary health care giver in making a more

informed decision about a patient's diagnosis and/or about efficacy of treatment. An additional goal of the original work was to bridge the neuroscientific gap at the systems level of study by developing standardized sensory measures that could be not only utilized in clinical or clinical research settings, but could be directly correlated with the observations obtained directly from high resolution laboratory animal experimentation.

The tactile diagnostic system that was developed was conceptually designed to investigate differences in cortical information processing strategies between people with autism and people without. Thus, a number of tests specifically target diminished capacities known to exist in autism from genotypic, physiological and anatomical studies. The question that were subsequently addressed is whether or not the strategy that was devised for investigating a population with a neurodevelopmental disorder can be broadly applied to a number of neurological disorders. In other words, it is considered that the changes manifested by the neurodevelopmental disorder autism to be systemic, in that large scale alterations in cortical processing are impacted because of changes that occur throughout the cortex. If systemic cortical alterations occur in other neurological disorders, could they also be detected in the same manner?

Proof-of-concept studies in a number of clinical research areas demonstrated that these newly developed metrics were sensitive to systemic cortical alterations. For example, a metric of central adaptation was obtained in a large cohort of subjects from multiple populations, and it was found that this metric in all of these subject populations was significantly impacted. This is not particularly surprising, as a number of cortical mechanisms play significant roles in adaptation (or can lead to maladaptive behavior). GABAergic and NMDA receptor mediated neurotransmission, as well as neuron-glial interactions play significant roles in the cortical dynamic process that allows the CNS to quickly modify and adapt to environmental stimuli. Among the subject populations that were identified as having below-normative values for adaptation (and suspected impacted cortical mechanisms) are autism (GAD deficiency or low GABA levels; Tannan et al, 2008),

concussion/TBI (white matter damage; neuron-glial interactions), pharmacological manipulation (DXM blocks NMDA receptors; Folger et al, 2008), and chronic pain (fibromyalgia, VVS, migraine, IBS and TMJD -often treated with GABA agonists and/or NMDA antagonists). One question that emerges from this data is that most of these neurological disorders result in some type of altered central sensitization, no matter what the cause – whether it be neurodevelopmental, neurodegenerative, pharmacological or trauma induced – in which there is a significant change in the balance between excitation and inhibition.

The scientific aim of the dissertation work was to determine if sensory perceptual metrics, similar to those that were used to successfully distinguish subjects with autism from healthy control populations, could be used to reliably distinguish – on an individual basis – subjects with neurological disorders that are not neurodevelopmental in nature. Towards that goal, subjects from two broad categories of neurological disorders - chronic pain and trauma induced systemic alterations – were targeted. The engineering aim – and the most significant part of this dissertation – was the hardware and software development of a low cost, portable vibrotactile stimulator that could be widely distributed and used virtually anywhere. Widespread distribution of the device allowed for a large number of proof-of-concept studies in a diverse spectrum of neurological disorders to be feasible.

The potential impact of this work is highly significant for multiple communities. A simple, fast, non-invasive, cost-effective means for assessing CNS health that could be utilized by health care providers could have an overwhelming impact. To date, there are no standardized, quantitative measures for assessing altered central sensitization. The advantage of the proposed methodology is that it will be low cost, easy to use and effective at both providing information about a patient or subject that would enable a diagnostician to make a radically more informed choice about treatment, AND it would provide a means for assessing treatment efficacy. Is a drug effective in treating a patient's pain, and if so, is it at the proper dose? Is it safe for a concussed athlete to return to play? These are the

types of everyday, practical questions that could be addressed by the methodology that has been developed. Additionally, as all of the methods developed are based on decades of neuro-scientific findings in the lab (both from our lab and many others) from observations of non-human primates, the clinical tool that has been developed could provide a direct (and iterative) translational link from the lab to the clinic.

CHAPTER 2: CM4: A FOUR-POINT VCA BASED VIBROTACTILE STIMULATOR[1]

Overview

Current methods for applying multi-site vibratory stimuli to the skin typically involve the use of multiple, individual vibrotactile stimulators. Limitations of such an arrangement include difficulty with both positioning the stimuli as well as ensuring that stimuli are delivered in a synchronized and deliberate manner. Previously, we reported a two-site tactile stimulator that was developed in order to solve these problems (Tannan et al., 2007a). Due to both the success of that novel stimulator and the limitations that were inherent in that device, we designed and fabricated a four-site stimulator that provides a number of advantages over the previous version. First, the device can stimulate four independent skin sites and is primarily designed for stimulating the digit tips. Second, the positioning of the probe tips has been re-designed to provide better ergonomic hand placement. Third, the device is much more portable than the previously-reported stimulator. Fourth, the stimulator head has a much smaller footprint on the table or surface where it resides. To demonstrate the capacity of the device for delivering tactile stimulation at four independent sites, a finger agnosia protocol, in the presence and absence of conditioning stimuli, was conducted on seventeen healthy control subjects. The study demonstrated that with increasing amplitudes of vibrotactile conditioning stimuli concurrent with the agnosia test, inaccuracies of digit identification increased, particularly at digits D3 and D4. The results are consistent with prior studies (Tommerdahl et al. 2007) that implicated synchronization of adjacent and near-adjacent cortical ensembles with conditioning stimuli in impacting TOJ performance.

[1]This chapter previous appearted in the Journal of Neuroscience Methods. The original citiation is as follows: Holden JK, Nguyen RH, Francisco EM, Zhang Z, Dennis RG, Tommerdahl M. "A novel device for the study of somatosensory information processing." *J Neurosci Methods*, 2012 Mar 15;204(2):215-20. Epub 2011 Dec 4.

Introduction

For the past several years, our research group has been working towards the development of a portable tactile stimulator that could effectively be used to study changes in sensory information processing in clinical and clinical research venues across a diverse spectrum of neurological disorders. Thus far, we have gone through several iterations in the development of this stimulator. The first prototype of the device (Tannan et al., 2005a) was used to demonstrate changes in spatial acuity with repetitive stimulation. A subsequent report described that this change did not occur with individuals with autism, strongly suggesting a lower-than-normal inhibitory response (Tommerdahl et al., 2007a). A second iteration of the device (Tannan et al., 2007a) was much more portable as well as more robust and reliable in its ability to deliver well-controlled vibrotactile stimuli to the skin. The device proved extremely useful, and a number of studies were conducted with it that demonstrated the ability to reliably and reproducibly obtain metrics of neuro-adaptation (Tannan et al., 2007b), temporal order judgment (TOJ) and the impact of synchronized conditioning stimuli on TOJ (Tommerdahl et al., 2007b), the absence of the impact of those same conditioning stimuli on TOJ in individuals with autism (Tommerdahl et al., 2008), the relationship between spatial acuity and amplitude discrimination (Zhang et al., 2008), a method for the study of tactile-thermal interactions (Zhang, 2009), a reliable means for measuring amplitude discriminative capacity and a robust near-linear relationship between duration of repetitive conditioning stimuli and the impact of that conditioning on amplitude discriminative capacity (Tannan et al., 2007b), the below-normal adaptation metrics in autism (Tommerdahl et al., 2007), the impact of NMDA receptor block on adaption metrics (Folger et al., 2008), a demonstration of Weber's law (Francisco et al., 2008; Holden et al., 2011) and a robust relationship with neurophysiological data (Francisco et al., 2008), and differences in timing perception in Parkinson's Disease (Nelson et al., 2011). More recently, we have developed a newer, more portable and ergonomic model of the device, which is much more suited for a clinical or clinical research environment, and is capable of delivering

vibrotactile stimuli to four fingers: the index (D2), middle (D3), ring (D4), and little (D5) fingers. The utility of this device has been recently reported in a paper that reported phenotypic differences within a spectrum of patients with vulvodynia (Zhang et al., 2011), and in a paper that describes its utility for describing phenotypic differences within the autism spectrum via modulating vibrotactile stimuli (i.e., sinusoidal stimuli that dynamically change in amplitude), but the device itself, as well as a demonstration of its capability to deliver four-digit protocols, has not been fully described, which is the purpose of this report. In a subsequent paper, a magnet-compatible version of this device will be reported.

Methods

Hardware. The Cortical Metrics (CM-4; see Figure 1) stimulator was developed in our laboratories for use in series of experiments such as those described in this report. The system was designed using state-of-the-art rapid manufacturing technology to allow multiple identical systems to be built and used in different locations. Also, the use of rapid manufacturing permitted very rapid design evolution, thereby potentiating the production of special fixtures and changes to geometry as needed for special applications. The device consists of two separate parts: the main body and a detachable head unit. The flat plates of all exterior housing and other components of approximately planar geometry are direct manufactured using laser-machined 6 mm acrylic sheet, cut on a 120 Watt CO2 laser engraving system, model number X660 (Universal Laser Systems, Scottsdale, AZ). The more complex housing and internal mechanism components are direct manufactured from ABS plus, by fusion deposition modeling (FDM) on a StrataSys Dimension bst 1200es (StrataSys, Inc., Eden Prairie, MN). The cylindrical trays forming the disks of the head unit are CNC machined from 1" thick Acetal (Delrin) plate. All housing and mechanism components and assemblies were solid modeled prior to fabrication using SolidWorks solid modeling software (SolidWorks Corporation, Concord, MA).

Figure 2.1: Four Site Vibrotactile Stimulator. Each of the four probe tips is positioned by rotating the four independently-positioned drums to maximize contact between finger pads and the stimulator tips. During an experimental session, subjects were seated comfortably in a chair with their arm resting on the arm rest attached to the head unit of the device. Digits D2 through D5 were then positioned for vibrotactile stimulation.

The internal mechanism of the head unit is comprised of identical cylindrical disks placed sideways and four abreast (130 mm in diameter, 11 mm in depth) between two plastic supports. Each disk can be independently rotated to adjust for differing finger lengths for each test subject. A voice coil actuator (VCA) and an optical position sensor are mounted in each disk. Each VCA is attached to a plastic probe (5 mm diameter) which slightly protrudes through a hole (7 mm diameter) in the side of the cylinder. The amount of protrusion for each probe is independently adjustable as are the positions of the holes to accommodate the length of the subject's fingers. The VCAs drive the plastic stimulator probe tips according to prescribed sinusoidal waveforms. The moving components of the stimulator tips are directly manufactured from Polycarbonate (PC) by 3-D FDM as a single

compliant mechanism component integrating a mounting flange, a thin-beam four-bar linkage, a magnet coil bobbin, an optical displacement sensor vane, and the extension to the mechanical stimulator tip. The compliant four-bar linkage mechanism allows the coil, optical position sensor vane, and tip to be displaced vertically along a straight line for a distance of ±1 mm. The 4-bar compliant mechanism also provides a very low hysteresis linear restoring force to center each tip vertically when no current is applied to the VCA coil. The VCA coil is 400 turns of 34 AWG magnet wire (approximately 30 Ohms total resistance), wrapped in a rectangular bobbin permanently solvent bonded into the four-bar mechanism. The entire four-bar mechanism is 5.3 mm in thickness, and is positioned such that the VCA coils sit directly between two opposed rectangular N42 rare-earth-element magnets (catalog number BCC2, K & J Magnetics, Jamison, PA) similar to those found in computer hard drives. The resulting VCA motors generate extremely linear force outputs as a function of drive current with very low hysteresis due to the "frictionless" nature of the single-piece bearing-less four-bar compliant mechanism. The position of the vibrating tips is detected by non-contacting optical displacement sensors, one for each tip, similar in configuration to ones we have previously employed in precision optical force transducers (Dennis and Kosnik, 2002). When the tips are not being driven, the optical position sensors can act as a highly-sensitive contact or force sensor. By employing the optical position sensor, the tips can be driven to contact the skin, and the contact force of each tip can be adjusted independently due to the fact that the spring constant of each VCA four-bar linkage mechanism is identical.

The custom electronics were designed using free CAD software from ExpressPCB (www.expresspcb.com). The printed circuit boards were manufactured using the resulting CAD files, also by ExpressPCB. The hybrid circuit includes signal amplifiers for the position sensors, an analog controller to allow either "force" or "position" control of each VCA motor and tip, a tunable analog PID controller for position control of each tip, and a bipolar push-pull high-current op-amp output stage to drive each VCA motor. This hybrid circuit is

interfaced via four parallel pin connectors (2 banks of 50 pins for digital signals and 2 banks of 34 pins for analog signals) to an internal NI-USB-6259 data acquisition (DAQ) board. The DAQ board then interfaces via a USB connection to any standard PC running Microsoft Windows XP or later.

Software. A custom line-of-business application was developed for the Microsoft .Net platform using the C# programming language and Windows Presentation Foundation (WPF) framework to control the stimulator and administer the data collection protocols. The interface was designed to be intuitive, extensible, and aesthetically pleasing. The software needed to be extensible to facilitate the development of future protocols for a device as flexible as the CM-4. The core extensibility was achieved by using a "plugin" architecture with a shell application whose function is to discover, load and execute small plugins. The shell exposes a software contract (an inheritable C# class) that is consumed and extended by each plugin. Each task described in this paper represents one such plugin. Most traditional neuropsychological protocols using the standard X-alternative forced-choice (X-AFC) tracking method (Cornsweet, 1962) can be created with only a couple dozen lines of C# code. While most plugins interact directly with the CM-4 stimulator, this is not a requirement of the plugin contract. Plugins can, for example, be designed to collect arbitrary subject information pertinent to the given study (e.g. participant demographics, relevant medical history, various surveys, etc.). The net effect is not only a significant reduction in the amount of clinical paperwork that needs to be completed by each participant, but also a marked reduction in data-entry time for clinicians. All data collected by the application are stored in an encrypted (128-bit RC4) SQLite database in a user-specified location. Each database can be shared with multiple instances of the shell application, providing a mechanism for seamless networking of CM-4 stations (Holden, et al, 2011). The software is also capable of storing, as well as creating and customizing, all relevant initialization information for each plugin, such that a given battery of protocols can be administered repeatedly and in a consistent manner, while maintaining flexibility for future projects. The

batteries allow for greater reuse of each plugin, resulting in shorter development times a more efficient workflow throughout an experiment.

Protocols. In order to demonstrate exemplary use of the CM-4, a finger agnosia test, in the presence and absence of conditioning stimuli, was performed. The finger agnosia test was designed to assess the capacity of subjects to recognize and identify stimulated digits, an assessment similar to tactile finger recognition or localization tests (Boll, 1974; Reitan and Wolfson, 1993) utilized in current neuropsychological diagnostics.

Subjects. Seventeen healthy subjects (8 males and 9 females), ranging from 22 to 57 (39.1±2.9) years of age, were recruited for the study. None of the subjects reported any neuropsychological impairment and all were naïve to both the study design and issue under investigation. The study was performed in accordance with the Declaration of Helsinki, all subjects gave their informed consent, and the experimental procedures were reviewed and approved in advance by an institutional review board.

Experimental Procedure. During an experimental session, the subjects were seated comfortably in a chair with the right arm resting on the device. Because the lengths of fingers typically vary among subjects, the positions of the probe tips were individually adjusted to ensure that they contacted the glabrous, padded tips of the fingers of each subject. These loci were chosen in order to allow the convenience of access and comfort of participants as well as for the wealth of neurophysiologic information that exists for the corresponding somatotopic regions of cortex in primates (Chen et al., 2003, 2007, 2009; Francisco et al., 2008; Friedman et al., 2008; LaMotte and Mountcastle, 1975; Mountcastle, 1969; Tommerdahl et al., 1993, 1998, 2002, 2005, 2006, 2010). As depicted in Figure 1, probe tip positioning was accomplished by loosening a set screw and rotating each of the drums independently to conform to the natural hand shape of each subject. After proper positioning, if the probe tips still failed to make proper contact with the digits, the tips themselves were either raised or lowered. Once adjusted, the probe tips were locked in place prior to initiation of the battery so that they would remain immobile during testing. At

the start of each run, the four tips were driven towards the tips of the fingers in order to ensure good contact with the skin.

During the assessment, the device delivered constant-amplitude sinusoidal skin displacements (vibrations) via flat Delrin probes (5-10 mm in diameter) positioned to make contact with the tips of the index (D2), middle (D3), ring (D4), and little (D5) fingers of the right hand. The independent probe tips were computer-controlled and capable of delivering a wide range of vibrotactile stimulation of varying frequencies (Hz) and amplitudes (μm). Stimulus parameters were specified by test algorithms that were based on specific protocols as well as subject responses during those protocols.

Subjects viewed a computer monitor that provided continuous visual cueing during the experimental session. Specifically, an onscreen light panel indicated to the participant when stimuli were being delivered and when subjects were to respond. Training trials were not included prior to testing, and the subjects were not given performance feedback or knowledge of the results during data acquisition. The sensory testing session was conducted by application of low frequency (25 Hz) vibration to selected fingers. Each battery of testing lasted between 15 and 20 minutes depending on the protocols being run and on subject performance. Each individual protocol typically lasted 2 to 3 minutes.

Finger Agnosia Protocol. Finger agnosia tests are typically utilized to diagnose the ability of subjects to recognize and identify stimulated digits (Boll, 1974; Reitan and Wolfson, 1993). In order to assess the ability of the subject to discriminate one digit from another, a four-alternative forced-choice (4-AFC) protocol was implemented. Figure 2 represents a timeline for the finger agnosia protocols evaluated. The device delivered a short pulse or tap (300 μm, 25 Hz, 40 ms) to one of the four digits in a pseudo-random order on a trial-by-trial basis, and subjects were queried as to which digit was stimulated (Figure 2). The simple test was used in order to determine baseline values for each subject. A more complex agnosia test was subsequently administered in which test stimuli were delivered to the skin as a tap as in the previous test (300 μm, 25 Hz, 40 ms), but in the

presence of conditioning stimuli at variable amplitudes. In each case, a 25 Hz, 500 ms conditioning stimulus was delivered to all four digits at one of four amplitudes: 30, 40, 50, and 100 μm. The conditioning stimulus was delivered 500 ms prior to, and 500 ms following, the tap of the test digit (Figure 2). For all finger agnosia tasks, subjects indicated which finger was perceived to have received the large amplitude tap by choosing the respective digit on an image of the dorsal side of a hand presented on a computer monitor. Test stimuli sites were pseudo-randomized on a trial-by-trial basis. The subjects were assessed on their accuracy over a total of 16 trials (4 trials for each digit as the test stimulus).

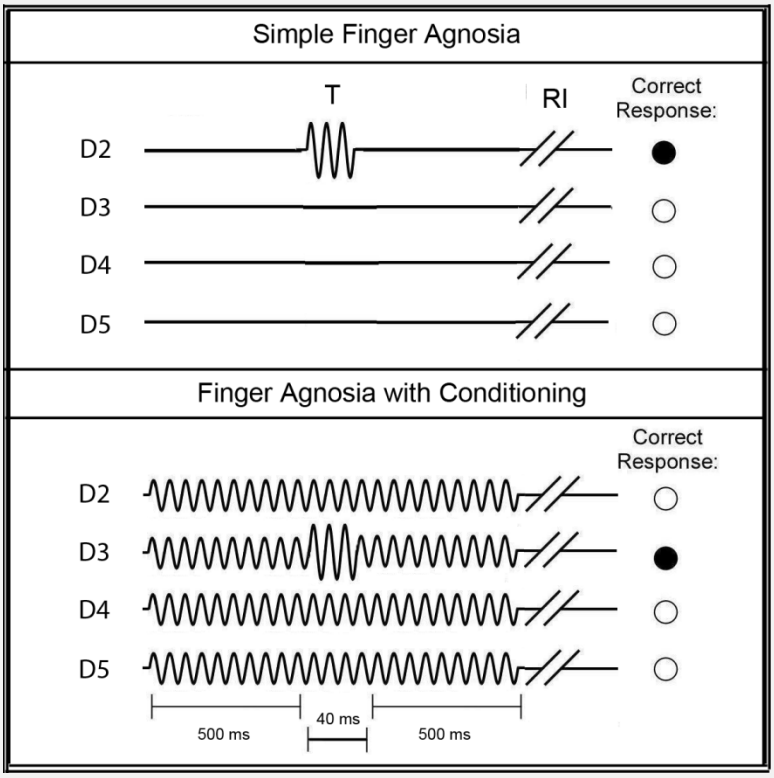

Figure 2.2: Schematics of Finger Agnosia Protocols. The simple finger agnosia assessment (top panel) consisted of a 4AFC protocol where a short test (T) pulse (300 μm, 25 Hz, 40 ms) was delivered to one of the four digits followed by a subject response interval (RI). The finger agnosia test was also conducted in the presence of conditioning stimuli of amplitudes 30, 40, 50, or 100 μm (bottom panel). The conditioning stimulus was delivered 500 ms prior to, and 500 ms following, the tap of the test digit. For all finger agnosia tasks, subjects indicated which finger was perceived to have received the large amplitude tap by choosing the respective digit on an image of the dorsal side of a hand presented on a computer monitor. Test stimuli sites were pseudo-randomized on a trial-by-trial basis.

Analysis. For the finger agnosia protocols, accuracy percentages were calculated by analyzing the ratio of correct to total responses of the subjects. Percent accuracies were trial-independent and reflected accuracies across all 16 trials. The 100 μm conditioning condition was chosen for further analysis because of the significantly lower percent accuracy compared to the simple agnosia task. Percent inaccuracies were quantified for the 100 μm conditioning stimulus by calculating the frequency at which digits were incorrectly chosen. Results were calculated in this manner in order to compare percent inaccuracies with difference limens (DLs), where lower value might suggest higher accuracies and increased discriminative capabilities. The data were analyzed for significance by calculating p-values across mean inaccuracy metrics for each digit. Histograms were plotted in order to visualize the differences among each of the digits with respect to standard error of the means. Statistical t-tests were used to evaluate the difference of the performance of each subject under different conditions. A probability value of less than 0.05 was considered statistically significant.

Auditory Cue Analysis. To ensure that the stimulator did not produce any audible clues during the agnosia task, an auditory output analysis was conducted using a standard USB microphone and the open source software suite Audacity. The microphone was placed on a table 31 cm from the stimulator head unit. Four one-second recordings were created with each condition consisting of an initial 250 ms period of silence followed by a single-channel 300 μm 25hz sinusoidal vibration lasting 500 ms and ending with another 250 ms period of silence. Audacity provides a contrast analysis tool in compliance with the Web Content Accessibility Guidelines (WCAG 2.0), Success Criteria 1.4.7. This tool was used to calculate the RMS amplitude in decibels (dB) during each vibration and period of silence.

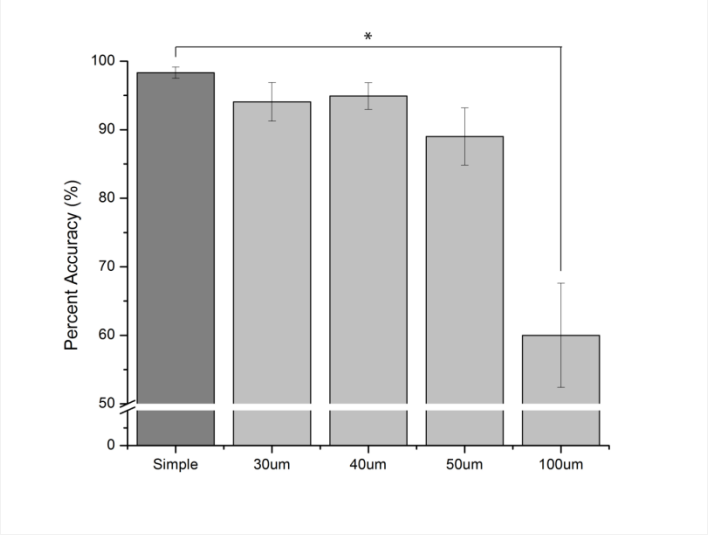

Figure 2.3: Average Percent Accuracy the Effect of Conditioning Stimuli on the Finger Agnosia Task. The average percent accuracy in absence of conditioning stimuli was 98.2±0.9% (n=17). In the presence of 30, 40, 50, and 100 μm conditioning stimuli, the percent accuracies gradually decreased with increased amplitude of conditioning stimuli: 93.7±3.0% at 30 μm (n=17), 94.9±4.2% at 40 μm (n=16), 89.0±4.2% at 50 μm (n=17, $p<0.06$), and 60.0±7.6% at 100 μm(n=5, $p<0.01$).

Results

This study employed a finger agnosia protocol, in the presence and absence of conditioning stimulation, on healthy subjects in order to demonstrate the capacity of the device for delivering well-controlled vibrotactile stimuli at four independent sites. The auditory cue analysis found no indication of any auditory cues produced being produced by the stimulator during a vibration. The peak amplitude for any channel during a vibration was -42.64 dB (silence is considered to be in the range of -30 dB for humans). The average RMS amplitude (during all vibrations) was -58.90±0.11 dB. The average RMS amplitude during the periods of silence was -58.83±0.10 dB. Comparing each condition's vibration to the immediately preceding silence yielded an average difference in RMS amplitude of 0.05±0.13 dB. The finger agnosia task was evaluated in order to quantify the ability of subjects to recognize and identify stimulated digits in the absence and in the presence of conditioning stimuli at different amplitudes. This task included seventeen healthy subjects (8 males and 9 females) ranging from 22 to 57 (39.1±2.9) years of age. As shown in Figure 4, the average percent accuracy in the absence of conditioning stimuli was 98.2±0.9%

(n=17), and accuracy across subjects decreased with increasing amplitude of conditioning stimuli. Conditioning amplitudes of 30 and 40 μm resulted in percent accuracies of 93.7±3.0% and 94.9±4.2%, respectively, and were not statistically significant compared to subject performance in the absence of conditioning stimuli. The effect of conditioning on the finger agnosia task became statistically significant at conditioning amplitudes greater than 50 μm: 89.0±4.2% at 50 μm ($p<0.06$) and 60.0±7.6% at 100 μm ($p<0.01$). Because the conditioning stimuli at 100 μm resulted in the most significant percentage of incorrect responses compared to the simple finger agnosia protocol, the frequency of inaccurate responses for each digit was quantified (Figure 4). The results suggested that subjects, on average, made the largest number of inaccurate responses when the correct answer should have been D3 and D4 (percent inaccuracies of 60.0±10.0% and 55.0±14.6%, respectively). Subjects were relatively better at identifying stimulation of D2 (inaccuracy of 15.0±10.0% significantly better than that for D3, $p<0.01$) and better at identifying D5, though not statistically significantly more.

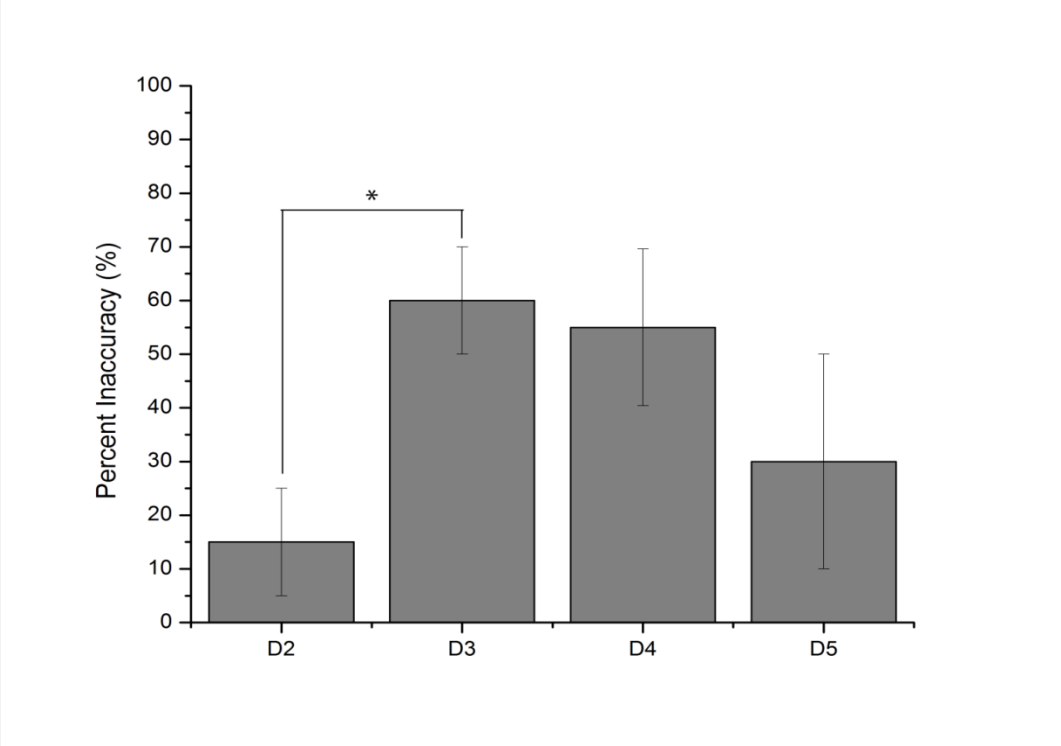

Figure 2.4: Average Percent Inaccuracy on Finger Agnosia with 100 μm Conditioning Stimuli

. Digits D3 and D4 showed the highest percent inaccuracies of 60.0±10.0% and 55.0±14.6%, respectively. There was a statistically significant observation in accurately recognizing and identifying stimulation of D2 at 15.0±10.0% versus D3 at 30.0±20.0% ($p<0.01$) and slight discrimination difference between D2 and D4 ($p<0.08$) in the presence of the 100 μm conditioning stimuli. The other the digit combinations showed no statistical significance in discrimination capability.

Discussion

The delivery of sinusoidal displacements to a single skin site via mechanical transducer has been used extensively for the study of flutter vibration in both psychophysical and neurophysiological settings for a number of decades. Exemplary uses of such a device are described in Goble and Hollins, 1993; Juliano et al., 1989; LaMotte and Mountcastle, 1975; Mountcastle et a., 1969; Tannan et al., 2006; Tommerdahl et al., 1993, 1998, 2002; and Vierck and Jones, 1970. Typically, stimuli that can be delivered through mechanical transducers – vertical displacement stimulators such as the one originally described by Chubbuck (1966) – were used for studies of somatosensation and are very well equipped to deliver sinusoidal stimuli at a frequency range (1 to 250 Hz) with

amplitudes of sufficient size (between 0 and 1000 μm) to activate a broad range of mechanoreceptors. However, in order to stimulate more than one skin site – either during the course of human psychophysical testing or animal experimentation – it is necessary to position a second vertical displacement stimulator over the second skin site. Our previous device (described in Tannan et al. 2007a) was designed to address this issue by allowing dual site stimulation with automated two-dimensional probe positioning. Although the device reported by Tannan and colleagues was successfully utilized in a number of studies (Tannan et al., 2005b, 2006, 2007b, 2008; Tommerdahl et al., 2007a, 2007b, 2008), it was cumbersome and not ideal for clinical and clinical research venues. The CM-4, described in this report, has the capacity to quickly and easily adjust to fit to most adult, and many juvenile, hand sizes and can deliver vibrotactile stimuli to the tips of four digits. The ability to simultaneously deliver vibrotactile stimuli to a number of digits allows for a great deal of protocol diversity.

In this report, we described a relatively simple four-site finger agnosia protocol to demonstrate the potential utility of the device. The principle finding in the results of this study is that there is an increase in inaccuracies with increases in the amplitude of concurrent conditioning stimulation delivered during the agnosia task, and the ability to perform the task accurately in the presence of that conditioning stimulation is diminished more in digits D3 and D4 than in digits D2 and D5. The decrease in accuracy with increasing amplitudes of synchronized sinusoidal stimulation is consistent with prior reports of increasing inaccuracies in temporal order judgment (TOJ) in the presence of synchronized and periodic conditioning stimuli. In a study by Tommerdahl and colleagues (Tommerdahl et al., 2007), it was demonstrated that TOJ results obtained from a number of pairs of stimulus sites – unilateral as well as bilateral – were comparable. However, in the presence of a 25Hz conditioning sinusoidal stimulus which was delivered both before, concurrently and after the TOJ task, there was a significant increase in the TOJ measured when the two stimuli were located unilaterally on digits D2 and D3. In the presence of the same 25Hz

conditioning stimulus, the TOJ obtained when the two stimuli were delivered bilaterally was not impacted. This led to the speculation that the impact that the conditioning stimuli – which only had an impact if they were sinusoidal, periodic and synchronous – had on TOJ measures was due to the synchronization of adjacent cortical ensembles in somatosensory cortex, and that the synchronization of these cortical ensembles could have been responsible for the degradation in temporal order judgment. The conditioning stimuli in this study were also synchronized, periodic and simultaneous, and if the degradation in test performance was due to synchronization of adjacent cortical ensembles similar to what was speculated in the TOJ report, then inaccuracies due to this synchronization would be lower on the digits on the perimeter of the cortical ensemble (i.e., D2 and D5), and the results reflect this prediction. Future studies will consider whether or not subjects with neurological disorders are not impacted by conditioning stimuli, as was found to be the case in subsequent TOJ studies (e.g., TOJ metrics of subjects with autism were not impacted significantly by conditioning stimuli; Tommerdahl et al., 2008).

The degree of inaccuracies in the different digits with increasing conditioning stimulation is also consistent with motor studies of digit interdependencies. In studying the autonomy of finger movements, intended motion in one finger often results in simultaneous movement, or enslavement, of other digits. More specifically, D3 and D4 show the most enslavement, or interdependency, of adjacent digits while D2 is characterized by the greatest independence (Häger-Ross and Schieber, 2000). In observing motor-related cortical potentials (MRCPs), the autonomous nature of D2 was shown to be significantly high while D4 showed the most dependency on other digits (Slobounov et al., 2002). In Figure 4, D2 demonstrates the lowest inaccuracies in the presence of conditioning stimulation while D3 and D4 exhibit the most; thus, in both the motor and sensory based studies, D2 demonstrates the most independence.

The role of neural communication between adjacent and non-adjacent cortical regions plays an important role in understanding the relationship between

neurophysiological mechanisms and sensory percept. The development of new, more versatile devices and methodologies, such as presented in this report, could contribute to bridging decades of neuroscientific research with human perceptual clinical and clinical research studies. One long term goal of our research is to develop sensory based instrumentation and methodologies for the diagnosis and assessment of treatment efficacies for a broad range of neurological disorders, and building this aforementioned bridge could provide new insights into fundamental information processing mechanisms as well as generating perceptual metrics that are more sensitive to alterations in central information processing capacity.

CHAPTER 3: CM3: A FOUR-POINT PIEZOELECTRIC BASED MRI/MEG COMPATIBLE VIBROTACTILE STIMULATOR[1]

Overview

Recently, we reported methods for applying multi-site vibratory stimuli to the fingertips. Typically, this involves the use of multiple, individual vibrotactile stimulator and limitations of such an arrangement include difficulty with both positioning the stimuli as well as ensuring that stimuli are delivered in a synchronized and deliberate manner. The device that we reported is a significant improvement on multiple independent stimulators (Holden et al, 2011), and due to both the success of that stimulator and the consequent need to validate a number of findings that had been made with both that device and the precursor of that device (Tannan et al, 2007a), we designed and fabricated a four-site stimulator that could be used in MRI and MEG compatible environments. The device can stimulate four independent skin sites and is primarily designed for stimulating the digit tips. The device is similar to the previously reported device in that it is portable and is ergonomically suited for delivering stimuli to the finger tips, but it has the advantage of being MRI and MEG compatible. However, the fundamental mechanisms of the device are significantly different from the device that we recently reported since the device is piezo-based rather than VCA based. To demonstrate the reliability of the device for delivering tactile stimulation at four independent sites, a temporal order judgment (TOJ) protocol, in the presence and absence of conditioning stimuli, was conducted on seventeen healthy control subjects. The study produced results that were consistent with prior studies that implicated synchronization of adjacent and near-adjacent cortical ensembles with conditioning stimuli in impacting TOJ

[1]A large portion of the work presented in this chapter was completed as a collaborative effort with the following researchers: Nguyen RH, Francisco EM, McGonigle D, Seidler R, Dennis RG and Tommerdahl M

performance (Tommerdahl et al., 2007). Additionally, the device was used in both an MEG and in MRI pilot studies, and those studies demonstrated that no detectable noise was introduced by the stimulator in those environments.

Introduction

For the past several years, our research group has been working towards the development of a portable tactile stimulator that could effectively be used to study changes in sensory information processing in clinical and clinical research venues across a diverse spectrum of neurological disorders. Thus far, we have gone through several iterations in the development of this stimulator and the protocols that can be delivered with that stimulator. The current design of the stimulator – as described most recently in Holden et al, 2011 – is optimized for the delivery of vibrotactile stimuli to the finger tips. This optimization was done in order to take advantage of the well-known somatotopic relationships with the concept in mind that delivering stimuli to adjacent digit tips would evoke cortical activity in adjacent and/or near adjacent cortical regions, and that the interactions that result from such stimulus evoked activity will be robustly impacted by alterations in cortical information processing.

The first prototype of the system (Tannan et al., 2005a) was used to demonstrate changes in spatial acuity with repetitive stimulation. A subsequent report described that this change did not occur with individuals with autism, strongly suggesting a lower-than-normal inhibitory response (Tommerdahl et al., 2007a). A second iteration of the device (Tannan et al., 2007a) was much more portable as well as more robust and reliable in its ability to deliver well-controlled vibrotactile stimuli to the skin. The device proved extremely useful, and a number of studies were conducted with it that demonstrated the ability to reliably and reproducibly obtain metrics of neuro-adaptation (Tannan et al., 2007b), temporal order judgment (TOJ) and the impact of synchronized conditioning stimuli on TOJ (Tommerdahl et al., 2007b), the absence of the impact of those same conditioning stimuli on TOJ in individuals with autism (Tommerdahl et al., 2008), the relationship between spatial acuity

and amplitude discrimination (Zhang et al., 2008), a method for the study of tactile-thermal interactions (Zhang, 2009), a reliable means for measuring amplitude discriminative capacity and a robust near-linear relationship between duration of repetitive conditioning stimuli and the impact of that conditioning on amplitude discriminative capacity (Tannan et al., 2007b), the below-normal adaptation metrics in autism (Tommerdahl et al., 2007), the impact of NMDA receptor block on adaption metrics (Folger et al., 2009), a demonstration of Weber's law (Francisco et al., 2008; Holden et al., 2011) and a robust relationship with neurophysiological data (Francisco et al., 2008), and differences in timing perception in Parkinson's Disease (Nelson et al., 2011). More recently, we have developed a newer, more portable and ergonomic model of the device, which is much more suited for a clinical or clinical research environment, and is capable of delivering vibrotactile stimuli to four fingers: the index (D2), middle (D3), ring (D4), and little (D5) fingers (CM4; Holden et al, 2011). The utility of this device has been demonstrated in a report of phenotypic differences within a spectrum of patients with vulvodynia (Zhang et al., 2011a), in a report that described stability of cortical plasticity across a wide age spectrum (Zhange et al, 2011b), and in a paper that describes its utility for describing phenotypic differences within the autism spectrum via modulating vibrotactile stimuli (i.e., sinusoidal stimuli that dynamically change in amplitude; Francisco et al, 2011).

Due, in part, to the fact that we have experienced a great deal of success in demonstrating phenotypic differences between and within a number of neurological alterations, we determined that it would be useful to design and fabricate a magnet-compatible stimulator that had the same, or nearly the same, capabilities as the CM4. Such a device would allow for validation studies of a number of ideas that have been proposed by previous behavioral findings and would possibly elucidate the underlying mechanisms that lead to differential responses by different subject populations. In this report, a magnet-compatible version of the CM4 device, the CM3, is described.

Magnet compatible stimulators are typically designed to use pneumatic or piezo-ceramic parts. Each has its own advantages and disadvantages. Pneumatic devices for use in magnetic environments are typically built with plastic and latex tubing, with the controlling electronics kept away from the magnets. These devices typically have a low frequency range with a maximum near 100Hz and require pressurized air to operate properly (Briggs et al, 2004;) Golaszewski et al (2002) was able to avoid using compressed air canisters by using a BP cuff and their use of a DC motor and pneumatic by-pass line gave a wider range (1-150Hz) and larger amplitude (up to 2mm) than most devices. The device designed by Briggs et al had the potential to support multiple probe tips, each with a different frequency, amplitude, and pattern, though the prior calculations were necessary to lower the risk of bursting the latex diaphragm. The one major disadvantage of any pneumatic device is the possibility of inexact and difficult to reproduce measurements (Briggs et al, 2004; Golaskzewski et al, 2002). Piezo-ceramics are the other typical option for use in a magnetic environment. These often have larger frequency ranges (up to 300Hz) than pneumatic devices (Harrington et al, 2000; Francis et al, 2000), with the ability to target a small frequency band such as the 16-34Hz band that Hegner et al (2010) targeted with precise frequency steps of 2Hz. Piezo-ceramics typically require large voltages to create a small amplitude (50V for 169um in Harrington et all, 2000; 100V for 400um in Francis et al, 2000). A work-around to get a large amplitude (though high voltages were still necessary) involves using piezo-ceramic wafers with multiple rods that can be individually controlled (Hegner et al, 2010). The high voltages required to move these amplitudes require that a non-conducting surface interacts with the subjects, such as plastic probe tips or non-conducting piezo-ceramic wafers. A piezo-ceramic stimulator offers more control than a pneumatic stimulator, though they are often more expensive and require large voltages.

Methods

Hardware. The cortical metrics (cm-3; see figure 1) stimulator was developed in our laboratories for use in the series of experiments described in this report. The principle driving design requirement for the CM3 stimulator system is to allow up to four vibrotactile stimulator mechanisms to interact with a test subject's fingertips while their cortex is being imaged in a magnet-based imaging system such as fMRI. The system was designed using state-of-the-art rapid manufacturing technology to allow multiple identical systems to be built and used in different locations. Also, the use of rapid manufacturing permitted very rapid design evolution, thereby facilitating the production of special fixtures and changes to geometry as needed for special applications. The device consists of two separate parts: the controller/power box and one, or in some cases two, detachable stimulator head unit(s) connected together by a 40-conductor shielded twisted-pair ribbon cable, 2 meters in length. The flat plates of all exterior housing and other components of approximately planar geometry are direct manufactured using laser-machined cast acrylic sheet, cut on a 120 Watt CO2 laser engraving system, model number X660 (Universal Laser Systems, Scottsdale, AZ). The more complex housing and internal mechanism components are direct "3-D" manufactured from ABS plus thermoplastic material, by fusion deposition modeling (FDM) on a StrataSys Dimension bst 1200es (StrataSys, Inc., Eden Prairie, MN). The four large cylindrical components forming the four movable disks of the stimulator head units are CNC machined from 1" thick Acetal (Delrin) plate. All housing and mechanism components and assemblies were solid modeled prior to fabrication using SolidWorks solid modeling software (SolidWorks Corporation, Concord, MA).

Figure 3.1: Four Site Vibrotactile Stimulator. Each of the four probe tips is positioned by rotating the four independently-positioned drums to maximize contact between finger pads and the stimulator tips. During an experimental session, subjects were seated comfortably in a chair with their arm resting on the arm rest attached to the head unit of the device. Digits D2 through D5 were then positioned for vibrotactile stimulation.

The internal mechanism of the head unit is comprised of identical cylindrical disks placed sideways and four abreast coaxially (130mm in diameter, 24mm in depth) between two acetal side panels. Each disk can be independently rotated to adjust for differing finger lengths for each test subject. A servo mechanism comprising a non-metallic piezo bender actuator and a compliant four-bar link linear motion mechanism are mounted inside each disk. The piezo bender actuators (P/N: Q2C, formerly Q220-A4NM-303YB) are custom manufactured by Piezo Systems, Inc., in Cambridge MA. Each piezo bender is .5mm thick x 12.5mm wide x 32mm in length, and require approximately 200 to 300 volts for actuation. Each piezo bender is attached to a cylindrical plastic probe (5mm diameter) which slightly protrudes through a hole (7mm diameter) in the side of each 130 mm diameter acrylic disk,

which serves to mechanically isolate the test subject from the internal piezo driver voltages. The amount of protrusion for each probe is independently adjustable as are the positions of the holes to accommodate the length of the subject's fingers as he/she wraps their hand around the stimulator head unit. The piezo bender motion is converted into linear displacement by the four-bar compliant mechanism to drive the cylindrical plastic stimulator probe tips linearly into and out of each 130mm diameter disk in the stimulator head unit, according to prescribed sinusoidal waveforms. The moving components of the stimulator tips are directly manufactured from ABS "plus" material by 3-D FDM as a single compliant mechanism component integrating a mounting flange, a thin-beam four-bar linkage, coupling lugs for attaching one piezo bender into each actuator mechanism, and the extension to the mechanical stimulator tip. The compliant four-bar linkage mechanism allows the stimulator tip to be displaced vertically along a straight line for a distance of ± 1 mm. The 4-bar compliant mechanism also provides a very low hysteresis linear restoring force to center each tip vertically when no voltage is applied to the piezo benders. The entire four-bar mechanism is 5.3 mm in thickness, and is positioned such that the stimulator tips move along a radial line extending from the center of each 130mm disk, perpendicular to the outer circumference of each disk. The resulting linearized piezo bender mechanisms generate extremely linear force outputs as a function of drive voltage with very low hysteresis due to the "frictionless" nature of the single piece bearing-less four bar compliant mechanism. The position of the vibrating tips is not sensed for the CM3 units, unlike the optical position sensors in the previously reported CM4 systems (Holden et al, 2011). Care was taken throughout the design of the CM3 stimulator head to exclude magnetic and/or electrically conductive components that might interfere with or be damaged by the presence of strong external magnetic fields associated with modern magnet-based imaging systems.

The custom electronics were designed using free CAD software from ExpressPCB (www.expresspcb.com). The printed circuit boards were manufactured using the resulting

CAD files, also by ExpressPCB. The hybrid circuit is interfaced via four parallel pin connectors (2 banks of 50 pins for digital signals and 2 banks of 34 pins for analog signals) to an internal NI-USB-6259 data acquisition (DAQ) board. The DAQ board then interfaces via a USB connection to any standard PC running Microsoft Windows XP or later.

Software. A custom line-of-business application was developed for the Microsoft .Net platform using the C# programming language and Windows Presentation Foundation (WPF) framework to control the stimulator and administer the data collection protocols. The interface was designed to be intuitive, extensible, and aesthetically pleasing. The software needed to be extensible to facilitate the development of future protocols for a device as flexible as the CM-3. The core extensibility was achieved by using a "plugin" architecture with a shell application whose function is to discover, load and execute small plugins. The shell exposes a software contract (an inheritable C# class) that is consumed and extended by each plugin. Each task described in this paper represents one such plugin. Most traditional neuropsychological protocols using the standard X-alternative forced-choice (X-AFC) tracking method (Cornsweet, 1962) can be created with only a couple of dozen lines of C# code. While most plugins interact directly with the CM-3 stimulator, this is not a requirement of the plugin contract. Plugins can, for example, be designed to collect arbitrary subject information pertinent to the given study (e.g. participant demographics, relevant medical history, various surveys, etc.). The net effect is not only a significant reduction in the amount of clinical paperwork that needs to be completed by each participant, but also a marked reduction in data-entry time for clinicians. All data collected by the application are stored in an encrypted (128-bit RC4) SQLite database in a user-specified location. Each database can be shared with multiple instances of the shell application, providing a mechanism for seamless networking of CM-3 stations (Holden, et al, 2011). The software is also capable of storing, as well as creating and customizing, all relevant initialization information for each plugin, such that a given battery of protocols can be administered repeatedly and in a consistent manner, while maintaining flexibility for future projects. The

batteries allow for greater reuse of each plugin, resulting in shorter development times a more efficient workflow throughout an experiment.

Protocols. In order to demonstrate exemplary use of the CM-3, 3 studies were conducted. First, Temporal Order Judgment (TOJ), in the presence and absence of conditioning stimuli, was collected and compared with data previously reported with a VCA based stimulator (Tommerdahl et al, 2007b). Second, pilot studies with fMRI were conducted in order to ascertain compatibility of the stimulator in an MRI environment. Third, pilot studies in an MEG environment were conducted in order to determine whether or not the CM3 introduced noise in that environment. Additionally, both MEG and MRI studies compared the responses evoked by stimulating different finger tips.

Subjects. Thirty healthy subjects ranging from 22 to 26 years of age, were recruited for the TOJ study. None of the subjects reported any neuropsychological impairment and all were naïve to both the study design and issue under investigation. The study was performed in accordance with the Declaration of Helsinki, all subjects gave their informed consent, and the experimental procedures were reviewed and approved in advance by an institutional review board.

Experimental Procedure – TOJ with and without background noise. During an experimental session, the subjects were seated comfortably in a chair with the right arm resting on the device. Because the lengths of fingers typically vary among subjects, the positions of the probe tips were individually adjusted to ensure that they contacted the glabrous, padded tips of the fingers of each subject. These loci were chosen in order to allow the convenience of access and comfort of participants as well as for the wealth of neurophysiologic information that exists for the corresponding somatotopic regions of cortex in primates (Chen et al., 2003, 2007, 2009; Francisco et al., 2008; Friedman et al., 2008; LaMotte and Mountcastle, 1975; Mountcastle, 1969; Tommerdahl et al., 1993, 1998, 2002, 2005, 2006, 2010). As depicted in Figure 1, probe tip positioning was accomplished by loosening a set screw and rotating each of the drums independently to conform to the

natural hand shape of each subject. After proper positioning, if the probe tips still failed to make proper contact with the digits, the tips themselves were either raised or lowered. Once adjusted, the probe tips were locked in place prior to initiation of the battery so that they would remain immobile during testing. At the start of each run, the four tips were driven towards the tips of the fingers in order to ensure good contact with the skin.

During the assessment, the device delivered sinusoidal skin displacements (vibrations) via flat Delrin probes (5-10 mm in diameter) positioned to make contact with the tips of the index (D2), middle (D3), ring (D4), and little (D5) fingers of the right hand. The independent probe tips were computer-controlled and capable of delivering a wide range of vibrotactile stimuli of varying frequencies (Hz) and amplitudes (μm). Stimulus parameters were specified by test algorithms that were based on specific protocols as well as subject responses during those protocols.

Subjects viewed a computer monitor that provided continuous visual cueing during the experimental session. Specifically, an onscreen light panel indicated to the participant when stimuli were being delivered and when subjects were to respond. Training trials were included prior to testing, and the subjects were given performance feedback only prior to trials during data acquisition. The sensory testing session was conducted by application of low frequency (25 Hz) vibration to selected fingers. Each battery of testing lasted between 15 and 20 minutes depending on the protocols being run and on subject performance. Each individual protocol typically lasted 2 to 3 minutes.

Temporal Order Judgement, without (TOJs) and with carrier (TOJc) stimulus. All participants received the temporal order judgement tasks (n=30). In the temporal order judgement task (TOJ), two single vibrotactile pulses (40 ms, 25 Hz, 200 μm) were delivered on two digits (D2, D3, D4 or D5) separated temporally by a starting ISI of 150 ms (the first pulse was assigned pseudo-randomly) within a 1 s interval. Participants were asked to respond to the digit that received the first pulse. The ISI was modulated with 1 up/1 down tracking for the first 10 trials and a 2 up/1 down tracking for the remainder of the task (ISI

was decreased for correct answers and increased for incorrect answers). In one condition, there was no concurrent stimulation (TOJs) and in the second condition (TOJc), a 25 Hz concurrent carrier (20 μm) stimulus was delivered throughout each 1 s trial-interval. The tasks were performed for six digit combinations on each subject: D2-D2, D2-D4, D2-D5, D3-D4, D3-D5 and D4-D6. Noise introduction in the MRI environment

The amount of noise introduced into the MRI environment by the CM3 was measured by collecting MRI data, in the absence of a human subject, with the CM3 in four different locations or situations: 1) The CM3 was not in in the scan room; 2) the CM3 was placed on the scanner table but not connected to either power or computer; 3) the CM3 was placed on the scanner table and connected to the driving hardware in the control room, without the power turned on; and 4) the CM3 was connected to both computer and power, was turned on and the stimulators were turned on.

The stability scans were acquired on a 3T GE Signa LX MR scanner (Waukesha, WI). A GE structural phantom was scanned using a reverse spiral acquisition (TR/TE/FA=1000/27.5/60, 200 cm FOV, 13 slices, 5/1 thickness/gap, 64x64 matrix, 180 frames collected).

Using a region of interest, temporal and spatial signal-to-noise ratio (SNR), the temporal drift and normalized frequency magnitude were calculated. In addition, the summed absolute temporal difference of the time course was calculated and plotted, as a measure of frame-to-frame stability. Comparisons were made between the scans obtained in the four different conditions.

Results

This study employed a TOJ protocol, in the presence and absence of conditioning stimulation, on healthy subjects in order to demonstrate the capacity of the device for delivering well-controlled vibrotactile stimuli at four independent sites. The study also confirmed a previous finding (Tommerdahl et al, 2007b) that demonstrated that performance on the TOJ task, in the presence of synchronized and periodic vibrotactile

stimulation, is reduced. Additionally, DLs for the TOJ task with synchronized conditioning stimuli were not significantly elevated when the task was performed across D2-D5. In other words, when cortical distance was greatest between the stimulus sites, the impact of the conditioning stimulus was smallest.

Studies were also conducted in the presence and absence of MEG and MRI environments in order to ascertain whether or not the device introduced noise and was magnet compatible. There was no detectable noise evoked by the CM3 stimulator in either of these environments.

The TOJ task was evaluated in order to quantify the ability of subjects to recognize and identify stimulated digits in the absence and in the presence of conditioning stimuli.

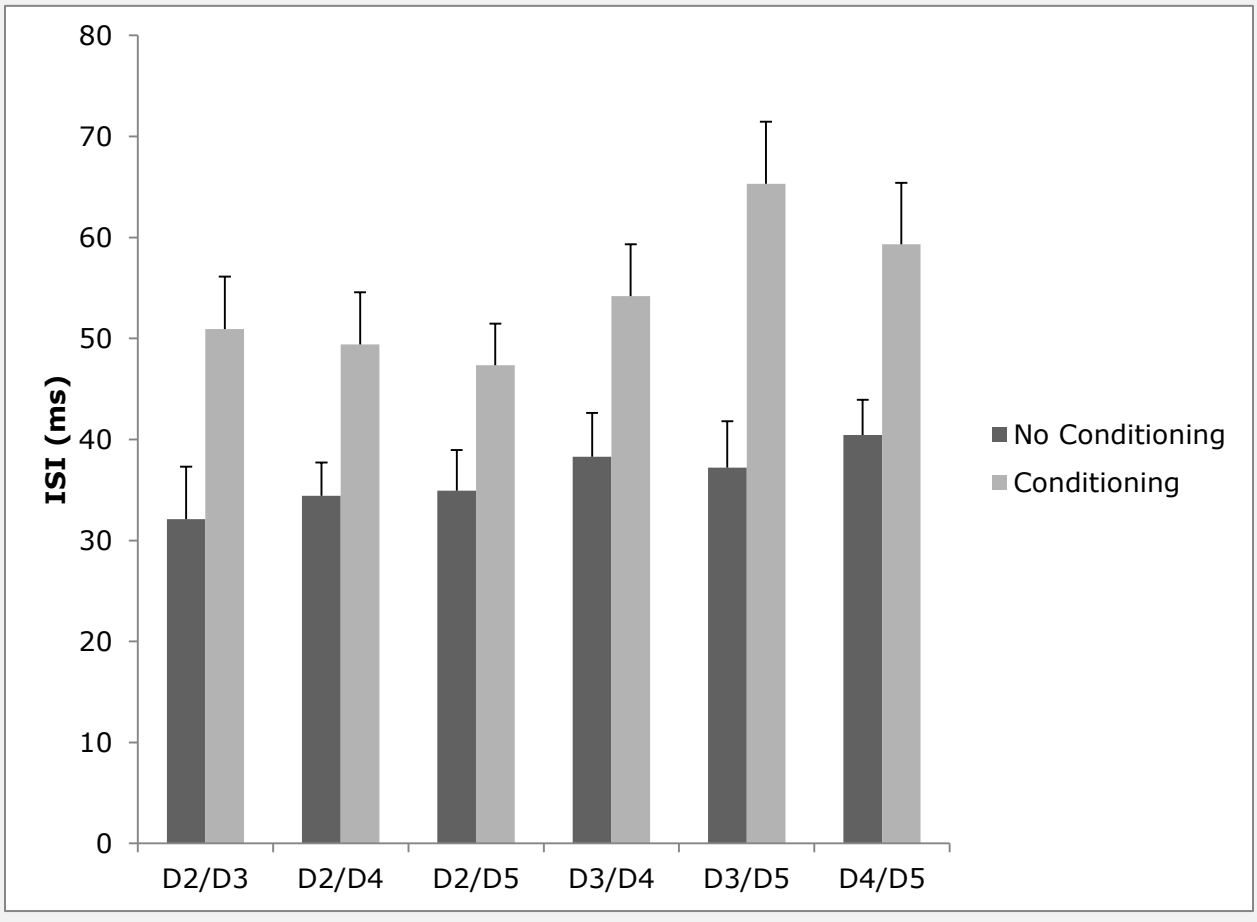

Figure 3.2: Impact of Conditioning Stimulus on TOJ Performance

MRI recording results. There were no significant differences observed in any of the recordings that were obtained during scans in the four different conditions of CM3 placement and operation. No dominant noise spikes were observed in either the frequency spectrum or difference time course, and with steady temporal and spatial SNR in each case (1 – no CM3 present, 2- CM3 present, 3 – CM3 plugged in and 4- CM3 operating): 1) 117:180, 2) 148:190, 3) 135:177, 4) 140:178. Thus, the device induced no detectable MR artifacts.

Discussion

The delivery of sinusoidal displacements to a single skin site via mechanical transducer has been used extensively for the study of flutter vibration in both psychophysical and neurophysiological settings for a number of decades. Exemplary uses of such a device are described in Goble and Hollins, 1993; Juliano et al., 1989; LaMotte and Mountcastle, 1975; Mountcastle et a., 1969; Tannan et al., 2006; Tommerdahl et al., 1993, 1998, 2002; and Vierck and Jones, 1970. Typically, stimuli that can be delivered through mechanical transducers – vertical displacement stimulators such as the one originally described by Chubbuck (1966) – were used for studies of somatosensation and are very well equipped to deliver sinusoidal stimuli at a frequency range (1 to 250 Hz) with amplitudes of sufficient size (between 0 and 1000 μm) to activate a broad range of mechanoreceptors. However, in order to stimulate more than one skin site – either during the course of human psychophysical testing or animal experimentation – it is necessary to position a second vertical displacement stimulator over the second skin site. Our previous device (described in Tannan et al. 2007a) was designed to address this issue by allowing dual site stimulation with automated two-dimensional probe positioning. Although the device reported by Tannan and colleagues was successfully utilized in a number of studies (Tannan et al., 2005b, 2006, 2007b, 2008; Tommerdahl et al., 2007a, 2007b, 2008), it was cumbersome and not ideal for clinical and clinical research venues. The CM-4, described in Holden et al, 2011, has the capacity to quickly and easily adjust to fit to most adult, and

many juvenile, hand sizes and can deliver vibrotactile stimuli to the tips of four digits. The ability to simultaneously deliver vibrotactile stimuli to a number of digits allows for a great deal of protocol diversity. The ability to deliver these stimuli in an MRI and MEG environments expands the functionality of the stimulator. Not only can behavioral tests be performed, but neurophysiological correlates can be obtained as well.

In this report, we described the use of a relatively simple protocol – Temporal Order Judgment (TOJ) in the presence and absence of conditioning stimuli. This protocol has been previously described (Tommerdahl et al, 2007x, 2008x), and in those studies, stimulation was provided to D2 and D3 in order to observe the impact that synchronized and periodic stimuli had on TOJ performance. Performance on the TOJ task itself was relatively robust across the digit combinations, although performance with D4-D5 appears to be worse than other digit combinations, and this would be expected due to partial overlap between D4-D5 representations. Post-conditioning, there were significant differences with the task using different digit combinations. As the separation between the test sites located between D2 and the other digits increased (D2 was paired with D3, D4 and D5 on separate tests), there was a decrease in the impact of the conditioning stimulus. Specifically, there was little impact of conditioning on the D2-D5 pair although there was impact on performance when D2 was paired with D3 or D4. The interpretation of this finding is that there is a critical distance between cortical representations that needs to occur before the conditioning stimulus no longer has an effect. In the case of the D4-D5 pairing, the cortical distance is already minimized and thus, the conditioning stimulus that normally impacts TOJ performance with D2-D3 pairing by functionally linking those cortical representations, has effectively already linked the D4-D5 sites.

The principle finding in the results of this study is that there is an increase in inaccuracies with concurrent conditioning stimulation delivered during the TOJ task, and the ability to perform the task accurately in the presence of that conditioning stimulation is diminished more in digits D3 and D4 than in digits D2 and D5. The decrease in accuracy

with synchronized sinusoidal stimulation is consistent with prior reports of increasing inaccuracies in temporal order judgment (TOJ) in the presence of synchronized and periodic conditioning stimuli. In a study by Tommerdahl and colleagues (Tommerdahl et al., 2007), it was demonstrated that TOJ results obtained from a number of pairs of stimulus sites – unilateral as well as bilateral – were comparable. However, in the presence of a 25Hz conditioning sinusoidal stimulus which was delivered both before, concurrently and after the TOJ task, there was a significant increase in the TOJ measured when the two stimuli were located unilaterally on digits D2 and D3. In the presence of the same 25Hz conditioning stimulus, the TOJ obtained when the two stimuli were delivered bilaterally was not impacted. This led to the speculation that the impact that the conditioning stimuli – which only had an impact if they were sinusoidal, periodic and synchronous – had on TOJ measures was due to the synchronization of adjacent cortical ensembles in somatosensory cortex, and that the synchronization of these cortical ensembles could have been responsible for the degradation in temporal order judgment. The conditioning stimuli in this study were also synchronized, periodic and simultaneous, and if the degradation in test performance was due to synchronization of adjacent cortical ensembles similar to what was speculated in the TOJ report, then inaccuracies due to this synchronization would be lower on the digits on the perimeter of the cortical ensemble (i.e., D2 and D5), and the results reflect this prediction. Future studies will consider whether or not subjects with neurological disorders are not impacted by conditioning stimuli, as was found to be the case in subsequent TOJ studies (e.g., TOJ metrics of subjects with autism were not impacted significantly by conditioning stimuli; Tommerdahl et al., 2008).

The role of neural communication between adjacent and non-adjacent cortical regions plays an important role in understanding the relationship between neurophysiological mechanisms and sensory percept. The development of new, more versatile devices and methodologies, such as presented in this report, could contribute to bridging decades of neuroscientific research with human perceptual clinical and clinical

research studies. One long term goal of our research is to develop sensory based instrumentation and methodologies for the diagnosis and assessment of treatment efficacies for a broad range of neurological disorders, and building this aforementioned bridge could provide new insights into fundamental information processing mechanisms as well as generating perceptual metrics that are more sensitive to alterations in central information processing capacity.

CHAPTER 4: VIBROTACTILE STIMULATOR SOFTWARE INTERFACE

Both the CM3 and CM4 vibrotactile stimulators were designed to leverage identical data acquisition (DAQ) circuitry produced by National Instruments. Each DAQ board is accompanied by a software license to a set of application development software libraries developed by National Instruments for creating end-user applications that interface with their DAQ hardware. The availability of application development tools from the hardware vendor was a primary driving force in selecting the data acquisition board. Versions of the application development libraries exist for several different programming languages and operating systems, but the CM3 and CM4 devices only utilize the versions for Microsoft's .NET Framework and National Instruments' own LabVIEW integrated development environment (IDE). A series of software applications had to be created to calibrate and control the delivery of the aforementioned vibrotactile stimuli.

The first such application was developed in LabVIEW to calibrate each pair of voice coil actuators and optical feedback mechanisms tips using the DAQ board's analog-to-digital (ADC) and digital-to-analog (DAC) capabilities. The USB-6259 DAQ board possesses 32 16-bit analog input channels, capable of 1 million samples per second (SPS) in aggregate, and 4 16-bit digital output channels, capable of 2.8 million SPS. These capabilities were far beyond the requirements of basic sinusoidal function generation of tactile flutter range frequencies, and thus ensured that development of vibrotactile stimulation protocols would not be hindered by data acquisition inadequacies. The first step to verify that the DAQ system was capable of delivering controlled sinusoidal vibrations was to plot the analog signal coming from the CM4 optical position sensor.

Figure 4.1: Optical Sensor Readings Verify Sinusoid Generation

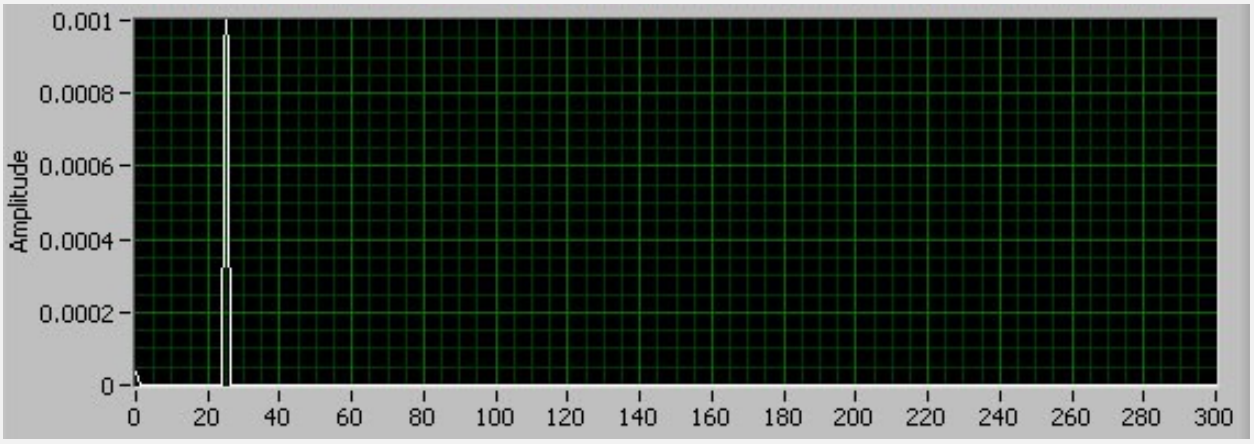

Figure 4.2: FFT of Measured Sinusoid in Figure 1

As demonstrated above, the frequency response for the actuator was perfect, but the pre-calibration amplitude of the sinusoid reached an error level that was unacceptable, and thus software calibration of each actuator was necessary. A simple paradigm was used to perform this calibration: For each frequency that the actuator could possibly deliver during a behavioral protocol, a simple linear calibration was performed across the entire amplitude

range. Nine desired amplitudes were chosen in the range of 50 to 700 microns. A sinusoid lasting one second representing the un-calibrated command signal calculated for each amplitude was administered and the position was recorded from the optical sensor at a sample rate of 10kHz. The peak-to-peak amplitudes of the recorded optical waveforms were calculated at 200ms intervals and averaged together as a measure of the average peak-to-peak amplitude for the entire sinusoid. The difference of the commanded and measured amplitude was calculated for each sinusoid and a simple linear regression equation was then calculated for each frequency. The procedure was then replicated using the calibrated command signal to verify that the measured and commanded amplitudes now matched. The figures below show an example output from this calibration program and demonstrate its effectiveness.

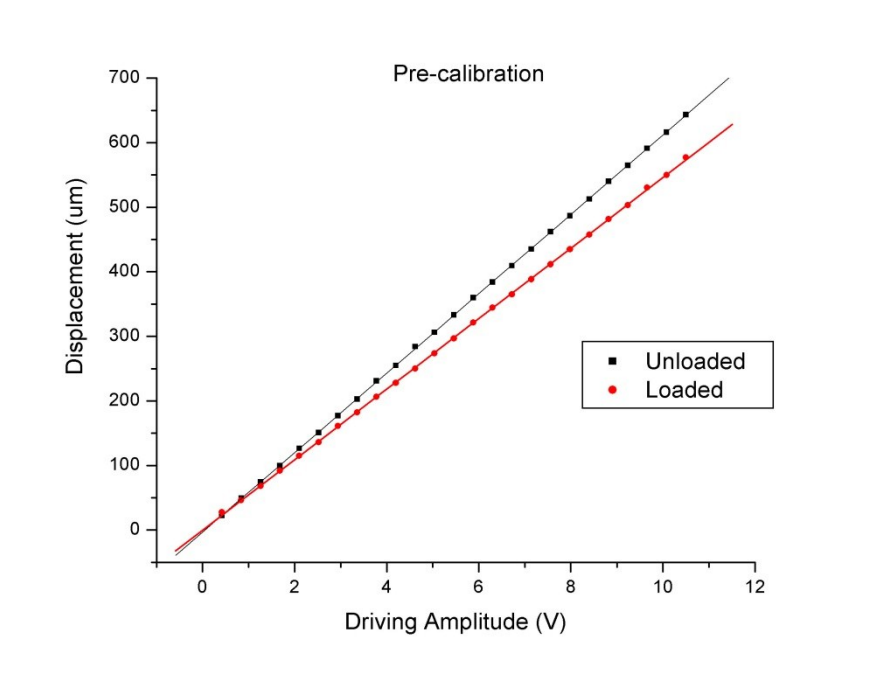

Figure 4.3: Pre-calibration Driving Amplitude Discrepancy

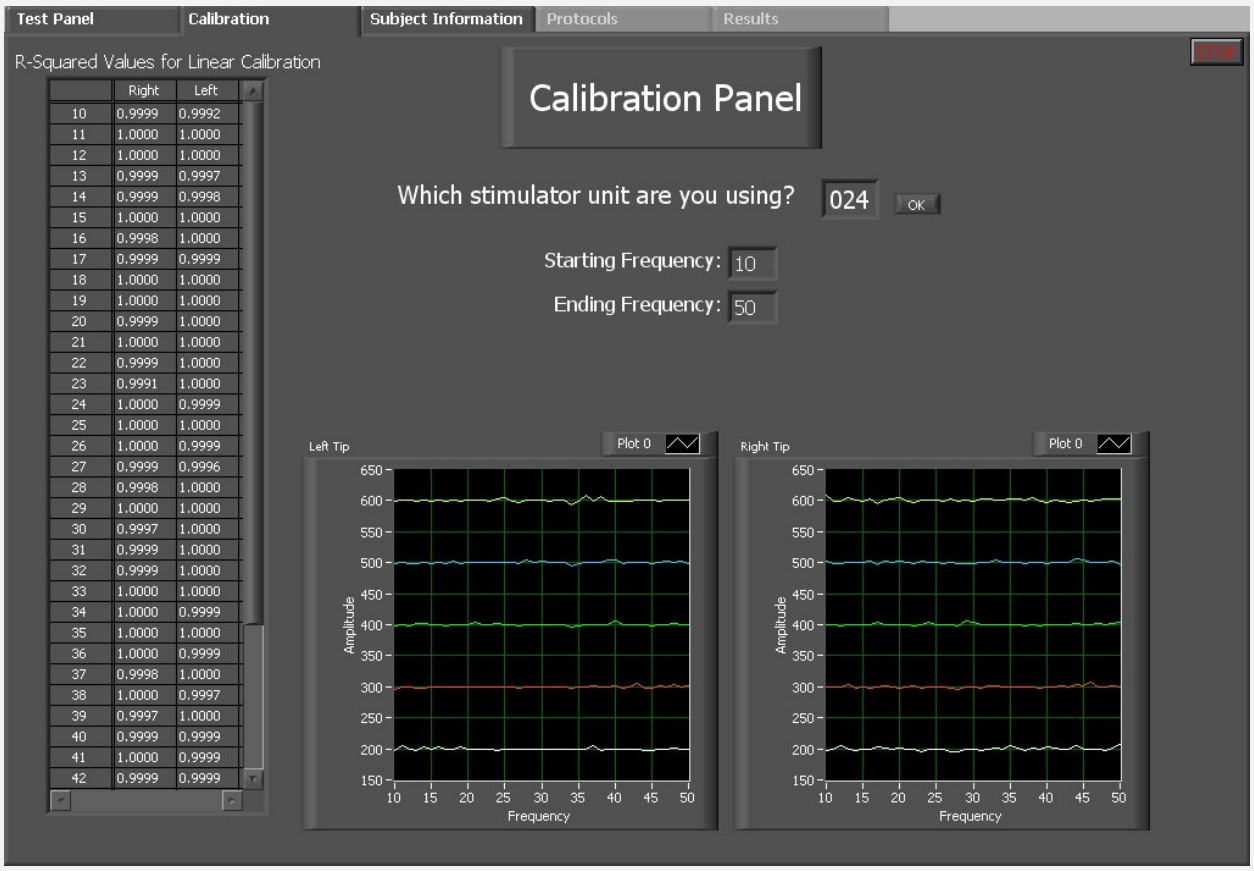

Figure 4.4: VCA Calibration Application - Output from a completed calibration exercise. The coefficients of determination for the VCAs are all > 0.999. The measured amplitudes are graphed for command amplitudes ranging from 200 microns to 600 microns across frequencies from 10 to 50hz.

After demonstrating the ability to successfully and accurately replicate arbitrary sinusoidal waveforms, the design of a framework for the creation and execution of the behavioral protocols described herein was the next logical step. The majority of the behavioral protocols that allow for the quantitative assessment of a wide array of cortical processes follow a similar pattern. Identifying this pattern allowed for the extraction and encapsulation of common elements into independent software modules that could be more easily combined and extended during the development of new behavioral protocols. Just like for the stimulator itself, one of the design considerations for the protocol execution framework was portability. The software package would need to be executed on dozens of computers in such a way that did not end up requiring a particular computer to be manually paired with a particular stimulator. Another important design consideration would be the

user interface. In order for this system to be successful at a clinical level, the interface would have to be intuitive and aesthetically pleasing enough for an experimenter without intimate knowledge of the entire system to navigate. These requirements would ultimately result in a shift from the laboratory-centric LabVIEW programming language to the more widespread C#.

C# is an object-oriented programming language (OOP) built on Microsoft's .NET Framework. Its syntax is similar to both of its predecessors, Java and C++. Like Java, C# applications are not compiled directly into machine language, but to an intermediate language (Microsoft Intermediate Language (MSIL)) that gets executed in a virtual runtime environment. This gives developers lots of conveniences not afforded by other languages like C/C++. For example, memory management in both C# and Java is handled by the runtime unless explicitly overridden by the developer leading to fewer software memory leaks and thus greater application stability. With all of the similarities between Java and C#, choosing between the two came down to their ability to create modern graphical user interfaces (GUIs).

In 2006, Microsoft released the Windows Presentation Framework (WPF), a framework for facilitating the creation rich user interfaces. It introduced a markup language called the Extensible Application Markup Language (XAML), based on the Extensible Markup Language (XML), which separates the 'view' logic used to control a user interface from the underlying 'model' logic. This concept is not new in software development, and it is generally accepted as best practice to decouple the logic specific to the user interface from the underlying business logic when attempting to create an extensible, maintainable and long lasting application. To facilitate this separation of logic, WPF included an efficient and robust implementation of GUI data binding. Data binding in this context refers to the coupling of a simple object (in the OOP sense) with its visual representation in the GUI. This enables the developer to manipulate simple data objects and have changes to those objects automatically synchronized with their visual representations within the user

interface. By leveraging this data binding capability, WPF was also able to provide a flexible animation framework that significantly reduced the amount of development time required to create aesthetically pleasing transitions within the GUI. Those key features ultimately led to the selection of C# as the language of choice for developing the first clinical GUI for our behavioral protocols. It should be noted that the only majorly obvious flaw of C# (and WPF) was that it was limited to running on the Windows® operating system. However, this was not a significant concern since the hardware drivers for the DAQ board also shared this limitation.

Device Driver Library

After choosing C#, the first iteration of the application was divided into three separate parts. The first task was to create a relatively low level interface to the embedded DAQ board. Although the DAQ system was capable of streaming arbitrary waveforms to the actuators, sinusoidal waveforms would be used exclusively in the behavioral protocols. Thus, the main job of this low level interface library was to create an abstraction for the generation of sinusoids that could be utilized by the upper layers of the software package. A simplification of the class diagram below displays the functional relationship between classes.

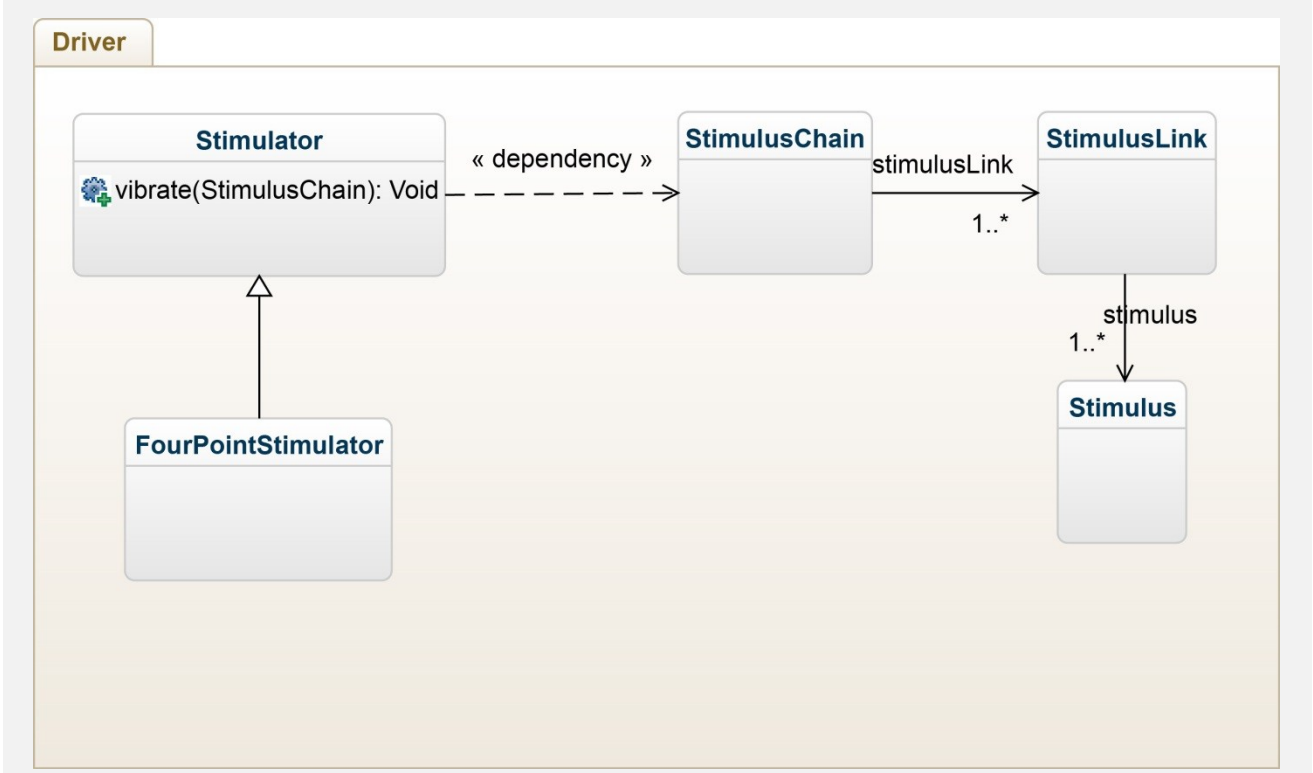

Figure 4.5: Abbreviated Driver Library Class Diagram

The main Stimulator class served to encapsulate all of the functionality available to the upper layers. It is important to note that the Stimulator classes utilizes the Factory pattern (Gamma et al 1994) and does not expose a public constructor function. This prevents the upper software layers from attempting to create an instance of a Stimulator object when there is no physical hardware connected to the computer, and allows the Stimulator class to manage multiple devices plugged in to the same machine simultaneously. The Stimulator class is responsible for managing the state of position control mechanisms as well as using an embedded calibration database to generate amplitude and frequency accurate sinusoids for any CM vibrotactile stimulator. It also contains the mappings for hardware actuator channels to human digit tips. If a person places his or her right hand on the head unit of a stimulator, the channel mappings would be the opposite of those used for a left hand. This allows the upper layer to make function calls referencing a person's digit tips (e.g. D2,D3) instead of hardware channels (e.g. 0,1),

which is significantly more intuitive when developing behavioral protocols. Complex sinusoidal vibrations are pieced together by using a chain of simple sinusoids. The most basic Stimulus class represents a single sinusoidal waveform with a given amplitude, frequency, and duration. An instance of the StimulusLink class represents a single base Stimulus with an optional second Stimulus that will be superimposed. The duration of the superimposed stimulus is ignored, as it must be the same as the base sinusoid. One or more StimulusLinks can be sequenced to form a StimulusChain. The StimulusChain class includes helper functions to pad a chain to a given duration or to introduce delays without having to manually create 0 amplitude sinusoids. A set of StimulusChain objects is passed to the 'vibrate' method of a Stimulator instance to where each chain is converted to the appropriately calibrated driving voltages for a given DAQ hardware channel and ultimately passed to the stimulator via the USB connection. It should be noted that the upper software layers can subscribe to a software event that will be fired just before the USB transfer begins to enable synchronization with user interface elements to which this low layer is completely naïve. This library is used in every software application that controls a CM3 or CM4 stimulator, regardless of the GUI.

Common Plugin Library

The next software layer was also a software library that cannot be executed as a standalone application. The broad scope of possible behavioral protocols that could be realized using a portable vibrotactile stimulator made it clear that our lab could not possibly perform all of the research tasks alone. In order to facilitate collaboration with other research labs, it was decided that the upper software layers should implement a 'plugin' architecture that could be extended by developers from other laboratories.

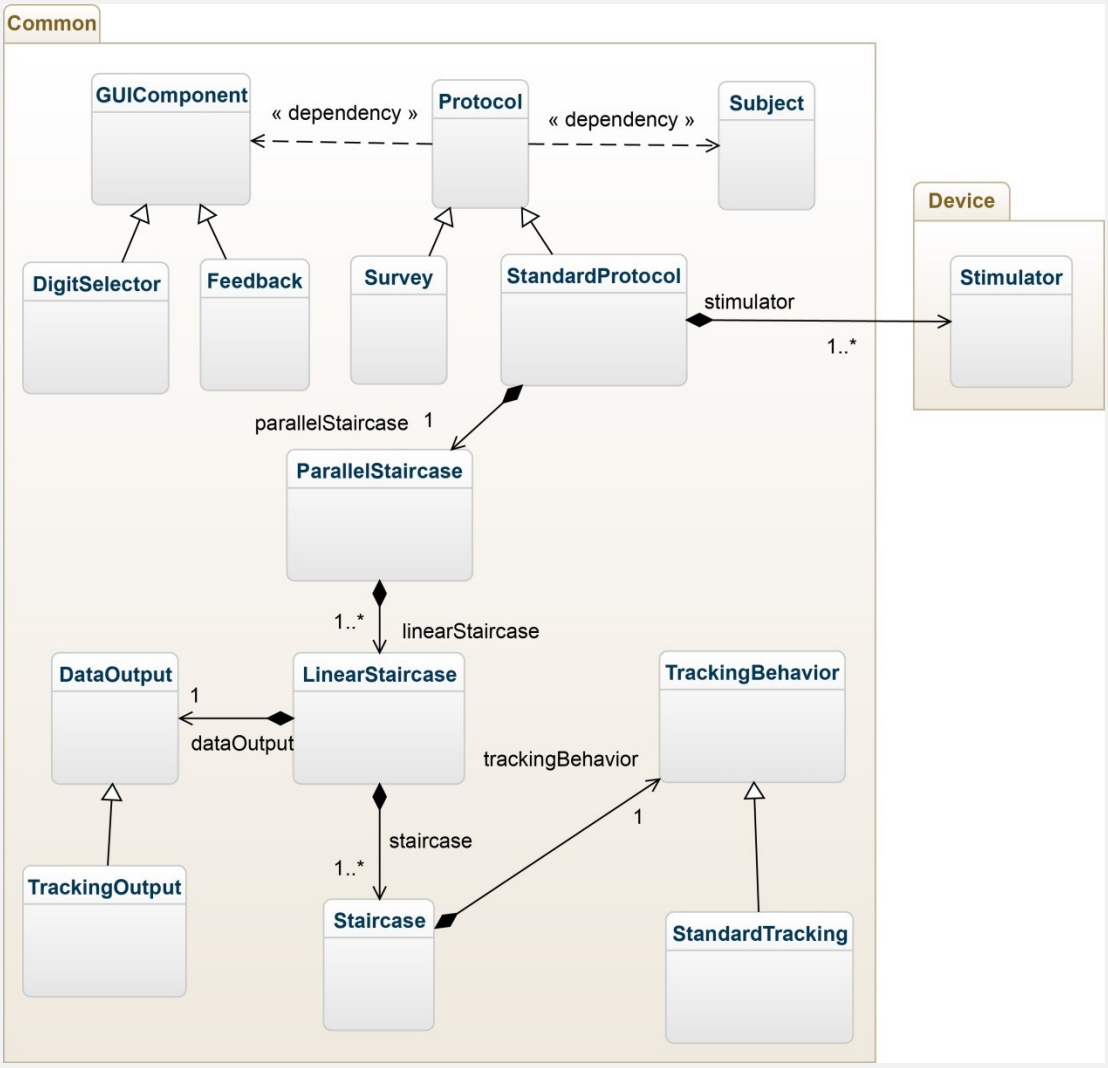

Figure 4.6: Abbreviated Class Diagram of Common Plugin Interface Library

The plugin architecture is centered around the implementation of a single base Protocol class. Implementation of this class is the bare minimum required to be recognized by the top software layer. In a nutshell, the Protocol class merely provides a small set of virtual public functions to initialize, start, stop and pause the Protocol that can be called from the top layer. The initialization function depends on the Subject class, which encapsulates the necessary demographic data to represent the person on whom the Protocol is being executed, and the return value is the GUI to be displayed to the Subject by the top software layer.

The simplest provided implementation of a Protocol is the derived class, Survey. The Survey class represents a Protocol that can be executed without a stimulator. Many clinicians had legacy demographical surveys that were administered on paper during each clinical visit by a particular subject, so the Survey class provided a simple way to collect that data electronically. An example of one such implementation of the Survey class is an electronic version of the Autism Quotient survey (Baron-Cohen et al 2001).

The other major subclass of the Protocol class is the StandardProtocol class. Classes that inherit from the StandardProtocol class require the presence of a CM stimulator and have a common execution flow directed by an overridden 'start' function of the Protocol class. All behavioral protocols that have been designed so far execute a sequence of trials with various methods of transitioning from one trial to the next. Instances of the StandardProtocols do this through the implementation of the ParallelStaircase class. A bottom-up approach is best to understand how this works.

At the lowest level, the Staircase class represents a simple list of trials and associated metadata. This metadata includes all of the information needed to execute and record data from a particular trial e.g. stimulus amplitude, user response, inter-stimulus interval etc. The Staircase class also contains an instance of a TrackingBehavior that describes the orderly transition from one trial to the next. An example of a TrackingBehavior is an implementation of a modified von Békésy tracking algorithm (Tannan et al 2005b). Each instance of the LinearStaircase class contains a list of Staircase instances that are to be executed sequentially. This allows the developer to build a series of trials using identical TrackingBehaviors while still maintain the ability to modify secondary parameters throughout the protocol. The most common example of this function is the modification of the bias parameter at the midway point of a tracking algorithm as described in Tannan 2005b. Since all Staircases encompassed by a LinearStaircase are executed sequentially, it is assumed that the trials exhibit linear dependence as well. This implies that the LinearStaircase should be responsible for recording the starting parameters for the

first trial in that dependence hierarchy, and thus is the logical place for an instance of the DataOutput class.

The DataOutput class is responsible for recording the aforementioned starting parameters as well as the raw data collected during execution of its parent LinearStaircase. After the last trial in a LinearStaircase is completed (according to the TrackingBehavior), the 'save' method of the DataOutput class is called to store the data to the computer's hard disk. The data can be stored either to a pair of plain-text files or an encrypted SQLite database depending on the security requirements of the environment in which the data was collected.

Finally, the ParallelStaircase class can encompass one or more instances of the LinearStaircase class that are executed simultaneously. Since data saving is controlled independently in each LinearStaircase, multiple sets of data can be generated for a single StandardProtocol if it happens to contain multiple LinearStaircases. The primary use for the ParallelStaircase class is during protocols that leverage tactile illusions that could also be a cue to the subject who understands the task. For example, a conditioning vibration that is always delivered at the same site as the 'test' stimulus of a 2AFC protocol could be considered a cue to the correct answer. In order to remove this confound, a second LinearStaircase with the conditioning vibration at the opposite site can be executed simultaneously with trials from each LinearStaircase randomly interleaved together.

The plugin library also exposes a few helper classes in order to facilitate the creation of custom rich user interfaces. Examples of such are the Feedback and DigitSelector classes. Some subclasses of the StandardProtocol class give the user various types of feedback after each response to a trial. The feedback can either be positive, negative, or neutral. Positive and negative feedback is generally reserved for training portions of a StandardProtocol where the subject must demonstrate an understanding of the proposed task by responding correctly several times in a row. Neutral feedback has been used in interfaces designed for children to keep them motivated to pay attention to the behavioral

task. In one such instance, a series of images similar to a short comic are presented after the completion of each trial, but they are unrelated to the correctness of the preceding response. The Feedback class is able to deliver all three types of feedback while remaining protocol agnostic and thus reusable across multiple behavioral tasks.

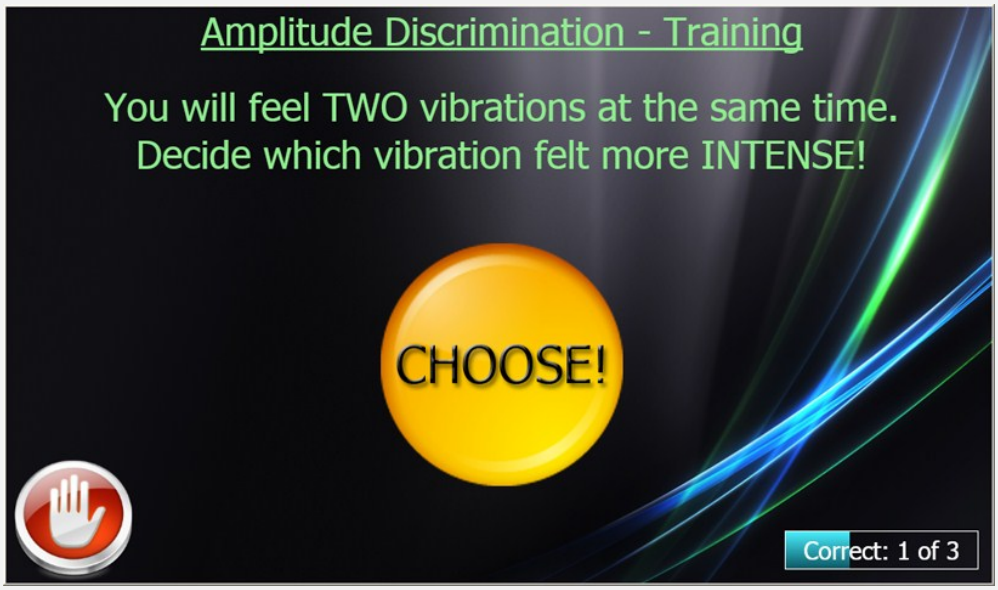

Figure 4.7: Example Plugin. Developed using the plugin library, this behavioral task is executed from the 'shell' layer

Shell Application

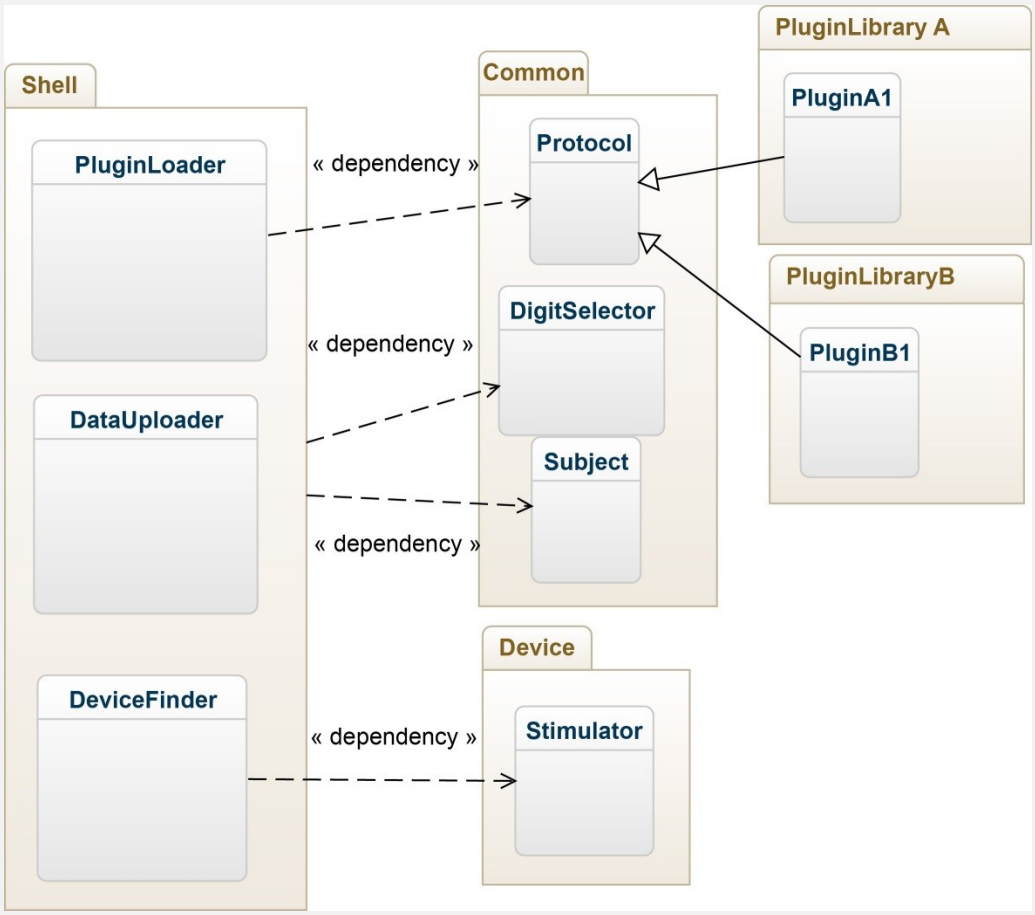

Figure 4.8: Abbreviated Class Diagram of Shell Application

The top software layer is the 'shell' layer. Its primary job is to locate, load, and execute plugins built using the common plugin library. In order to do this, it needs to provide two things to the plugins it executes: an instance of the Stimulator class and an instance of the Subject class. Therefore, it is also responsible for enumerating the attached stimulators and collecting the required information from the user to create a Subject. The shell also includes an interface to create batteries (XML representations of Protocol classes, appendix 4.3) of behavioral protocols with customized starting parameters that are executed sequentially without interference from the experimenter. In a clinical setting, this eliminates possible human error that could be introduced by manually loading each

behavioral task and modifying the appropriate starting parameters on-the-fly. Finally, the shell provides mechanisms for securely uploading collected behavioral data to a centralized database (where it will eventually be analyzed) as well as for automatically updating plugins for remote installations of the software package.

Database

Currently, there are ongoing academic and clinical collaborations in six countries worldwide, who have collectively performed tens of thousands of experimental runs on roughly 3000 participants. As this data began to accrue, storing it in an efficient and easily accessible format became a top priority. Most of the research data had previously been stored and analyzed using traditional tools like Microsoft Excel®. Excel was perfect for analyzing small datasets with an isolated set of conditions, but woefully inadequate for querying and analyzing the amount of data that is currently being collected. A relational database management system (RDBMS) (Codd et al 1970) was selected as the solution to this growing problem.

A RDBMS organizes data into two-dimensional tables with rows and columns. The tables are then mapped to each other through the concept of a 'relation'. In practice, relations are merely sets of rules that are applied to special columns (usually called a 'key' or 'index') within each table that facilitate fast and efficient access to data contained within the related tables. In each table, all rows must be unique. This is enforced through the concept of a 'primary key', which is defined as the minimum collection of columns used to uniquely identify each row. Often, the primary key will be an automatically generated and incremented integer that is Unrelated to the data in the table and only serves to satisfy the primary key requirement of the RDBMS.

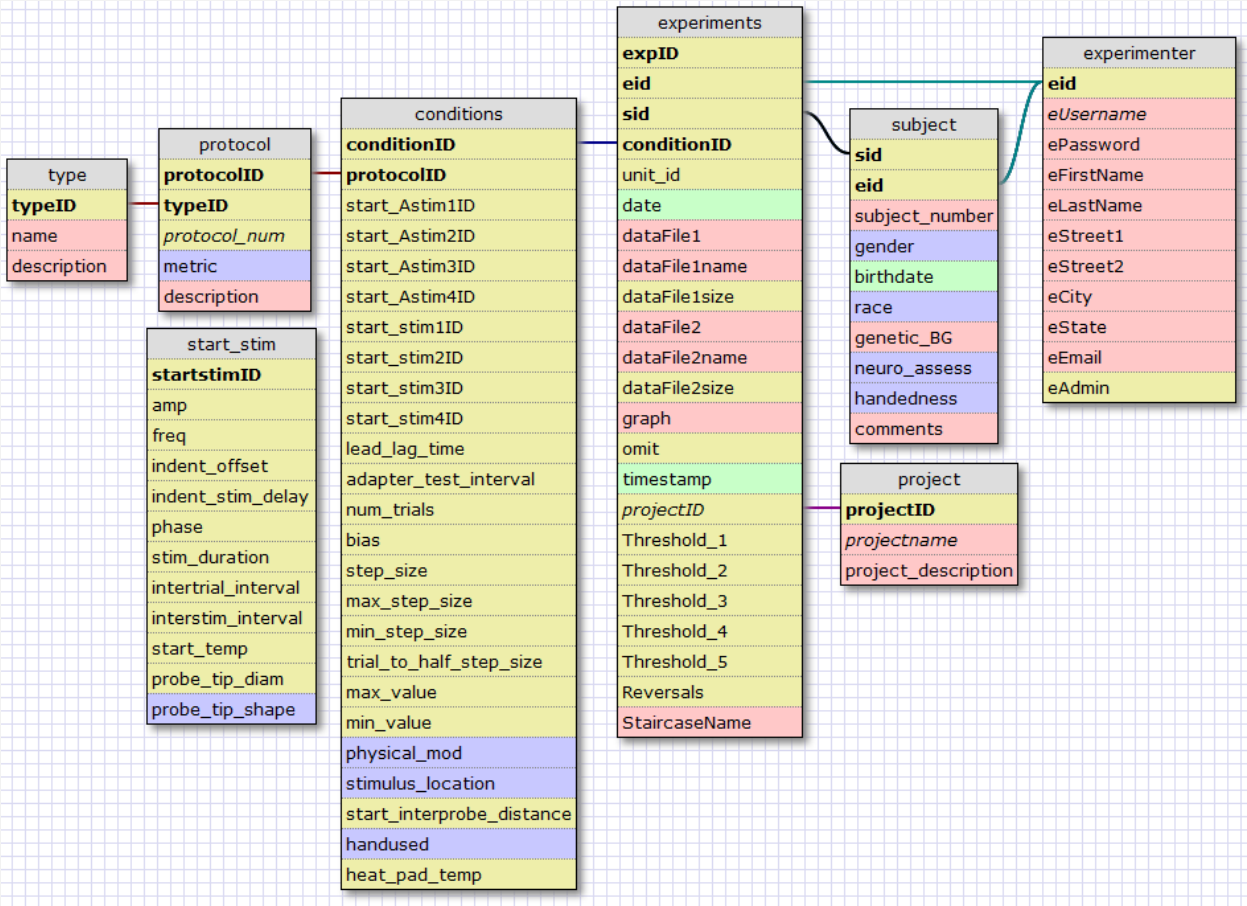

Figure 4.9: SQL Database Diagram for Quantitative Assessments

Accessing data contained in a RDBMS is usually done using some variation of the Structured Query Language (SQL), but this can vary according to the database implementation. The RDBMS implementation chosen to store data collected using the previously described software package was MySQL®. The database itself leveraged a few non-normalized (Codd et al 1971) optimizations to reduce the number of SQL JOIN commands issued for the queries most often executed on this particular database. Namely, in the conditions table, the stimulusID columns are, in practice, foreign keys to the start_stim table, but are not labeled as such in order to avoid creating the extra association table required for a many-to-many relationship.

The database is primarily accessed and queried through a web application hosted on the same server. The web application is powered by the open-source web2py (Di Pierro et

al. 2011) framework. Web2py is a python MVC full-stack web framework that provides mechanisms for handling sessions, authentication, cookies, database access, and of course web requests. Web2py uses a Database Abstraction Layer (DAL) that provides a consistent set of subroutines to interface with many different types of databases, both relational and otherwise. The diagram below explains the flow of data from the shell application, through the web application, into the database, back through the web application, and finally into the user's selected data analysis tool.

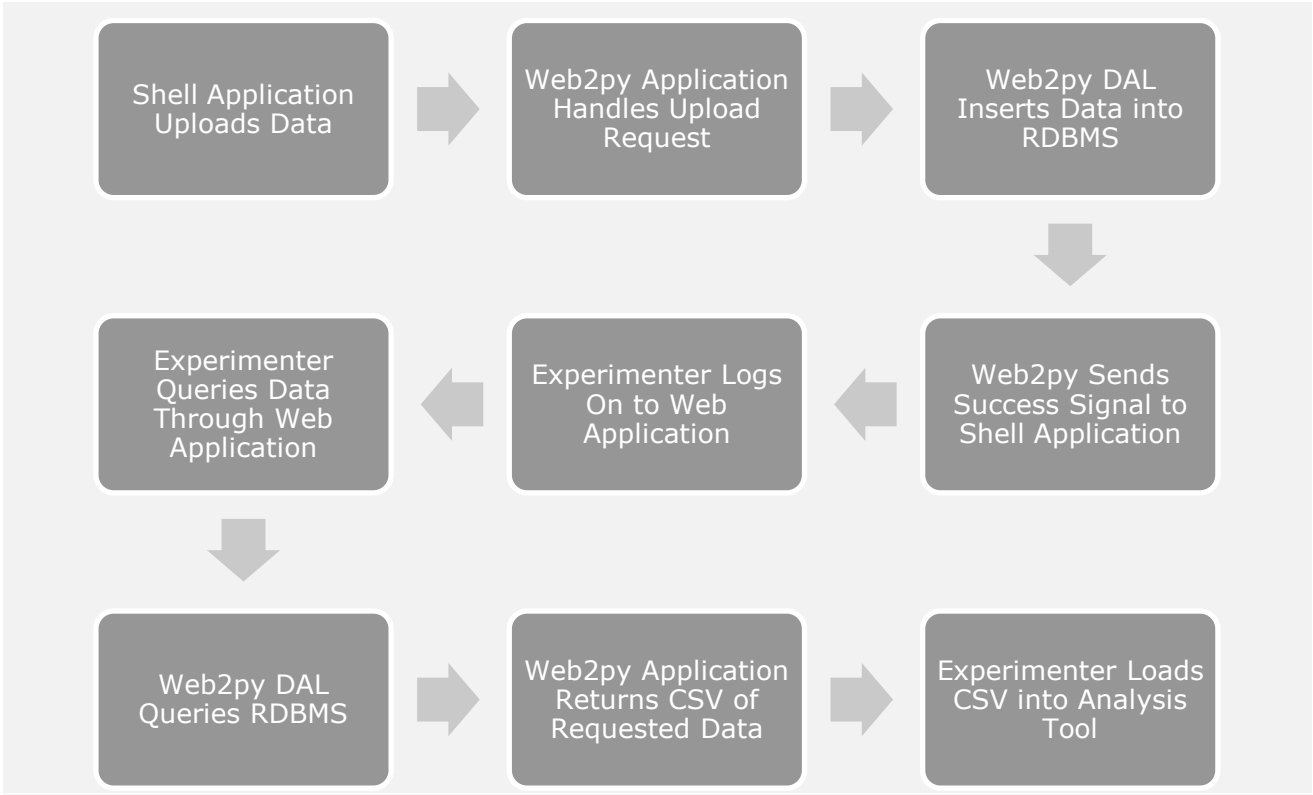

Figure 4.10 Data Flow Diagram

CHAPTER 5: APPLICATIONS

Utilizing the aforementioned software platform to control a CM vibrotactile stimulator, we have developed biologically based metrics for assessing brain health. The platform as a whole is able to non-invasively, quantifiably and inexpensively: 1.) Evaluate general brain health 2.) Detect certain disease states such as concussion, alcoholism, chronic pain, and age related deficits 3.) Measure treatment efficacy in a fraction of the time of traditional approaches, and 4.) Evaluate the efficacy of neurological drugs more quickly and accurately than current methodologies. No other existing system is able to non-invasively obtain quantitative and biologically based metrics about systemic changes in brain health at a resolution that effectively bridges decades of neuroscience research into a clinical environment.

Using Illusions to Quantify CNS Information Processing Capacity

In the Figure 5.1, pictured below, the center circles of each cluster appear to healthy individuals to be different sizes even though they are not. This context-dependent illusion is the result of a number of neural mechanisms being intact. In other words, if there was something wrong with an individual's CNS health, then he/she would not observe the illusion. His or her assessment, via visual percept of these 2 spheres, would be more accurate than that of someone who was not impaired. Thus, this would be a condition in which a CNS-impaired individual could outperform a healthy individual. This phenomenon is embedded in the CM system, which, in part, uses illusions of touch to quantitatively assess the degree to which CNS health impacts an individual's perception.

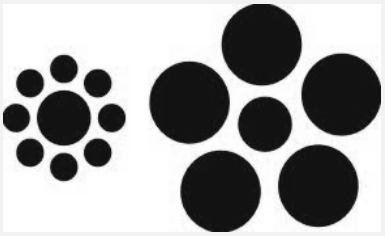

Figure 5.1: Example of Visual Illusion

The somatosensory system is ideally suited for the design of a CNS diagnostic system for a number of reasons. First, the organization of the somatosensory system is such that adjacent skin regions project to specific and unique adjacent cortical regions (i.e., it is somatotopic), and stimuli can be precisely controlled and delivered to these regions. Second, decades of neuroscience research have yielded a great deal of information about the nature of the interactions within and between the adjacent cortical regions that are being activated by tactile stimuli. Third, ambient environmental noise in the system can be easily controlled (i.e., it is less likely that a patient will be exposed to distracting tactile input than auditory or visual input). Fourth, the somatosensory system is the only sensory system that is highly integrated with the pain system, and this is often an important aspect of a patient's profile – particularly if they are suffering from chronic pain.

Percepts of Tactile Stimuli Can Be Measured Quantitatively.

We have developed several tests, made possible by our state-of-the-art tactile stimulator system, that differentiate healthy from impaired individuals by demonstrating that impaired individuals actually outperform healthy controls, making it difficult to cheat the system. This is accomplished by delivering stimuli to adjacent digit tips with the aforementioned portable stimulator and tracking subject responses. This methodology is analogous to a common eye exam. With an eye chart, a subject is queried with progressively more difficult or demanding questions – when the subject can no longer accurately determine what is on the chart, a very accurate assessment of their visual acuity has been obtained.

Impacts of Illusory Conditioning on Sensory Percepts Are Baseline Independent.

One of the biggest problems with using any type of measure – whether it be via modern medical imaging technologies, sensory perceptual metrics or some type of psychosocial questionnaire, is that it requires a baseline measure to be obtained before whatever CNS systemic alteration occurs. Not only is this impractical – the majority of patients seeking health care do not have baseline tests performed – but it is often inaccurate because of neurological shifts that occur naturally with aging, training, and/or experience. Importantly, a measure can be derived that is independent of a baseline shift. For example, consider following hypothetical situation. Healthy subjects are found to have "baseline" vision of 20/20, but when an illusory confound is introduced, they get much worse (20/60). Impaired subjects – whose vision might have gotten worse for a number of reasons (baseline of 20/30) do not get significantly worse with the introduction of an illusory confound. Thus, the critical measure is how much the illusory confound impacts the baseline measure. Several tactile illusory confounds have been developed and found to be sensitive to CNS health. Although all of these tests undoubtedly utilize multiple CNS mechanisms involved in interactions between adjacent and near-adjacent cortical regions, some play a more prominent role than others in each of the tests. This allows for a more powerful multi-parametric approach to be used in the analysis stage of profiling the CNS status of each individual. Each of these sets of tests takes approximately 2-3 minutes to complete.

Sensory Metric Category #1: Neuro-adaptation

Baseline Amplitude Discrimination. Stimuli are delivered to the two fingertips, D2 and D3, of different magnitudes, and the subject is asked which stimulus is larger. Among healthy subjects, this is a fairly robust measure across the age spectrum (Zhang et al, 2011b). However, the perception of which is larger is significantly impacted when the test stimulus is preceded by an illusory conditioning stimulus delivered to one of the two digits before the test (Tannan et al., 2006, 2007a, 2008; Tommerdahl et al., 2007, 2010b; Folger

et al., 2008; Francisco et al., 2011; Zhang et al., 2008, 2009, 2011a, 2011b). For example, stimulating D3 in the image above before performing the test has the effect of making the larger stimulus feel smaller than it really is because the fingertip adapts to the conditioning stimuli. This results in healthy subjects performing worse on the task because it is now more difficult to perceive that the larger stimulus is indeed greater in intensity than the smaller stimulus (compare baseline to confound for healthy controls in Figure 5.3).

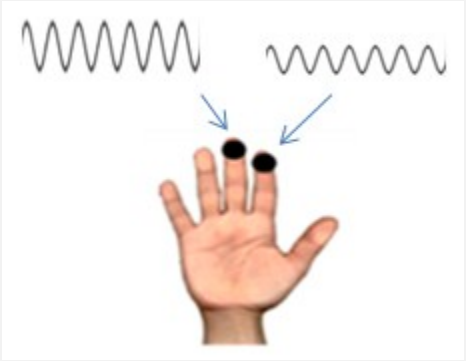

Figure 5.2: Diagram of Amplitude Discrimination

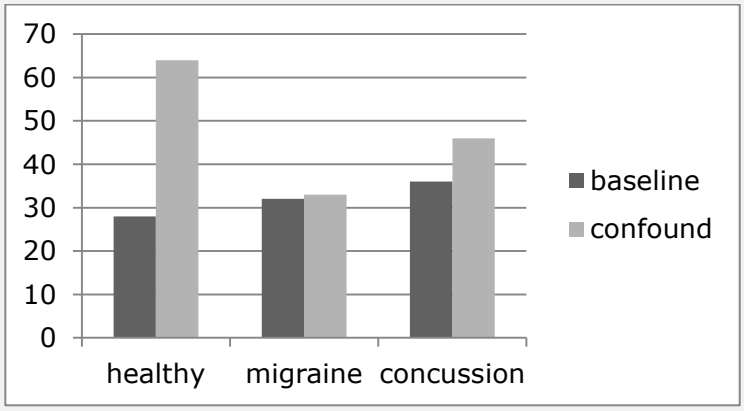

Figure 5.3: Task improvement for impaired populations

This metric is robustly consistent across the age spectrum for healthy controls (Zhang et al, 2011b). The telling metric is the percent difference between the baseline and confound measures, and is referred to as the adaptation metric. Note that in the migraine and concussion subject populations, the baseline metric is slightly elevated, but more significantly, the impact of the confound on the perceptual task is materially reduced. The

larger values for the confound in the healthy controls indicate that those subjects adapted – or habituated – normally, while the other two subject populations did not. This phenomenon is why, for example, someone with a migraine is more annoyed by a loud noise or bright light than a healthy patient—their brain cannot habituate normally.

Neuro-adaptation. Repetitive stimulation, such as occurs with the conditioning stimulus described above, normally results in an overall decrease in cortical response. In Figure 5.4, extracellular recordings are plotted in spikes/second (how frequently neurons fired) in response to a 25Hz sinusoidal mechanical stimulus that is delivered to the skin for 3 seconds. Note that initially, the response is on the order of 60-75 spikes/second, but as the stimulus continues, the response rate of the neurons decreases – down to approximately 25 spikes/second (Whitsel et al, 2002).

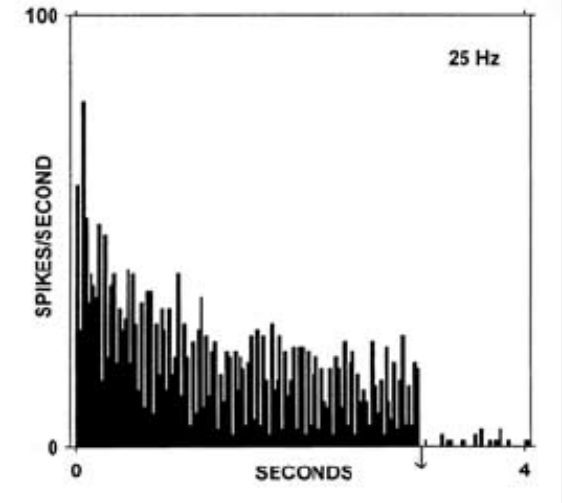

Figure 5.4: Extracellular response for 3s stimulation

Whenever there is a systemic cortical alteration, such as might occur with a neurological deficit, it usually results in an imbalance in excitation and inhibition, and the individual will not adapt normally. For this reason, they adapt less, and then outperform healthy controls because the conditioning stimulus does not alter their perception: thus, they perform better on a relative basis at the amplitude discrimination task post-illusory

conditioning. A number of studies have been performed to examine changes in responsivity of SI cortex to altered excitation. One early example is demonstrated in the figure at the left (from our early work – see Juliano et al, 1989). Note the difference in the extracellularly recorded response in the pre-drug (left side) vs. the post-drug (right side) topical application of a very small amount of a GABA agonist, which produces hyper-excitability to stimulation. The solid white bar at the top of the figure indicates when a tactile stimulus was applied to the central pad of the cat's forepaw. Increasing the excitation level of the cortex leads to less of a decrease in responsivity to repetitive stimulation (for review of dynamics involved, see Tommerdahl et al, 2010a) and will lead to changes in adaptation (for recent discussions, see Tommerdahl et al, 2010b; Zhang et al, 2011a).

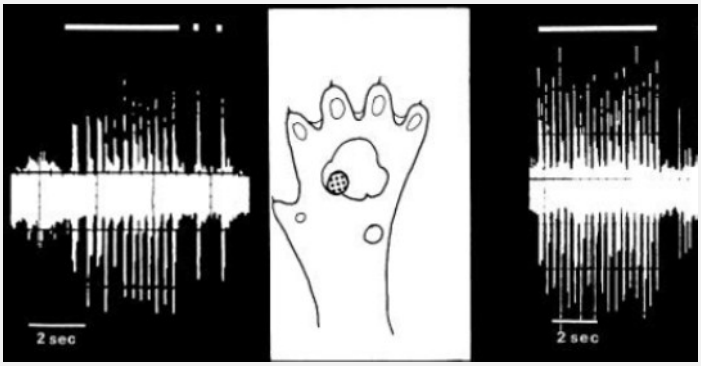

Figure 5.5: Pre/Post application of topical GABA agonist

Adaptation metrics will quantitatively assess the degree to which an individual's CNS is impacted by their condition, and the more that an individual is impacted by the neurological alteration, the less that performance will be impacted by adaptation. A degradation in performance will not be observed in healthy individuals.

Sensory Metric Category #2: Functional Connectivity

Temporal Order Judgement. Determination of which stimulus came first, as depicted at the left, describes an individual's temporal order judgment (TOJ) capacity. Typically,

healthy individuals have a TOJ capacity on the order of 30-40 msec. However, in the presence of an illusory conditioning stimulus, healthy controls perform significantly worse (Tommerdahl et al, 2007b).

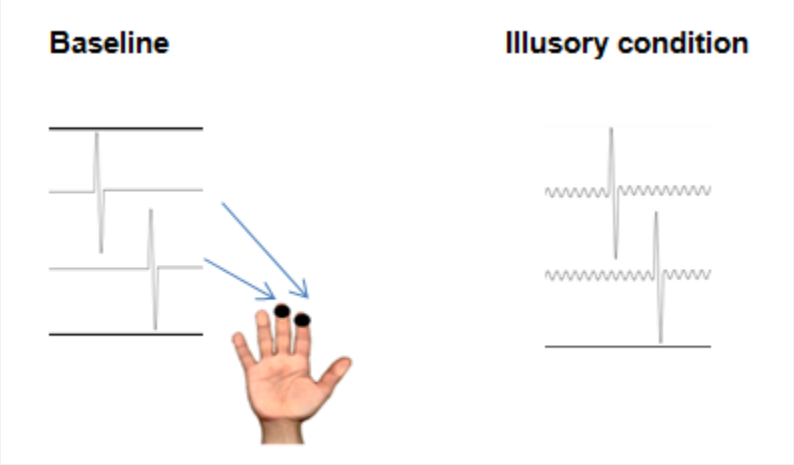

Figure 5.6: Diagram of Temporal Order Judgement Task

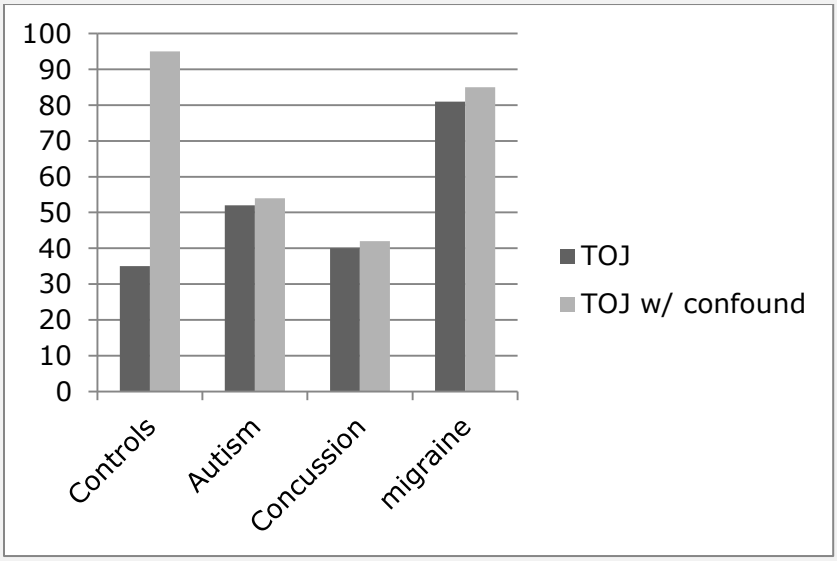

Figure 5.7: TOJ performance in impaired populations

Note that in each of the non-control subject populations in the graph above, individuals perform approximately the same in the presence of the confound (see Tommerdahl et al, 2007b and 2008 for more complete description). Functional connectivity

between adjacent cortical regions normally leads to a reduction in TOJ performance in healthy controls with the introduction of the confound, but not in CNS impaired individuals.

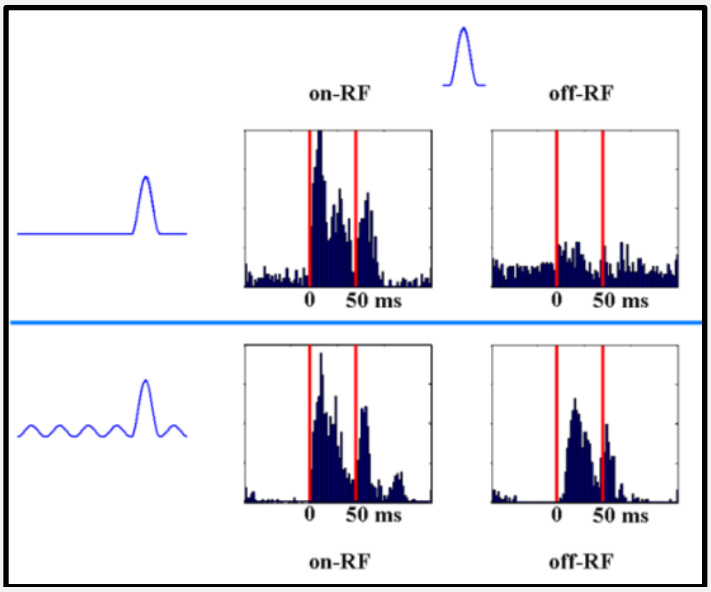

Figure 5.8: Synchronization via sub-threshold stimuli

Functional Connectivity. Consider the results displayed above. Extracellular recordings were obtained from SI cortical regions corresponding to D2 and D3 in a squirrel monkey. The figure at the top indicates relative positions (on-RF vs off-RF) of electrodes in somatosensory cortex (SI). When a vibrotactile pulse was delivered at D2 (note stimuli pictured at left), a significant above-background response was evoked at D2 (top left quadrant) but not at D3 (top right quadrant). When sub-threshold synchronized sinusoidal stimuli were delivered to both digits prior to the pulse (bottom half of figure), the pulse at D2 evokes a response in SI cortex at both the D2 and D3 representation. From this type of data, we hypothesized that this response was the result of functional connectivity between adjacent and/or near adjacent cortical ensembles, and that delivery of synchronized conditioning stimuli would impact the topography of temporal perception, unless there was a neurological deficit. Thus, this impact on temporal perception by illusory conditioning makes healthy brains perform worse at the TOJ task.

The degree to which a subject is impaired will be negatively correlated to the degree with which TOJ is impacted by the illusory confound. Individuals who are not impaired will perform worse at the TOJ task in the presence of the confound. Individuals without a neurological impairment will not be able to perform as well as on the confounded task as on the simple TOJ task.

Sensory Metric Category #3: Duration-Intensity Interactions.

Duration Discrimination. Typically, healthy individuals can accurately discern which of two stimuli last longer (delivered sequentially) when there is approximately a 10% difference (e.g., 500 vs. 550 msec). However, when the intensity of the shorter stimulus duration is increased, an illusion that the stimulus is longer is created, and duration discrimination capacity degrades (this is proportional to the increase in intensity; Francisco et al, 2012). Note that in the graph below, the difference limen (DL) gets worse with the introduction of the intensity confound for healthy controls. However, concussed and migraine subjects do not get worse with the introduction of the intensity confound.

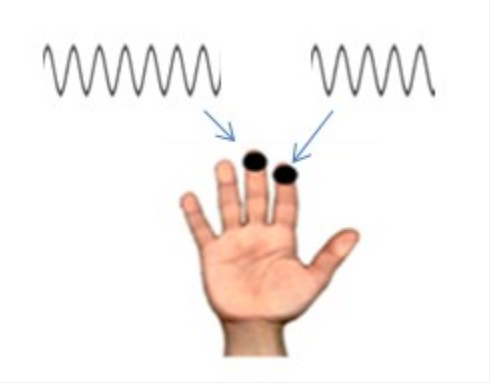

Figure 5.9: Diagram of Duration Discrimination

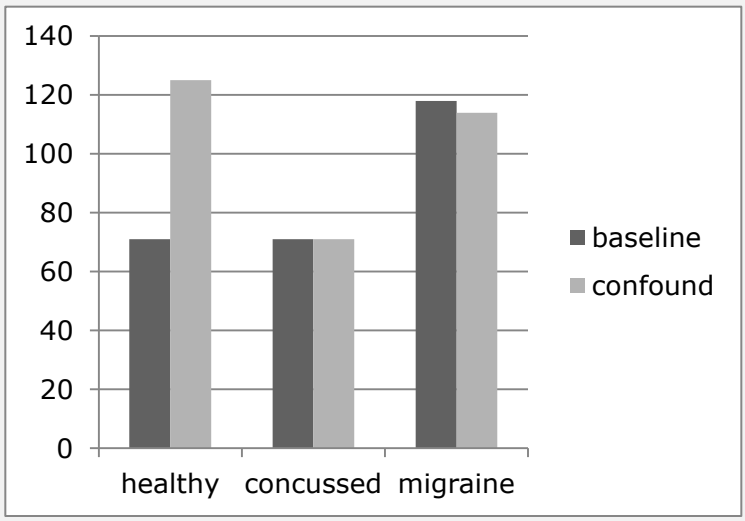

Figure 5.10: Duration Discrimination in impaired populations

Duration Intensity Interactions. We conducted several series of experiments in non-human primates using high resolution optical imaging methods (Simons et al, 2005, 2007). Observations from those experiments demonstrate that increasing the stimulus amplitude results in an increasing duration of the optical response (see figure to left); note the different durations of response for different magnitudes of stimulation).

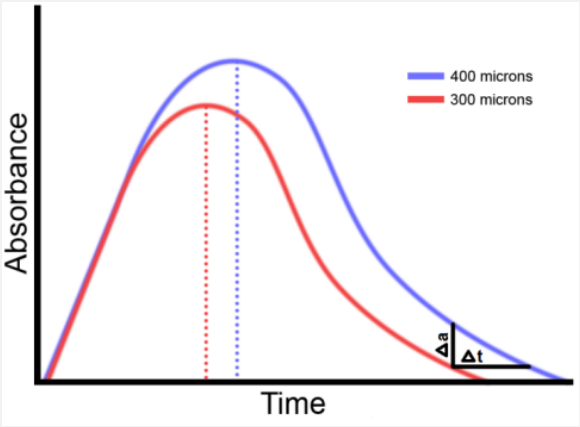

Figure 5.11: Effects of Amplitude modulation on OIS time-course.

Additional experiments examining the source of the optical signal (Lee et al, 2005) led us to hypothesize that if neuron-glial interactions were significantly impacted, such as they would be with neuro-inflammation, the response duration of the optical signal would

not be different with an increase in amplitude. Thus, we hypothesized that neuro-inflammation would lead to a reduction in the impact of the intensity confound on an individual's duration discrimination capacity.

The impact that an intensity confound has on duration discrimination capacity will be reduced with an increase in neurological impairment. Thus, subjects without impairment will not be able to outperform their baseline test.

Sensory Metric Category #4: Feed Forward Inhibition.

Stimulus Detection Threshold. The purpose of this metric is to determine the minimum stimulus that an individual can detect. This is accomplished by asking the subject to compare two stimuli – with one of them being zero – and tracking to their "static" detection threshold value. "Static" means that the stimulus (the larger one pictured to the left) does not change size during a test trial. The perceptual task that utilizes the illusory confound implements a "dynamic" or modulated stimulus. It starts out at a null value and increases in amplitude at a pre-determined rate (figurine at right). Even though the stimulus is not initially perceived by the subject, it has the effect of raising the subject's threshold. In other words, sub-threshold, or non-detectable, stimuli have an effect on perception, and the cortex tends to ignore the stimulus until it is much larger.

Dynamic thresholds have been demonstrated to be significantly elevated in healthy controls across the age spectrum (Zhang et al, 2011b). The significance of this is that although static threshold changes with age (due to skin physiology), the ratio between the two measures remains relatively constant. However, individuals with various types of CNS impairments (e.g. vulvodynia) demonstrate a reduction in that ratio, even though static thresholds remain the same (Tommerdahl et al, 2010; Zhang et al, 2011a). Thus, these impaired individuals outperform healthy controls in terms of ratio of dynamic to static thresholds. The graphs below summarize the results that we have obtained from several such populations.

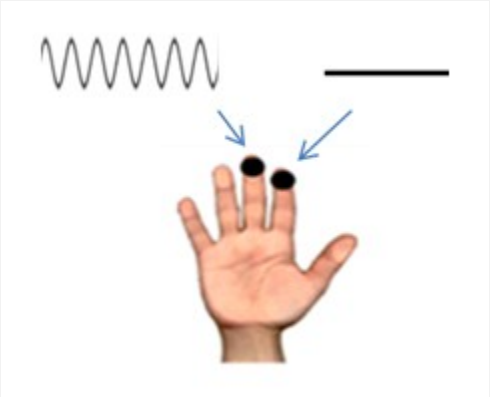

Figure 5.12: Diagram of Detection Threshold

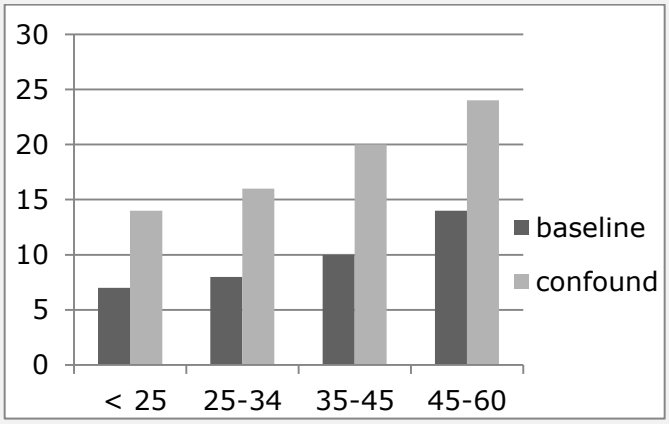

Figure 5.13: Static vs Dynamic Detection Thresholds across age groups

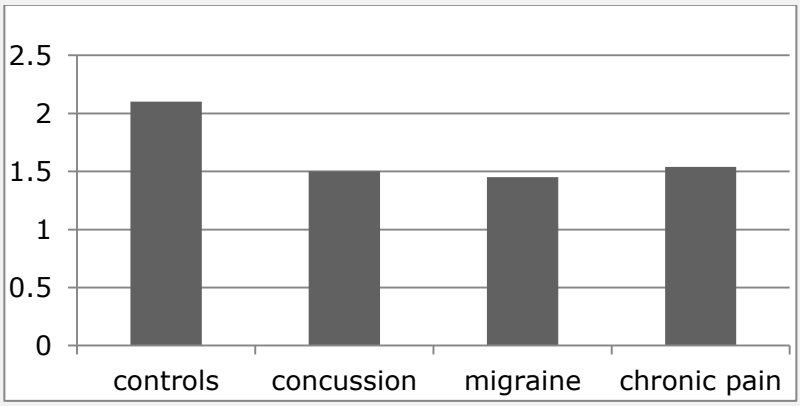

Figure 5.14: Static vs Dynamic Ratio in impaired populations

Feed Forward Inhibition. The role of sub-threshold stimulus-evoked inhibition – feed-forward inhibition and the role of within-column connectivity. A major well-documented feature of cortical functional organization is the presence of prominent feed-forward

inhibition in the input layer 4, in which local layer 4 inhibitory cells receive direct thalamocortical input and in turn suppress responses of neighboring layer 4 excitatory cells to their thalamocortical drive, thereby sharpening their RF properties (e.g., Douglas et al. 1995; Miller et al. 2001; Bruno and Simons 2002; Alonso and Swadlow 2005; Sun et al. 2006; Cruikshank et al. 2007). These inhibitory cells are more responsive to weak (near-threshold) afferent drive than are the excitatory layer 4 cells, and thus, sub-threshold or weak stimulus inputs will have the effect of raising the threshold at which excitatory layer 4 cells begin to respond to peripheral stimuli. In terms of sensory testing, this means that utilization of two different types of threshold tests – one with and one without subthreshold stimulus conditioning – should yield very different outcomes.

Deficiencies in the underlying mechanisms that support feed forward inhibition will result in significant reductions in the differences observed between static and dynamic thresholds of neurologically impaired subjects.

Enhancing Sensory Performance to Derive Measures of CNS Performance.

It has long been established that there are numerous conditions that will enhance performance on sensory perceptual tasks (for review, see Tommerdahl et al, 2010a). Just as specific illusory conditioning stimuli can be used to make performance worse for healthy individuals, but not for impaired individuals, some types of conditioning can enhance performance on a sensory task. This would be somewhat analogous to having someone read an eye chart before and after putting on the correct pair of eye-glasses.

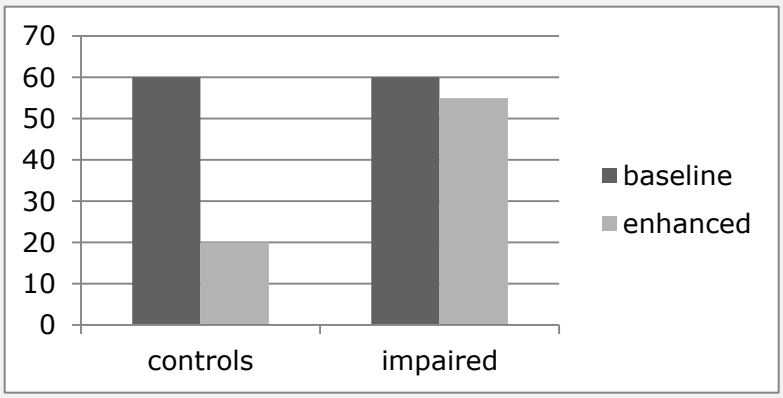

Figure 5.15: Applications Can Also Enhance Healthy Performance

The graph above summarizes this concept, which has been demonstrated in a number of studies (Tannan et al, 2005a, 2005b, 2006; Tommerdahl et al, 2005, 2006, 2010a, 2010b; Zhang et al, 2008, 2009; 2011a; Francisco et al, 2011, 2012). The key metric with this type of paired test would be the improvement in performance between the baseline and enhanced condition. For example, adaptation metrics – previously described as being derived from the use of an illusory conditioning stimulus – can be derived by obtaining measures reflecting the improvement in performance in certain tasks. Optimization of performance can be achieved with optimal conditions for a number of hypothesis driven tests, such as were described above for the illusory conditioning stimuli in Part I, and this parametric approach has been used to demonstrate heterogeneity across the autism spectrum (Francisco et al, 2011, 2012).

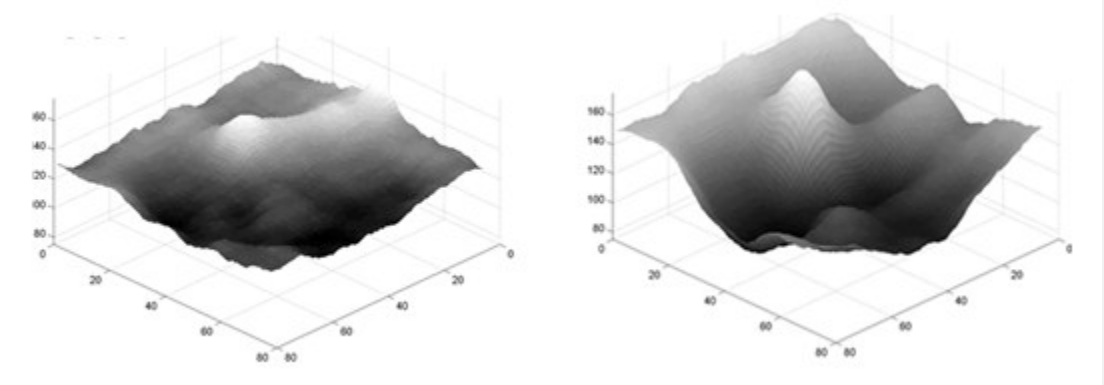

Figure 5.16: Cortical Contrast Enhancement Aids Perceptual Differentiation

With specific times of stimulation, particularly those that are repetitive, contrast enhancement is improved in the cortex and differentiation of sensory percepts is enabled. The two plots below were obtained from observations of somatosensory cortex (via optical imaging) and demonstrate that with time, the response becomes much more distinct (for full description and discussion, see Tommerdahl et al, 2002, 2010a). This improvement in contrast has been demonstrated to rely on both GABAergic and NMDA receptor mediated mechanisms, (Tommerdahl et al, 2010), and thus would be sensitive to changes in the status of those mechanisms, which play key roles in many neurological deficits/disorders.

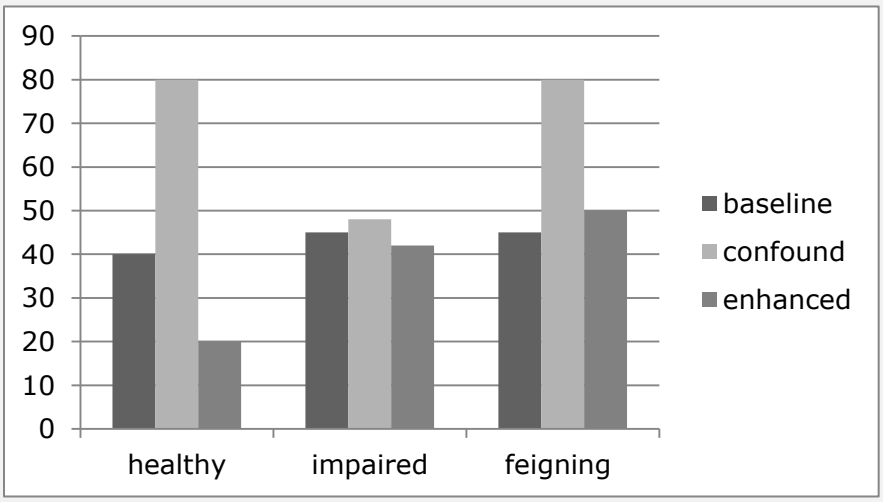

Figure 5.17: Cortical Metrics are Make it Difficult to Feign Impairment

Why bother with non-illusory conditioning tests? First, there are many such tests that have been performed on many different neurologically impaired subjects, both by our group and by others, and this foundation of research greatly facilitates interpretation of data. Second, these measures provide a baseline for subjects who may attempt to feign impairment. For example, we often obtain two metrics of adaptation from a subject – one with an illusory conditioning stimulus, and one with a non-illusory conditioning stimulus, and the metrics correlate extremely well. If a subject attempts to feign impairment, they will do poorly on the non-illusory test, but they will not outperform healthy controls on the illusory condition. The graph above summarizes this discrepancy in subject profiles.

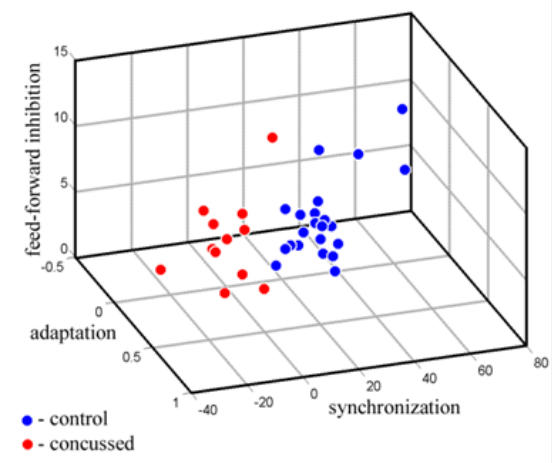

Figure 5.18: 3D Plot Demonstrating Separation Between Control and Impaired Populations

Analysis and Application

Just as a clinician would not base a full diagnosis of a patient by how they respond to only one question, we query subjects with multiple tests. A typical battery lasts 20-30 minutes, and this yields between 5 and 8 parameters (i.e., answers to different questions) that can be used to build a profile of a patient or subject. A 3-dimensional plot of two subject populations (controls vs. concussed) demonstrates how these populations can be differentiated. However, to fully appreciate the differences between subject populations, we utilize mathematical approaches that allow for the utility of more than 3 parameters. The

plot below was generated via PCA analysis with 5 parameters and differentiates concussed (orange) vs. non-concussed individuals with a 95% confidence level (via Hotelling's t-square statistic). With optimization of protocols and better parameter selection, we expect this to get much more precise.

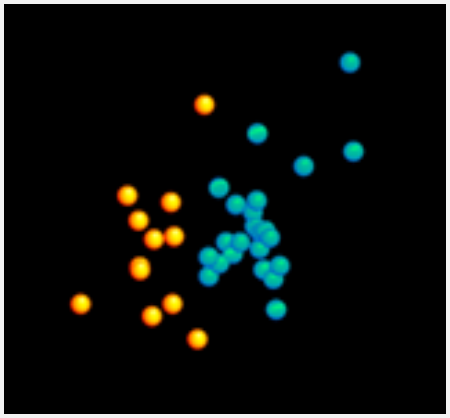

Figure 5.19: PCA Plot with 5 Paramters Differentiates Subject Populations

SVM (support vector machine; a machine learning algorithm) can be trained via clinical assessments to identify the markers that are most sensitive to different neurological categories as well as the sub-categories that might emerge. SVM utilizes all parameters in addition to clinical diagnostics to learn where segregation of data and/or categorization of groups occur. Data mining of the generated database will be utilized to optimize parameters for determination of degree of neurological impairment.

CHAPTER 6: FUTURE DIRECTIONS

Reduce Reliance on 3rd Party Data Acquisition

One of the biggest challenges we have faced since the initial publication of the CM4 vibrotactile stimulator was due to its reliance on the National Instruments DAQ board. When the CM4 was being designed, there were few commercial options available that met the standards necessary for the first prototype. The most important feature was a USB connection. Most traditional DAQ boards are integrated directly into a desktop PC through a PCI expansion slot, thus making them essentially unusable in a portable environment. At the time, there were other options for USB DAQ systems, but none of them provided four independent but synchronizable output (DAC) channels with the necessary precision (both ADC and DAC) to ensure +/- 1 micron accuracy. The USB-6259 far exceeded all of these requisites, but came at a cost. The DAQ portion was contributing almost 50% to the final materials cost of each stimulator. For the initial prototype, however, it was not worth the time investment required to create and test a custom DAQ solution.

After moving beyond the prototypal stage, the drawbacks of being tied to an expensive and vastly overpowered DAQ system started to outweigh the research time investment necessary to replace it. A complete redesign of the CM4 electronics took place. We decided to embed a generic 32-bit microprocessor (PIC32MX family) that would handle USB communication to the PC-based GUI as well as communication with discrete 16-bit ADC and DAC integrated circuits (ICs). Communication between the ADC, DAC and PIC32 was accomplished through the high-speed serial-peripheral interface (SPI) at rates up 40MHz. Simultaneously, the analog position control circuitry was eliminated and replaced by a digital PID algorithm. In addition to these changes, a custom H-bridge driving amplifier was designed to replace the high-cost solution in place in the CM4. Accomplishing this allowed

us to then replace the expensive dual-sided power supply that powered all of the analog amplifiers. The total cost of materials for the new stimulator, the CM5, was reduced by 96%. This is even more noteworthy considering that the CM4 was already an order of magnitude cheaper to produce than competing vibrotactile stimulators that are not even close to being portable. This cost reduction is crucial for clinical applications of cortical metrics.

The past six months has been a period of rapid development for the entire CM ecosystem. All new hardware has been prototyped while the previous version is maintained for distribution to our collaborators. This has led us to implement a more controlled development pipeline. Most of the new hardware research and development is focused on expanding the demonstrative capabilities. This is almost entirely an engineering task at this point, as the basic science has already started to be replicated and validated by researchers in six countries across the globe. At the same time, we are supporting and maintaining legacy systems for our ongoing clinical collaborations. We simply do not have the resources available to build and distribute CM devices to meet the demand. Streamlining the hardware development pipeline will be the first step to continued success over the next 6-12 months.

Hardware-wise we have transitioned from a Microchip PIC32 microcontroller to an ARM based STM32F4 microcontroller. This transition gave us a boost to several key aspects of future development. First, the raw computational power of the STM32F4 is significantly higher than that of the PIC32. This frees up more clock cycles to allow for implementation of additional sensors, such as for monitoring heart rate. Additional speed improvements are provided by the STM32's hardware digital signal processor (DSP) and floating-point unit (FPU). Currently, the implementation of the discrete position control algorithm on the PIC32 requires several dozen CPU cycles. This same algorithm leverages the hardware DSP of the STM32, reducing the number of required cycles by nearly 75%. Another advantage of the STM32 is its integrated 12-bit analog to digital converter (ADC), capable of 2.4 million

samples per second. This allows enough accuracy for a consumer level CM device to be developed without the need for an external high-precision ADC. Finally, the new hardware will hopefully address the long-term reliability issues we have experienced with previous revisions of the CM device. Research tools are notoriously fragile, so increasing the ruggedness of the device will be essential when moving to a primarily clinical environment.

The software development has at the very least kept pace with the hardware. A key component to future success of the CM platform is the generation of a comprehensive ontological database of sensory assessment data. A large database will allow for improved analysis techniques leveraging advanced mathematical models (e.g. principal component analysis (PCA)) for more effective differential diagnostic power. These mathematical tools can in turn accelerate the optimization of our assessment protocols, hopefully leading to shorter testing times that are thus less susceptible to problems like subject fatigue. The most recent revision of the software interface is the first step in that direction. Switching to an open-source web based software model allows for synchronization of client software with a secure online database and simultaneously streamlines the entire collaborative process for both researchers and clinicians. Also, the transition of programming languages from C# to Javascript provides a larger portion of the general public with a way to enhance the CM platform through 3rd party addons.

Therapeutic Potential

Up until now, we have primarily focused on using the vibrotactile capabilities of the CM system (hardware and software together) as a diagnostic tool for neurological disorders. Our overarching mission is to improve the standard of care for patients with neurological disorders, so facilitating a differential diagnosis of these disorders is only one half of the puzzle. One possible future direction that we could take would be to explore the capacity for vibrotactile stimulation to be used as a therapeutic treatment. Given the well documented existence of a perceptual relationship between innocuous touch and pain pathways (e.g. touch-gating of pain (Apkarian 1994), vibrotactile analgesia (Wall 1960)) as

well as experimental evidence that at least some portion of this interaction, at least for chronic pain, takes place in the primary somatosensory cortex (SI) (Vierck 2012), it seems likely that vibrotactile stimulation could be used therapeutically to treat certain types of pain.

Our understanding of the neural encoding of pain signals in both the peripheral and subcortical central nervous systems exceeds our understanding of how this information is processed cortically. Several studies by Willis et al circa 1978 demonstrated that dorsal horn neurons with thalamic projections maintain or combine response characteristics of various classes of peripheral nociceptors. They also demonstrated that the response of SI neurons was sufficiently similar to those in the dorsal horn and thus suggested that SI merely preserves a painful response, but does not transform it. At first glance, this would suggest that if mechanisms such as innocuous touch modified our perception of pain, it would have to be done either at the peripheral level, or in higher-order processing cortical levels receiving pain signals from SI. It has since been shown that experimental conditions play a significant role in the response of SI simultaneous nociceptive and vibratory inputs (Vierck 2012). One such condition was noted to be the level of anesthesia. Studies that have shown little variation in SI and dorsal horn responses to nociceptive inputs have relied on deep sedation techniques that have also been shown to both reduce and fundamentally alter neuronal responses (Favorov 1987). Vierck and colleagues went on to show that long lasting nociceptive input shifts the cortical response from the more posterior areas 3b and 1 to the anterior 3a. This suggests that chronic pain signals could be functionally

transformed in the primary somatosensory cortex and are therefore susceptible to cortical modifications known to target SI. While a CM device could be easily modified into a system capable of treating forms of minor to moderate acute pain by exploiting the aforementioned 'touch-gate', this type of pain is easily treatable pharmacologically with few noticeable side effects, so it would probably not be worth pursuing for possible clinical applications.

The form of chronic pain for which a vibrotactile system would have the greatest chance of being used as a successful beneficial therapy would be carpal tunnel syndrome. Carpal tunnel syndrome (CTS) is a form of neuropathy characterized by paresthesias and pain in digits 1, 2 and 3. These digits are all innervated by the median nerve and repetitive and long term compression of the median nerve is thought to be the underlying cause of CTS. Recently, a cortical complication of CTS was observed by Napadow and colleagues in 2006. Using Functional magnetic resonance imaging (fMRI), they found that the cortical distance between areas of SI somatotopically mapped to the affected digits was significantly less than that of healthy controls. This shift was concluded to be consistent with Hebian plasticity due to the correlated changes in median nerve afferent drive associated with paresthesias.

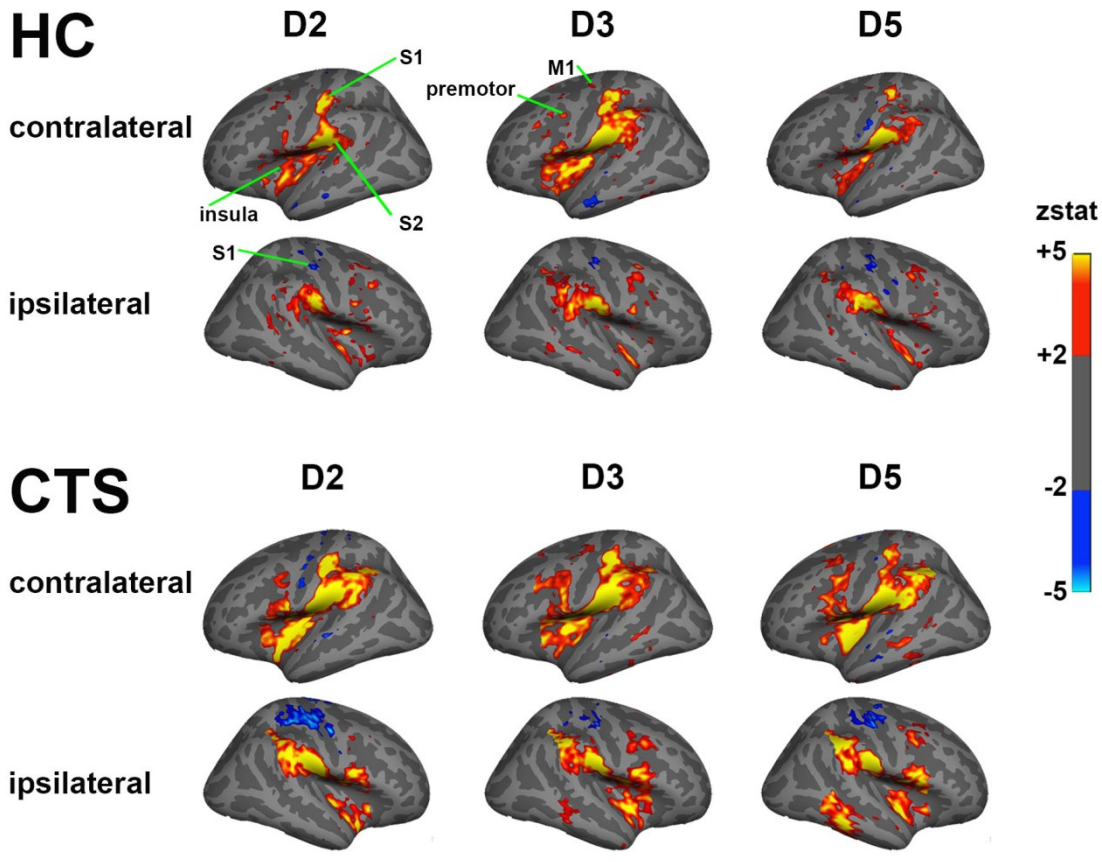

Figure 6.1: Functional MRI Activation in Patients with CTS

Traditionally, CTS is treated either with short term injections of corticosteroids or via surgery to sever the carpal ligament and thus widen the carpal tunnel, both of which have obvious negative side effects. Napadow et al explored acupuncture (effectively a long term conditioning stimulus) as a possible alternative treatment for CTS based on their earlier findings of altered cortical organization. They published in 2007 that they were able to use acupuncture induced plasticity to laterally shift the cortical representation of D2 (thereby increasing cortical separation between D2/D3). This shift was also significantly correlated to a reduction in paresthesias. Based on these, I believe the same results could be accomplished using a vibrotactile stimulator. I would also anticipate that passive vibrotactile protocols could be developed that would be even more effective in inducing cortical plasticity due to the ability of the CM device to easily and continually produce novel stimuli.

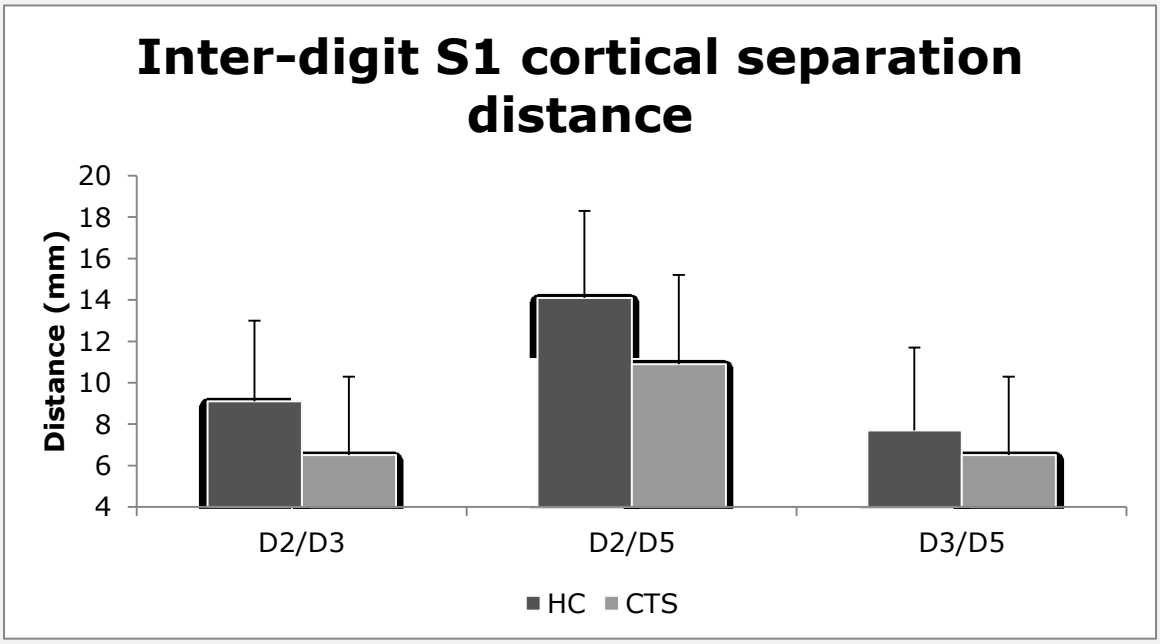

Figure 6.2: Cortical Digit Separation in SI for Patients with CTS

Outside of the realm of pain, the CM system as a whole could be used to provide therapeutic biofeedback to a wide range of neurologically impaired populations. There are

many complex sensory tasks that invoke higher-order cortical processing that could be developed to improve brain functions such as working memory (WM). We have already developed a form of the 'Simple Simon' game that can measure working memory. Using this task as a WM training exercise would just be a matter of repetition, and improvements in WM resulting from repetitive training has been shown to translate to other tasks (Klingberg 2010), thus demonstrating an improvement in brain function. Additionally and more interestingly, we are currently integrating extra biological sensors to measure things such as heart rate during our behavioral protocols. Since heart rate has been shown to correlate with stress, this information could be utilized in the creation of new tasks to promote stress reduction therapies. We have also just recently demonstrated a sensorimotor feedback protocol leveraging the raw power of the CM device's voice coil actuators (VCAs). The task requires the subject to deliver a fixed amount of force to the probe tips simultaneously. We provide a graphical interface with a couple of vertical progress bars to display the amount of force currently being exerted on the probes. We can then set a target position on these progress bars and measure how effectively a subject can control his/her gripping force. This type of protocol could be used in rehabilitation programs for many types of injuries that result in degradation of fine motor control.

Possibilities for Use with Large Non-Primate Mammals

A large portion of the fundamental biological basis for the aforementioned portable CNS diagnostic platform comes from in-vivo electrophysiological recordings and cortical optical imaging in non-human primates, specifically squirrel monkeys. Non-human primates were a natural first choice for correlating the results of invasive cortical observations due to their genetic similarities with humans. Primate research however has become more expensive and more restrictive in the U.S. in recent years, allowing for the exploration into non-primate animal models. An advantage of a large non-primate mammal model with a physiology similar to that of humans lies in the realm of trauma. CNS impairments, such as traumatic brain injury (TBI) from high force trauma, are best explored on mammals with a

mass and tissue density more similar to humans than small primates. A porcine TBI model has been gaining traction in the scientific community in the past several decades, so adapting the diagnostic platform to allow for correlation to these models could provide significant advancements in treatment methodology.

Optimal Location for Stimulation

Porcine models have become more popular in the past several decades primarily due to their biology being more similar to that of humans than more traditional mammal models such as rats or cats. The body surface areas of pigs and humans are more similar than other animal models, and some of their vascular structures are similar enough to be transplanted into humans (Swindle 2008).

Somatosensation relies on input from receptors in the skin, so the first design consideration would be to figure out how similar the dermis/epidermis of a pig is to that of a human. Luckily, that has already been done, and the porcine model has been popular in the field of dermatology for many years now (Swindle 2008). One thing to note here is that skin thickness does depend on the breed of the pig, so most dermatological studies have focused on miniature pigs of the Yucatan, Sinclair, and Hanford breeds. Humans have an average epidermal thickness ranging from 50-120um (Sauleau 2009), while mature Yucatan pigs average 40-100um depending on the location. The dorsum of the neck and back are thickest on pigs, so transmitting vibrations to receptors in the dermal layer could prove more difficult in those locations.

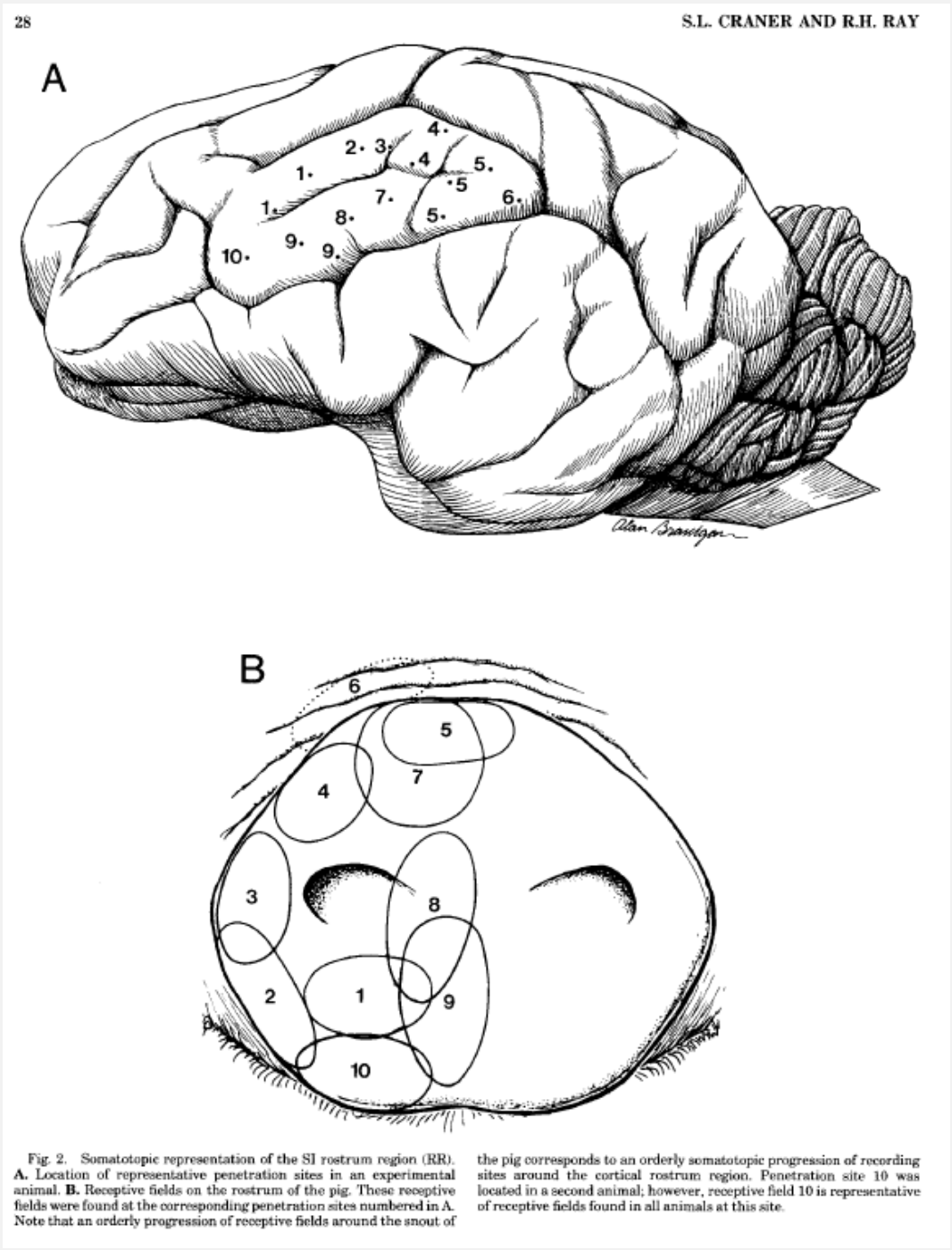

Fig. 2. Somatotopic representation of the SI rostrum region (RR). **A.** Location of representative penetration sites in an experimental animal. **B.** Receptive fields on the rostrum of the pig. These receptive fields were found at the corresponding penetration sites numbered in A. Note that an orderly progression of receptive fields around the snout of the pig corresponds to an orderly somatotopic progression of recording sites around the cortical rostrum region. Penetration site 10 was located in a second animal; however, receptive field 10 is representative of receptive fields found in all animals at this site.

Figure 6.3: Porcine Rostral Receptive Field Mapping

Since the porcine periphery is similar enough to that of a human, the next step is to factor in cortical representations of each possible mounting location. The primary somatosensory cortex of the neonatal pig was mapped using electrophysiological recordings

by Craner and Ray in 1991 (Craner et al 1991, Figure 6.4). Somatotopy was found as expected, with the largest area of SI being devoted to the rostrum (snout). This makes sense since the snout is the pig's primary tool for exploring its environment, much like hands for humans. Thus, from a cortical standpoint, the snout would be the best location for delivering controlled somatosensory input.

One of the most important nuances of our somatosensory testing in humans is the reliance on an orderly cortical organization for generating interactions between adjacent cortical regions. In the healthy human somatosensory cortex, regions somatotopically mapped to the fingertips are lined up with essentially no overlap between digits 2, 3 and 4. Digit 5 does have some overlap with digit 4 though, which makes performing independent motor tasks with those fingers difficult for most people, and also leads to performance reductions in sensory discrimination tasks using those digits. If we are to replicate our findings in pigs, we'll need a solution that can effectively stimulate adjacent cortical areas.

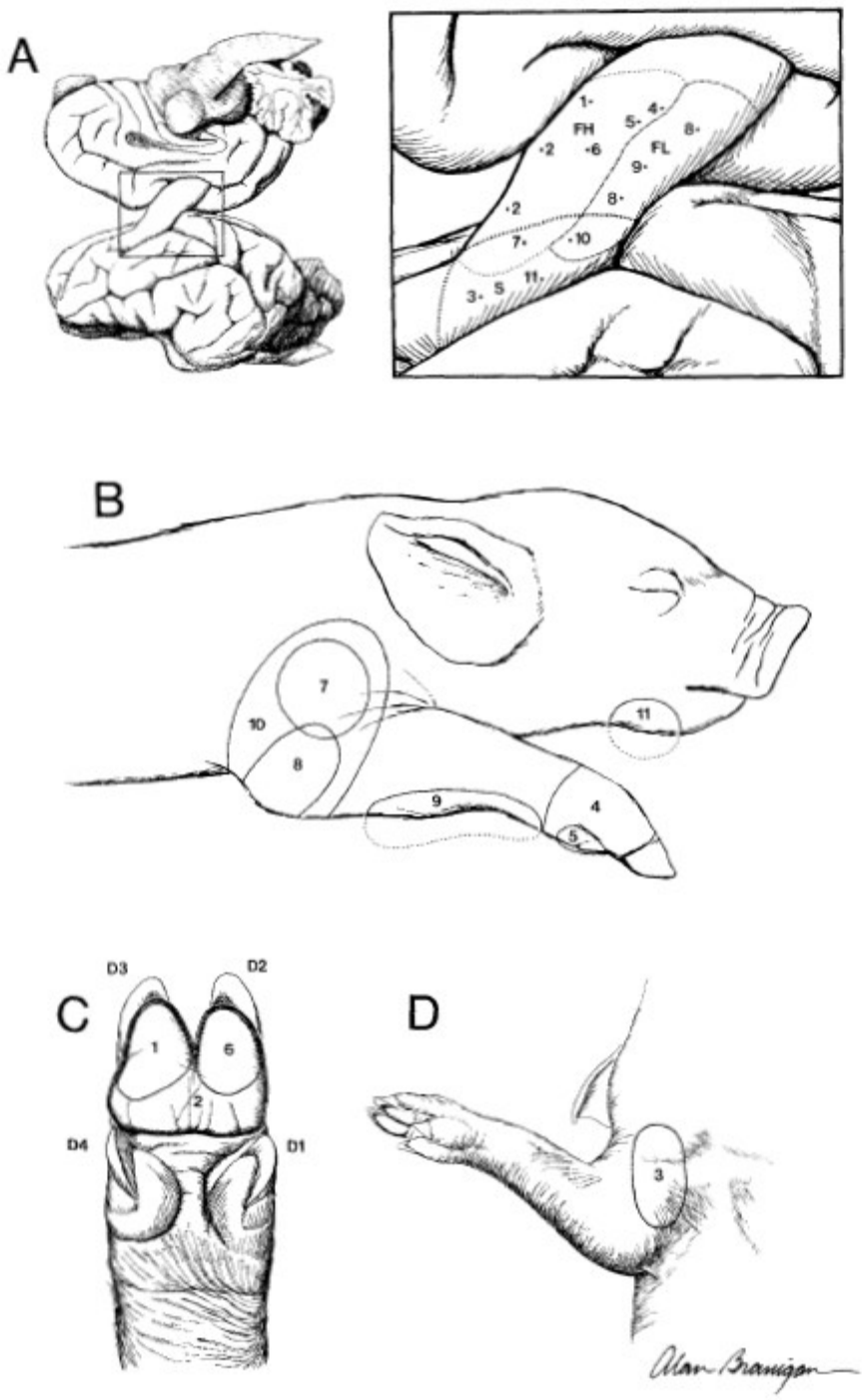

Fig. 4. Somatotopic representation of the SI forelimb region. **A.** Boxed area of cortex is enlarged in adjacent drawing. The enlargement illustrates composite representations of forehoof (FH), forelimb (FL), and shoulder (S), as well as representative penetration sites from an experimental animal. **B.** Receptive fields found on the forelimb and chin. **C.** Receptive fields found on ventral forehoof. D1 = digit 1, D2 = digit 2, D3 = digit 3, D4 = digit 4. **D.** Receptive field on ventral shoulder. Receptive fields in B, C, and D were found at the corresponding penetration sites in A.

Figure 6.4: Porcine Forelimb Receptive Field Mapping

Practically speaking, mounting a vibrotactile probe in such a way that it could stimulate the snout could prove to be extremely challenging, especially without impeding the pig's ability to navigate its environment effectively. In behavioral tasks, the snout is most often the tool used to access the reward, for example by pushing a lever (4). A mounted probe tip could impede this ability and thus add additional confounds to a behavioral study unintentionally. Looking at the receptive field mappings in the Craner and Ray paper (Fig. 2), it seems like the next-best spot would be the forelimbs. The downside of the forelimbs is that the receptive fields are rather large, so simultaneous stimulation of two or more points runs the risk of being perceived by the animal as single-site stimulation, thus making comparisons of multiple simultaneous stimuli significantly more difficult. Despite that risk, mounting a pair of vibrotactile probes to the forelimbs could potentially be much easier, and thus worth exploring as a possible 'Plan B'.

Necessary Device Modifications

While the choice of actuator design would be dictated by the location chosen, the control board for the CM-6/BG-1 could be used as-is. A few additions would have to be made for convenience. First, the BG-1 is designed to both communicate with and draw power from a PC via a USB cable. A wearable solution, for pigs (or otherwise), would require a Li-ion battery (or two) and a wireless communication module, which would be fairly trivial as the BG-1 board already exposes a both high-speed SPI and medium speed USART interface for future expansion. I would probably select the Roving Networks RN-42® Bluetooth® module as it has a UART port and comes with a Bluetooth® HID profile already built-in. A software migration would be trivial at that point as the data packets would be identical to their current form. The whole package only weighs a few ounces and could be easily strapped to even the smallest of pigs with some nylon fabric and Velcro in a fashion similar to a service animal's harness.

The actuators might have to be modified based on the desired stimulus location. To stimulate the rostrum, they would have to be much smaller than the current version. One

possibility for that would be to use a CM3 piezo actuator with a smaller arm bar linkage and probe tip. The downside is that a new position sensor mounting would have to be developed as well. A smaller position controlled VCA would be ideal, possibly with a fixed coil instead of fixed magnet. I would suggest targeting either receptive fields 3+4 or 4+5 (Fig. 1) on the dorsolateral edges of each nostril for a total of 4 actuators. This would hopefully leave enough of the rostrum exposed for the pig to navigate its environment effectively.

If 'Plan A' fails and we were forced to stimulate the forelimbs instead of the rostrum, we could probably get away with the current VCA in a package similar to the primate version of the probes. Unlike the primate version, we wouldn't want to expose too much of the probe tip to the elements in order to protect it from damage as the pig moves around. Mounting two primate tips side by side in opposing directions should give enough separation along the upper forelimb to stimulate receptive fields 7 and 8 as shown in Figure 2. This setup would be mirrored for the other forelimb, for a total of 4 actuators.

The mounting configurations would also be slightly different depending stimulation site, but both could be relatively simple modifications of existing designs. The rostrum actuators could be affixed to a muzzle, while the forelimbs could be affixed to the same harness that would hold the control circuitry. In both cases, I would most likely choose to design a housing with a strap tunnel adjacent to the probe tip so that it could be placed anywhere along a harness or muzzle strap. Most animal body harnesses are designed with adjustable straps anterior and posterior to the limbs, leaving the upper forelimb exposed almost perfectly above the targeted forelimb receptive field areas. The forelimb mounting strap would run from the anterior to the posterior harness straps while passing through the tunnels of both actuators. The strap could be loosened or tightened to adjust the amount of contact force from each actuator, and strap stops on either side of the assembly would allow the pair of actuators to be repositioned in multiple configurations along the strap to adjust for the shape of each animal.

Preventing damage to the actuators will probably be the biggest consideration for a successful mounting setup. Pigs like to roll around in the mud, and even the more manageably sized miniature pigs still clock in around 60lbs, therefore ruggedization will be unavoidable to ensure they can take a few bumps during the cognitive task training. The most likely damage to rostrum mounted stimulators would come from the animal's natural tendency to explore the ground with its snout. Thus, if the actuators are not sufficiently dorsal, they could easily end up being dragged through the mud. Damage to a forelimb mounted assembly would post likely be from inadvertent boundary collisions as they would most likely protrude farther laterally than the belly of the pig. That could be minimized by using smaller actuators like those proposed for rostral stimulation.

Test and Training Paradigms

Once the hardware is mounted and vibrotactile stimulation is delivered, we have to ask: Is the pig capable of performing a simple cognitive task with the presented sensory information? The literature seems to suggest, yes. A 2011 article by Gieling et al. serves as a review of the porcine cognitive ability and affirms that pigs can perform basic cognitive tasks with rapid learning when the task is properly designed. Most of the studies reviewed in the Gieling paper talk about gauging learning and memory functions using mazes with either positive or negative (stress-inducing) reinforcements. Positive rewards are usually either a sweet treat like an apple, or a social reinforcement such as access to its siblings and/or mother. To make the gustatory rewards even more appealing, food deprivation is commonly utilized prior to task training.

Based on those studies, I would propose a very simple task to test a pig's ability to differentiate various properties of simultaneous vibrations such as amplitude or frequency. A bilateral task would be easiest, as it would avoid the possibility of overlapping peripheral receptive fields. The pig would be placed in front of a gate. In front of the gate would be two identical paths, one of which leads to a positive reinforcement reward. At the start of the task, two simultaneous supra-threshold vibrations of sufficiently differing amplitude

would be delivered to both of the upper forelimbs. The limb that receives the higher amplitude vibration will indicate the correct path to the reward. As soon as the vibrations complete, the gate is opened and the pig is able to choose a path. The experiment could easily be modified to coerce the pig to activate a lever with its snout to dispense the reward instead. During the training, the vibrations would leverage Weber's Law and use a scaled difference limen so that the animal doesn't just learn to differentiate from a single fixed stimulus and actually selects based on proportional amplitude. Once (if) the pig has been trained to perform this task with high accuracy, the amplitude of the stimuli can be modulated such that the difference between the two amplitudes becomes progressively smaller. When the pig starts to select the wrong path (or lever), we can assume that its ability to differentiate the amplitudes has been sufficiently impaired, and the difference limen is calculated just as it is for humans. Additional layers of complexity could be added to this task rather easily. For example, the maze could be free roaming, using positional triggers to start a vibration as a big approaches either a fork in the maze or pair of snout levers.

Possible Experimental Pitfalls

Most of the possible pitfalls will lie in possible cues unrelated to the tactile vibrations. The most likely of which is an auditory cue. This would definitely be the case if using a piezo actuated probe. The current version of the CM stimulator uses a 20kHz sampling/update rate so that noise generated by the switching of the transistors in the driver circuit is beyond the audible range of human hearing. Pigs have been found to respond to a wider range of auditory frequencies, up to 41kHz (Gieling 2011). To test for this confound, we could simply offset the probes from their mounting points on the skin and see if the pig is still able to select the proper path with above-chance accuracy. In that case, a possible solution would be to raise the sampling rate to the 50kHz range. Consequently though, we would end up losing accuracy in the PWM signal generation. Other

alternatives could simply be to use ear plugs/muffs as is common in human studies, or add a white noise generator of sufficient volume to mask the transistor switching.

The second most likely cue would be olfactory. If the pig is able to smell the reward, we would know right away as accuracy would be higher than chance from the beginning of the task training session. The type of reward could simply be changed to be odorless, or if necessary, a more extreme bulbectomy could be performed (Gieling 2011).

APPENDIX 4.1: CLASS DIAGRAM FOR DEVICE DRIVER LIBRARY

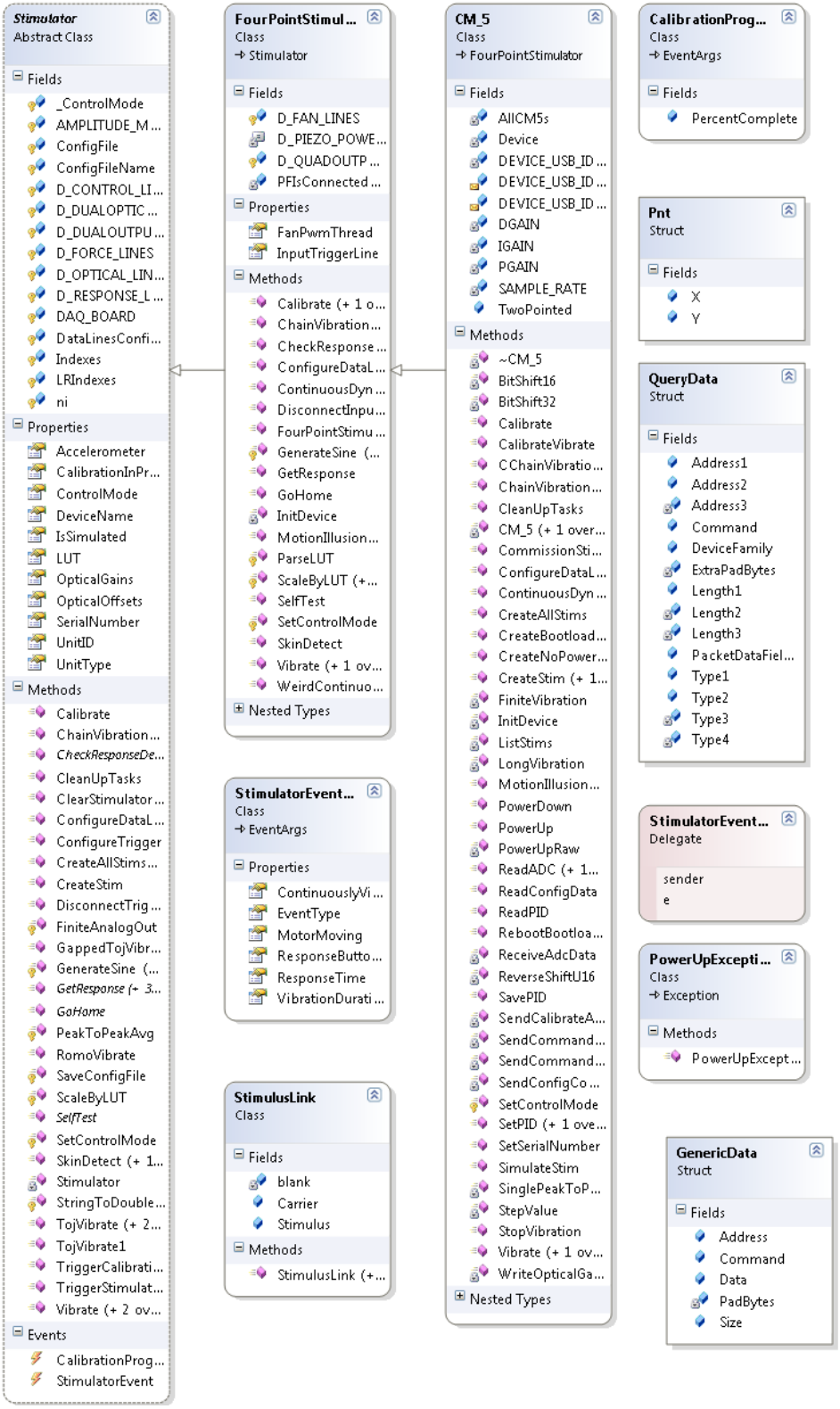

APPENDIX 4.2: CLASS DIAGRAM FOR SHELL AND PLUGIN LIBRARY

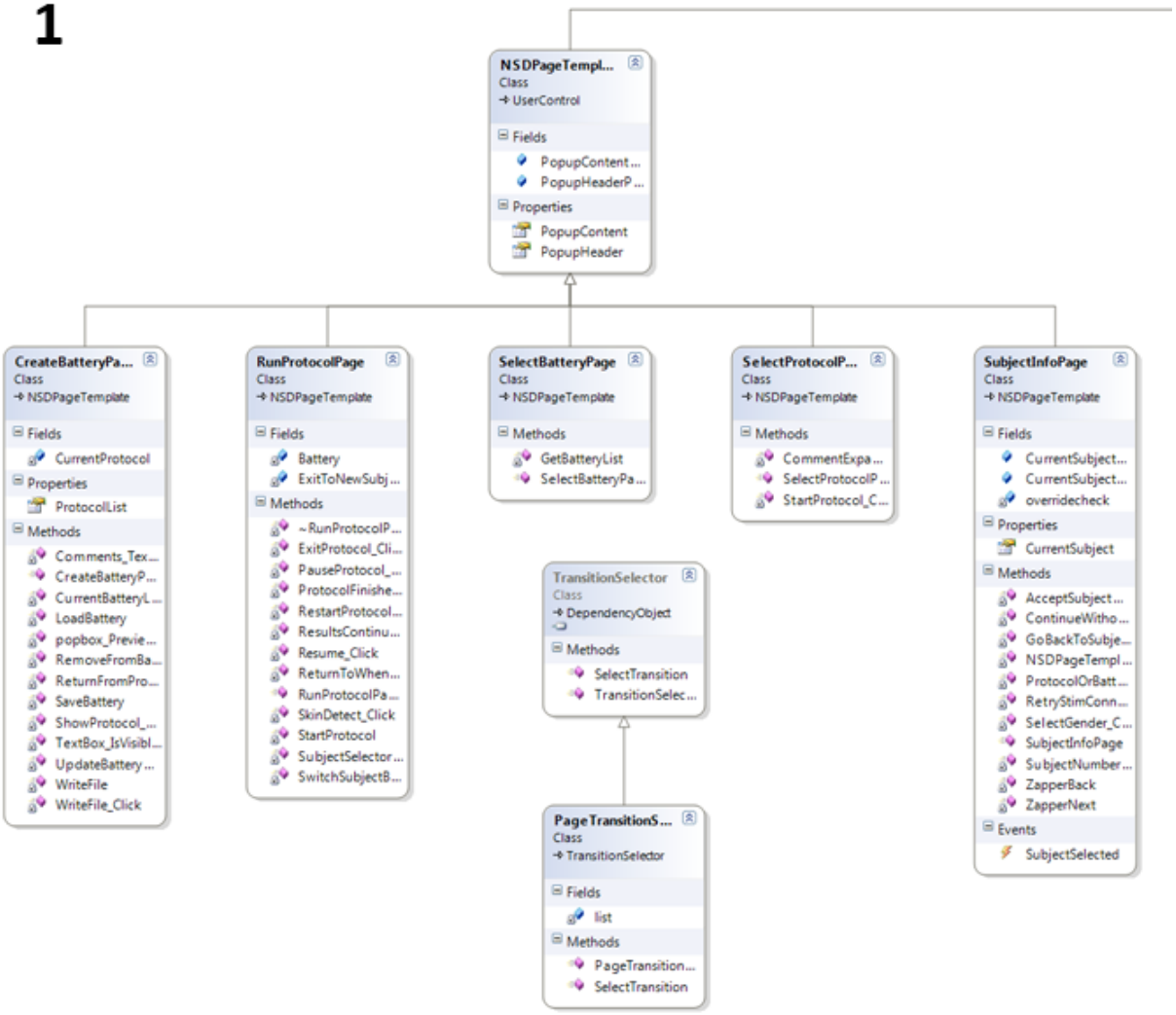

2

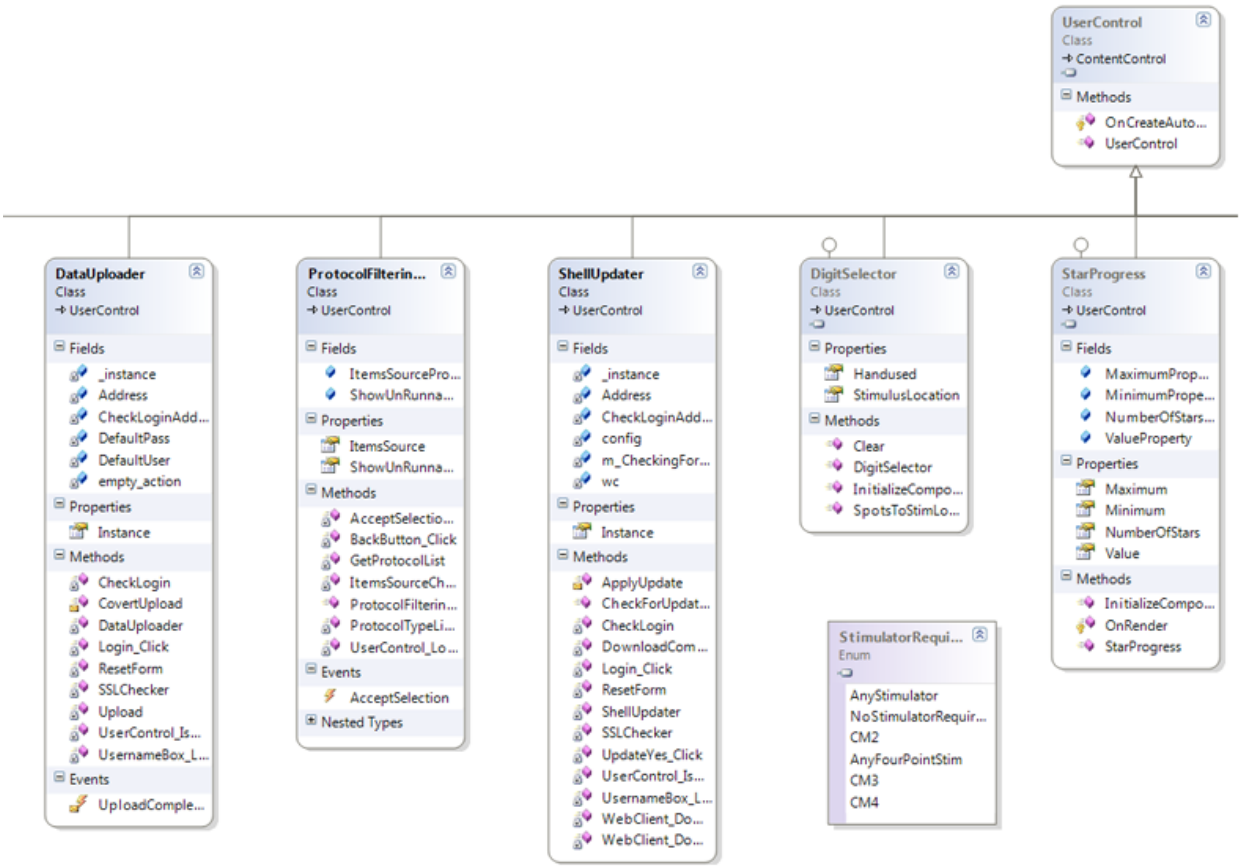
UserControl
Class
ContentControl
Methods
OnCreateAuto...
UserControl
DataUploader
Class
UserControl
Fields
_instance
Address
CheckLoginAdd...
DefaultPass
DefaultUser
empty_action
Properties
Instance
Methods
CheckLogin
CovertUpload
DataUploader
Login_Click
ResetForm
SSLChecker
Upload
UserControl_Is...
UsernameBox_L...
Events
UploadComple...
ProtocolFilterin...
Class
UserControl
Fields
ItemsSourcePro...
ShowUnRunna...
Properties
ItemsSource
ShowUnRunna...
Methods
AcceptSelectio...
BackButton_Click
GetProtocolList
ItemsSourceCh...
ProtocolFilterin...
ProtocolTypeLi...
UserControl_Lo...
Events
AcceptSelection
Nested Types
ShellUpdater
Class
UserControl
Fields
_instance
Address
CheckLoginAdd...
config
m_CheckingFor...
wc
Properties
Instance
Methods
ApplyUpdate
CheckForUpdat...
CheckLogin
DownloadCom...
Login_Click
ResetForm
ShellUpdater
SSLChecker
UpdateYes_Click
UserControl_Is...
UsernameBox_L...
WebClient_Do...
WebClient_Do...
DigitSelector
Class
UserControl
Properties
Handused
StimulusLocation
Methods
Clear
DigitSelector
InitializeCompo...
SpotsToStimLo...
StarProgress
Class
UserControl
Fields
MaximumProp...
MinimumPrope...
NumberOfStars...
ValueProperty
Properties
Maximum
Minimum
NumberOfStars
Value
Methods
InitializeCompo...
OnRender
StarProgress
StimulatorRequi...
Enum
AnyStimulator
NoStimulatorRequir...
CM2
AnyFourPointStim
CM3
CM4

3

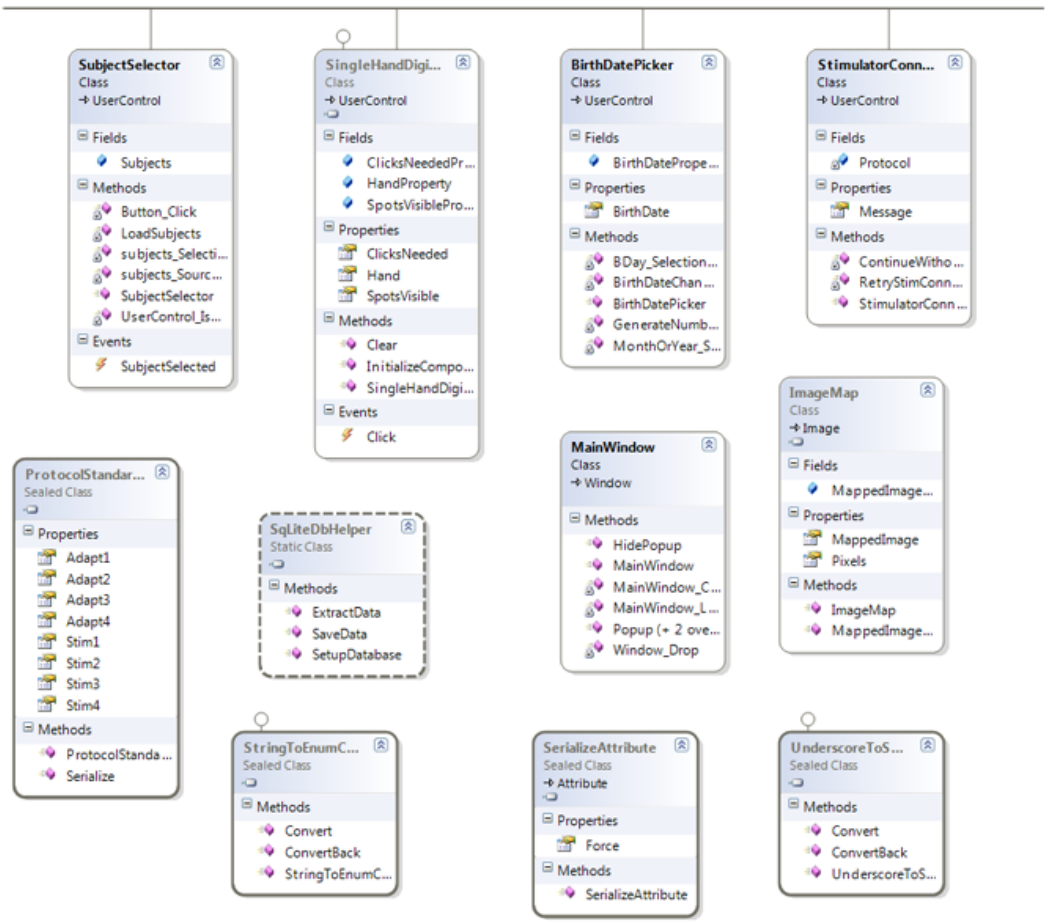
SubjectSelector
Class
UserControl
Fields
Subjects
Methods
Button_Click
LoadSubjects
subjects_Selecti...
subjects_Sourc...
SubjectSelector
UserControl_Is...
Events
SubjectSelected
SingleHandDigi...
Class
UserControl
Fields
ClicksNeededPr...
HandProperty
SpotsVisiblePro...
Properties
ClicksNeeded
Hand
SpotsVisible
Methods
Clear
InitializeCompo...
SingleHandDigi...
Events
Click
BirthDatePicker
Class
UserControl
Fields
BirthDatePrope...
Properties
BirthDate
Methods
BDay_Selection...
BirthDateChan...
BirthDatePicker
GenerateNumb...
MonthOrYear_S...
StimulatorConn...
Class
UserControl
Fields
Protocol
Properties
Message
Methods
ContinueWitho...
RetryStimConn...
StimulatorConn...
ImageMap
Class
Image
Fields
MappedImage...
Properties
MappedImage
Pixels
Methods
ImageMap
MappedImage...
MainWindow
Class
Window
Methods
HidePopup
MainWindow
MainWindow_C...
MainWindow_L...
Popup (+ 2 ove...
Window_Drop
ProtocolStandar...
Sealed Class
Properties
Adapt1
Adapt2
Adapt3
Adapt4
Stim1
Stim2
Stim3
Stim4
Methods
ProtocolStanda...
Serialize
SqLiteDbHelper
Static Class
Methods
ExtractData
SaveData
SetupDatabase
StringToEnumC...
Sealed Class
Methods
Convert
ConvertBack
StringToEnumC...
SerializeAttribute
Sealed Class
Attribute
Properties
Force
Methods
SerializeAttribute
UnderscoreToS...
Sealed Class
Methods
Convert
ConvertBack
UnderscoreToS...

4

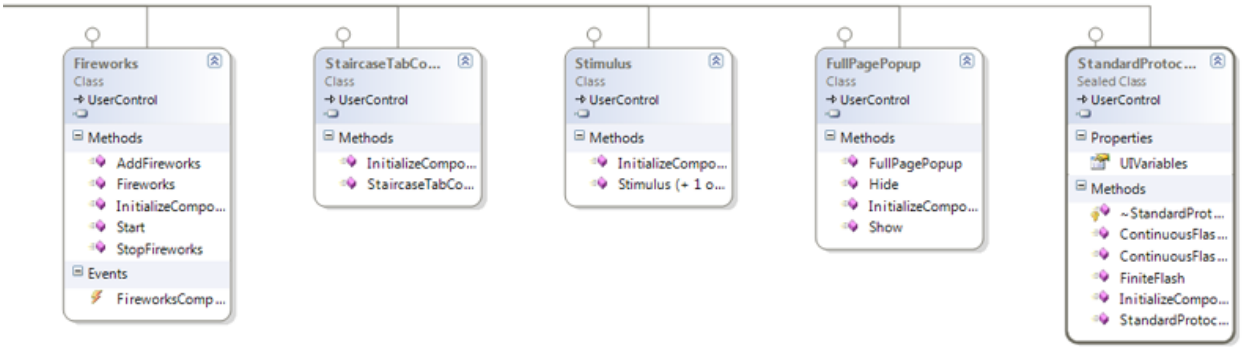
Fireworks
Class
UserControl
Methods
AddFireworks
Fireworks
InitializeCompo...
Start
StopFireworks
Events
FireworksComp...
StaircaseTabCo...
Class
UserControl
Methods
InitializeCompo...
StaircaseTabCo...
Stimulus
Class
UserControl
Methods
InitializeCompo...
Stimulus (+ 1 o...
FullPagePopup
Class
UserControl
Methods
FullPagePopup
Hide
InitializeCompo...
Show
StandardProtoc...
Sealed Class
UserControl
Properties
UIVariables
Methods
~StandardProt...
ContinuousFlas...
ContinuousFlas...
FiniteFlash
InitializeCompo...
StandardProtoc...

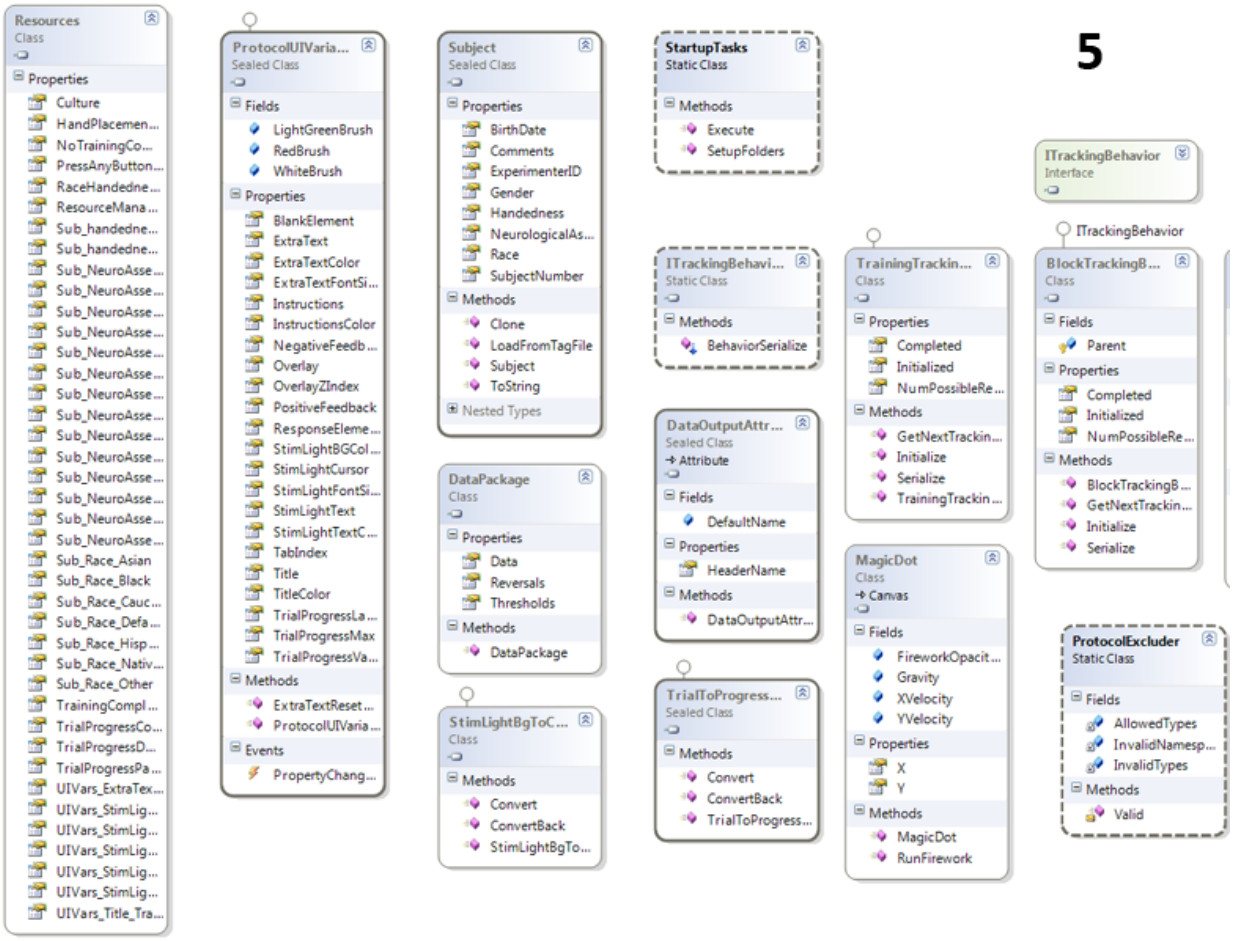
Resources
Class
Properties
Culture
HandPlacemen...
NoTrainingCo...
PressAnyButton...
RaceHandedne...
ResourceMana...
Sub_handedne...
Sub_handedne...
Sub_NeuroAsse...
Sub_NeuroAsse...
Sub_NeuroAsse...
Sub_NeuroAsse...
Sub_NeuroAsse...
Sub_NeuroAsse...
Sub_NeuroAsse...
Sub_NeuroAsse...
Sub_NeuroAsse...
Sub_NeuroAsse...
Sub_NeuroAsse...
Sub_NeuroAsse...
Sub_NeuroAsse...
Sub_NeuroAsse...
Sub_Race_Asian
Sub_Race_Black
Sub_Race_Cauc...
Sub_Race_Defa...
Sub_Race_Hisp...
Sub_Race_Nativ...
Sub_Race_Other
TrainingCompl...
TrialProgressCo...
TrialProgressD...
TrialProgressPa...
UIVars_ExtraTex...
UIVars_StimLig...
UIVars_StimLig...
UIVars_StimLig...
UIVars_StimLig...
UIVars_StimLig...
UIVars_Title_Tra...
ProtocolUIVaria...
Sealed Class
Fields
LightGreenBrush
RedBrush
WhiteBrush
Properties
BlankElement
ExtraText
ExtraTextColor
ExtraTextFontSi...
Instructions
InstructionsColor
NegativeFeedb...
Overlay
OverlayZIndex
PositiveFeedback
ResponseEleme...
StimLightBGCol...
StimLightCursor
StimLightFontSi...
StimLightText
StimLightTextC...
TabIndex
Title
TitleColor
TrialProgressLa...
TrialProgressMax
TrialProgressVa...
Methods
ExtraTextReset...
ProtocolUIVaria...
Events
PropertyChang...
Subject
Sealed Class
Properties
BirthDate
Comments
ExperimenterID
Gender
Handedness
NeurologicalAs...
Race
SubjectNumber
Methods
Clone
LoadFromTagFile
Subject
ToString
Nested Types
DataPackage
Class
Properties
Data
Reversals
Thresholds
Methods
DataPackage
StimLightBgToC...
Class
Methods
Convert
ConvertBack
StimLightBgTo...
StartupTasks
Static Class
Methods
Execute
SetupFolders
ITrackingBehavi...
Static Class
Methods
BehaviorSerialize
DataOutputAttr...
Sealed Class
Attribute
Fields
DefaultName
Properties
HeaderName
Methods
DataOutputAttr...
TrialToProgress...
Sealed Class
Methods
Convert
ConvertBack
TrialToProgress...
5
ITrackingBehavior
Interface
TrainingTrackin...
Class
Properties
Completed
Initialized
NumPossibleRe...
Methods
GetNextTrackin...
Initialize
Serialize
TrainingTrackin...
MagicDot
Class
Canvas
Fields
FireworkOpacit...
Gravity
XVelocity
YVelocity
Properties
X
Y
Methods
MagicDot
RunFirework
ITrackingBehavior
BlockTrackingB...
Class
Fields
Parent
Properties
Completed
Initialized
NumPossibleRe...
Methods
BlockTrackingB...
GetNextTrackin...
Initialize
Serialize
ProtocolExcluder
Static Class
Fields
AllowedTypes
InvalidNamesp...
InvalidTypes
Methods
Valid

6

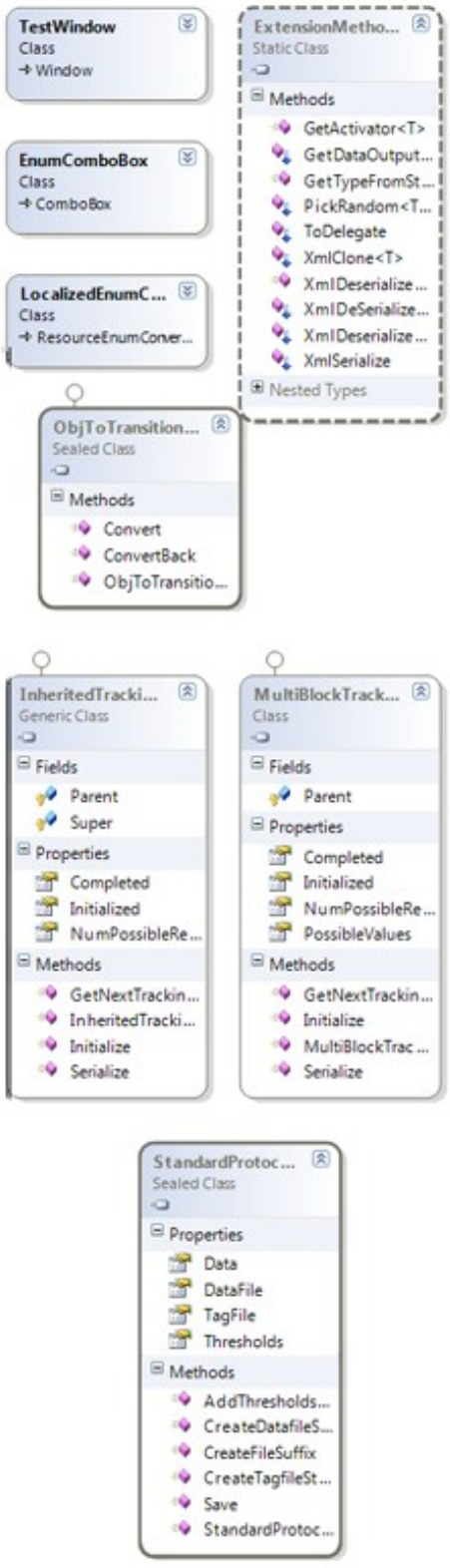
TestWindow
Class
Window
EnumComboBox
Class
ComboBox
LocalizedEnumC...
Class
ResourceEnumConver...
ExtensionMetho...
Static Class
Methods
GetActivator<T>
GetDataOutput...
GetTypeFromSt...
PickRandom<T...
ToDelegate
XmlClone<T>
XmlDeserialize...
XmlDeSerialize...
XmlDeserialize...
XmlSerialize
Nested Types
ObjToTransition...
Sealed Class
Methods
Convert
ConvertBack
ObjToTransitio...
InheritedTracki...
Generic Class
Fields
Parent
Super
Properties
Completed
Initialized
NumPossibleRe...
Methods
GetNextTrackin...
InheritedTracki...
Initialize
Serialize
MultiBlockTrack...
Class
Fields
Parent
Properties
Completed
Initialized
NumPossibleRe...
PossibleValues
Methods
GetNextTrackin...
Initialize
MultiBlockTrac...
Serialize
StandardProtoc...
Sealed Class
Properties
Data
DataFile
TagFile
Thresholds
Methods
AddThresholds...
CreateDatafileS...
CreateFileSuffix
CreateTagfileSt...
Save
StandardProtoc...

7

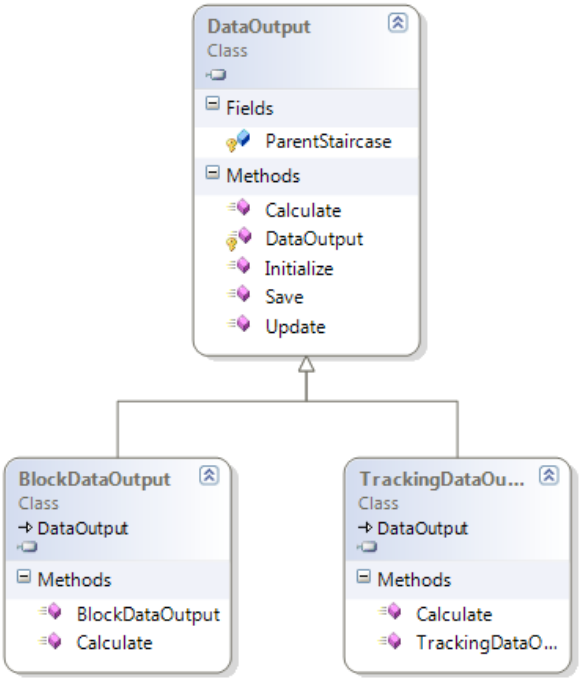
DataOutput
Class
Fields
ParentStaircase
Methods
Calculate
DataOutput
Initialize
Save
Update
BlockDataOutput
Class
DataOutput
Methods
BlockDataOutput
Calculate
TrackingDataOu...
Class
DataOutput
Methods
Calculate
TrackingDataO...

8

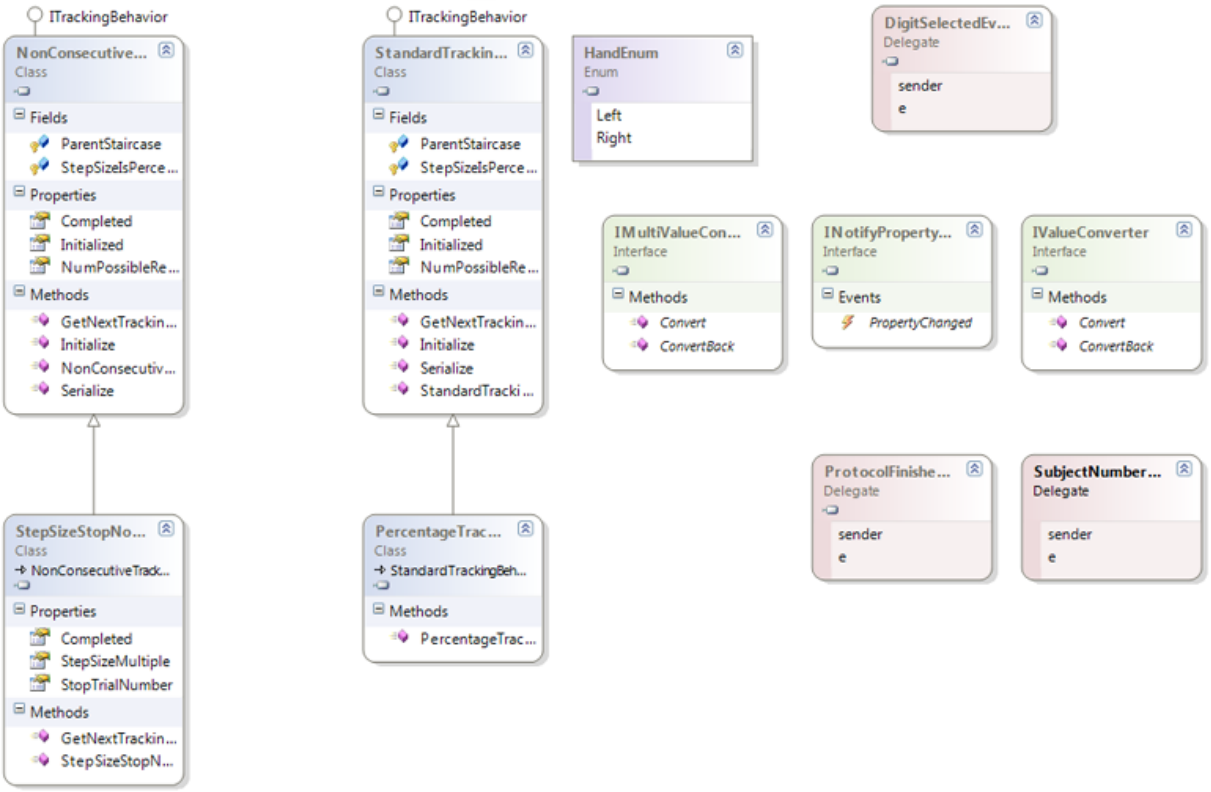
ITrackingBehavior
NonConsecutive...
Class
Fields
ParentStaircase
StepSizeIsPerce...
Properties
Completed
Initialized
NumPossibleRe...
Methods
GetNextTrackin...
Initialize
NonConsecutiv...
Serialize
StepSizeStopNo...
Class
NonConsecutiveTrack...
Properties
Completed
StepSizeMultiple
StopTrialNumber
Methods
GetNextTrackin...
StepSizeStopN...
ITrackingBehavior
StandardTrackin...
Class
Fields
ParentStaircase
StepSizeIsPerce...
Properties
Completed
Initialized
NumPossibleRe...
Methods
GetNextTrackin...
Initialize
Serialize
StandardTracki...
PercentageTrac...
Class
StandardTrackingBeh...
Methods
PercentageTrac...
HandEnum
Enum
Left
Right
DigitSelectedEv...
Delegate
sender
e
IMultiValueCon...
Interface
Methods
Convert
ConvertBack
INotifyProperty...
Interface
Events
PropertyChanged
IValueConverter
Interface
Methods
Convert
ConvertBack
ProtocolFinishe...
Delegate
sender
e
SubjectNumber...
Delegate
sender
e

9


Object
Class
Methods
~Object
Equals (+ 1 ove...
GetHashCode
GetType
MemberwiseCl...
Object
ReferenceEquals
ToString
StimulatorRequi...
Sealed Class
Attribute
Properties
Requirement
Methods
StimulatorRequ...

10

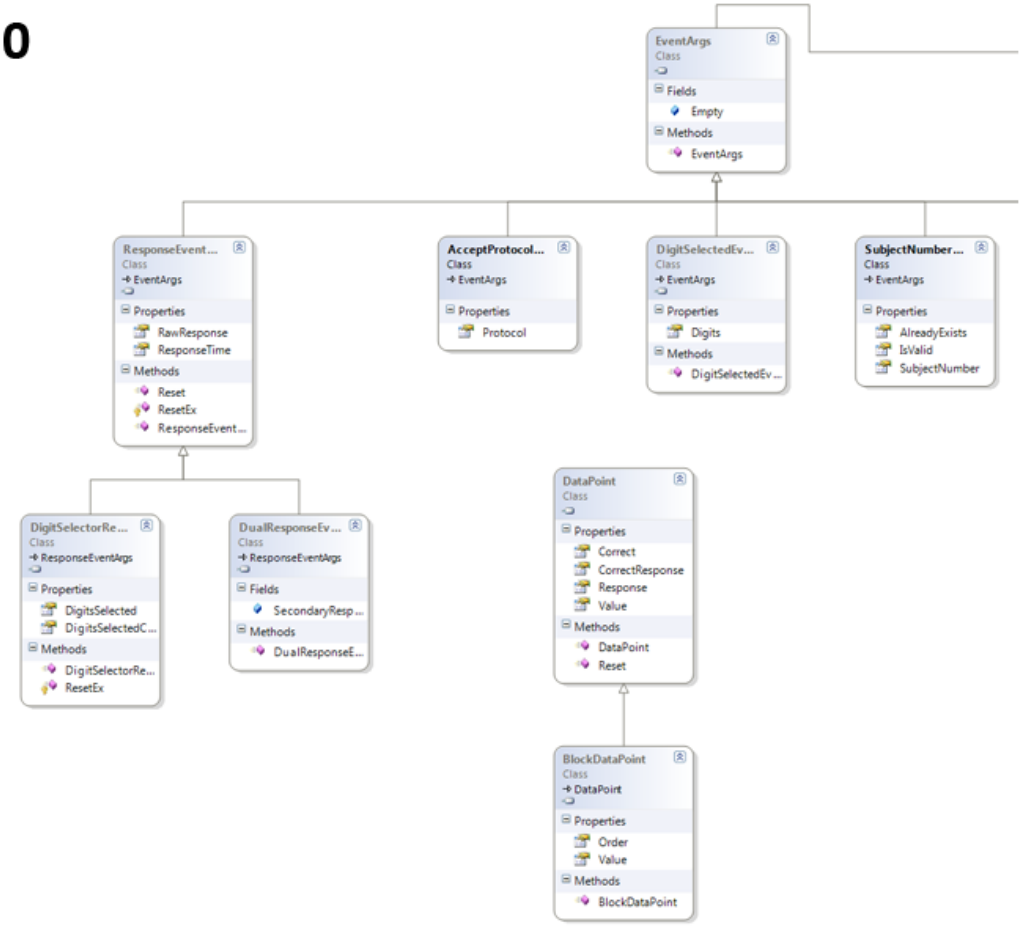
EventArgs
Class
Fields
Empty
Methods
EventArgs
ResponseEvent...
Class
EventArgs
Properties
RawResponse
ResponseTime
Methods
Reset
ResetEx
ResponseEvent...
AcceptProtocol...
Class
EventArgs
Properties
Protocol
DigitSelectedEv...
Class
EventArgs
Properties
Digits
Methods
DigitSelectedEv...
SubjectNumber...
Class
EventArgs
Properties
AlreadyExists
IsValid
SubjectNumber
DigitSelectorRe...
Class
ResponseEventArgs
Properties
DigitsSelected
DigitsSelectedC...
Methods
DigitSelectorRe...
ResetEx
DualResponseEv...
Class
ResponseEventArgs
Fields
SecondaryResp...
Methods
DualResponseE...
DataPoint
Class
Properties
Correct
CorrectResponse
Response
Value
Methods
DataPoint
Reset
BlockDataPoint
Class
DataPoint
Properties
Order
Value
Methods
BlockDataPoint

11

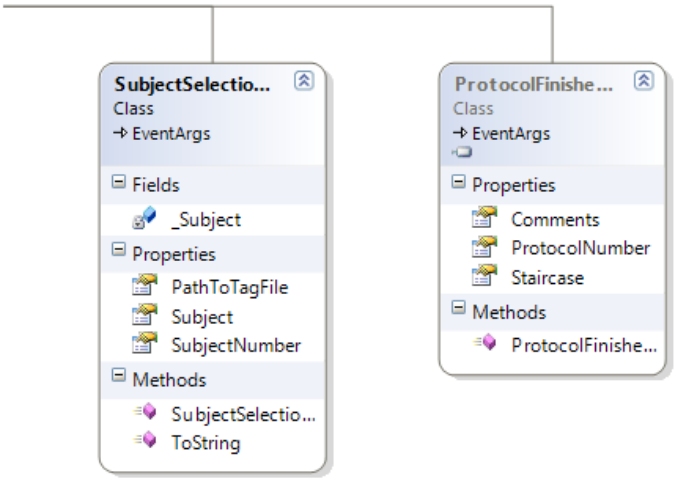
SubjectSelectio...
Class
EventArgs
Fields
_Subject
Properties
PathToTagFile
Subject
SubjectNumber
Methods
SubjectSelectio...
ToString
ProtocolFinishe...
Class
EventArgs
Properties
Comments
ProtocolNumber
Staircase
Methods
ProtocolFinishe...

12

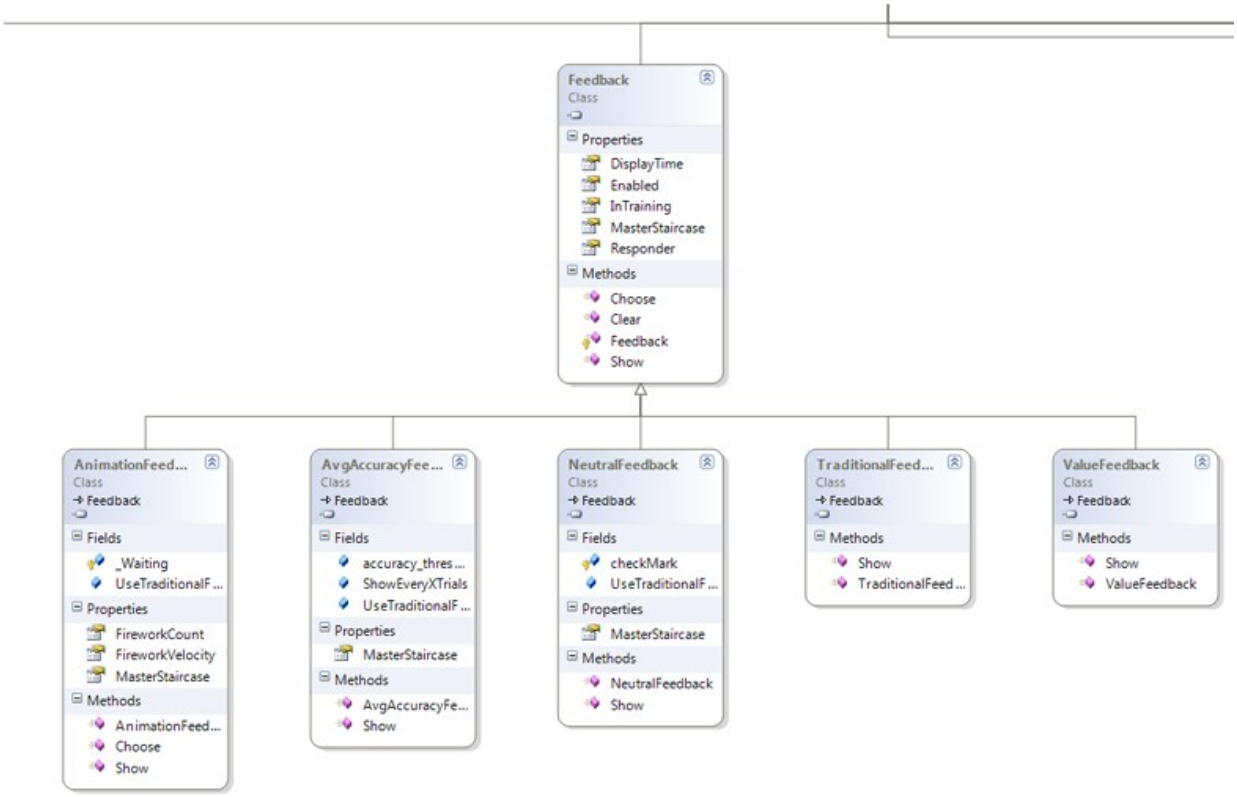
Feedback
Class
Properties
DisplayTime
Enabled
InTraining
MasterStaircase
Responder
Methods
Choose
Clear
Feedback
Show
AnimationFeed...
Class
Feedback
Fields
_Waiting
UseTraditionalF...
Properties
FireworkCount
FireworkVelocity
MasterStaircase
Methods
AnimationFeed...
Choose
Show
AvgAccuracyFee...
Class
Feedback
Fields
accuracy_thres...
ShowEveryXTrials
UseTraditionalF...
Properties
MasterStaircase
Methods
AvgAccuracyFe...
Show
NeutralFeedback
Class
Feedback
Fields
checkMark
UseTraditionalF...
Properties
MasterStaircase
Methods
NeutralFeedback
Show
TraditionalFeed...
Class
Feedback
Methods
Show
TraditionalFeed...
ValueFeedback
Class
Feedback
Methods
Show
ValueFeedback

13


ApplicationCom...
Sealed Class
Fields
_DebugProtocol
_ExitShell
_GotoCreateBat...
_GotoRunProto...
_GotoSelectBat...
_GotoSelectPro...
_GotoSubjectIn...
_HidePopup
_ShowPopup
_TogglePopup
_UpdateSoftware
_UploadData
Properties
DebugProtocol
ExitShell
GotoCreateBatt...
GotoRunProtoc...
GotoSelectBatt...
GotoSelectProt...
GotoSubjectInf...
HidePopup
ShowPopup
TogglePopup
UpdateSoftware
UploadData
Methods
ApplicationCo...
CollectGarbage
DebugProtocol...
DebugProtocol...
ExitShell_CanEx...
ExitShell_Execut...
GotoCreateBatt...
GotoCreateBatt...
GotoRunProtoc...
GotoRunProtoc...
GotoSelectBatt...
GotoSelectBatt...
GotoSelectProt...
GotoSelectProt...
GotoSubjectInf...
GotoSubjectInf...
HidePopup_Ca...
HidePopup_Exe...
ShowPopup_Ca...
ShowPopup_Ex...
TogglePopup_...
TogglePopup_E...
UpdateSoftwar...
UpdateSoftwar...
UploadData_Ca...
UploadData_Ex...
FileAssociation
Class
Methods
Associate
AssociateURL
IsAssociated
IStaircaseCombo
Interface
Properties
CompletedTrials
Count
CurrentTrial
IsCompleted
Methods
Initialize
NextStaircase
Save
Serialize
Events
Completed
ProtocolStandar...
Sealed Class
Properties
Bias
Comments
HandUsed
HeatPadTemp
IntervalBetwee...
ITI
LeadLagTime
MalingeringTrials
MaxVal
MinVal
NumTrials
StartInterprobe...
StepSize
StimControlMo...
StimulusLocation
TrainingTrials
Methods
ProtocolStanda...
Events
PropertyChang...
Globals
Sealed Class
Fields
_CorticalMetric...
_Stimulators
instance
Properties
BatteriesFolder
CorticalMetrics...
CurrentProtocol
CurrentSubject
Instance
ProtocolsFolder
SimulateStimul...
Stimulators
Methods
GetCorticalMet...
Globals
NetworkChang...
MasterStaircase
Class
Properties
CompletedTrials
Count
Current
CurrentTrial
IsCompleted
Methods
DeSerialize
IncrementIndex
Initialize
MasterStaircase
NextStaircase
Save
Serialize
Events
Completed
BoolToVisibility...
Class
Methods
Convert
ConvertBack
SingleInstance...
Class
WindowsFormsApplic...
Fields
app
Methods
OnStartup
OnStartupNextI...
Process
SingleInstance...
Staircase
Class
Fields
DeliverStimuli
Properties
Behavior
Count
CurrentIndex
CurrentTrial
Initialized
IsCompleted
StartingStimuli
Trials
UIVars
Vars
Methods
DeSerialize
GetFinalTrackin...
GetNextTrackin...
GetStandardPar...
Initialize
Reset
Serialize
SetResponse
Staircase (+ 1 o...
Resources
Class
Fields
resourceCulture
resourceMan
Properties
AdvMenuCancel
AdvMenuCreat...
AdvMenuExit
AdvMenuHeader
AdvMenuUpdate
AdvMenuUpload
AndPrompt
BatteryPrompt
Culture
DOBPrompt
GenderFemale
GenderMale
HandednessPro...
MoApril
MoAugust
MoDecember
MoFebruary
MoJanuary
MoJuly
MoJune
MoMarch
MoMay
MoNovember
MoOctober
MoSeptember
NoStimConnec...
NoStimConnec...
NoStimContinue
NoStimRetry
ProtocolPrompt
RaceHandedne...
RacePrompt
ResourceMana...
SelectGenderPr...
SubjectNumber...
Methods
Resources

14

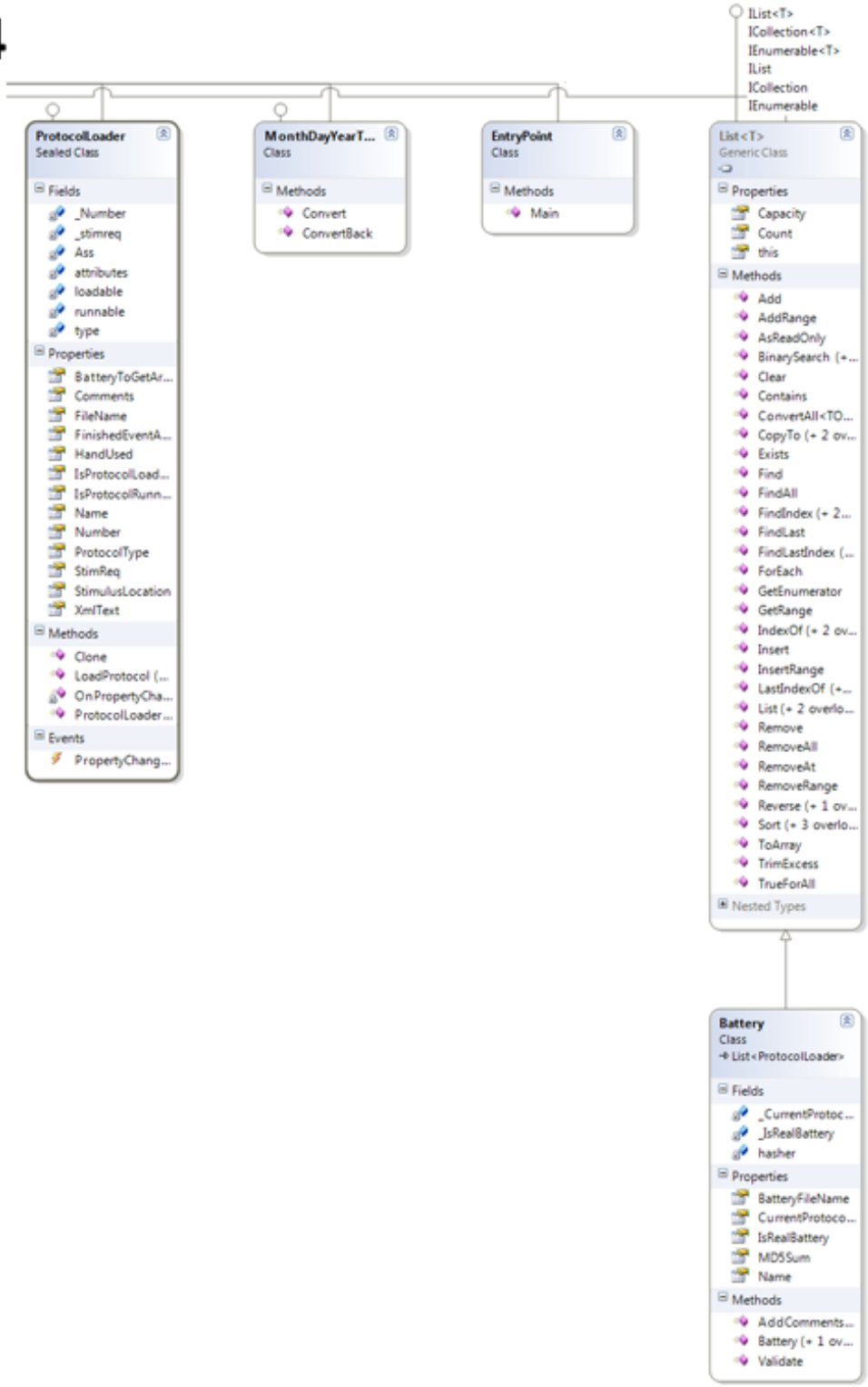
IList<T>
ICollection<T>
IEnumerable<T>
IList
ICollection
IEnumerable
ProtocolLoader
Sealed Class
Fields
_Number
_stimreq
Ass
attributes
loadable
runnable
type
Properties
BatteryToGetAr...
Comments
FileName
FinishedEventA...
HandUsed
IsProtocolLoad...
IsProtocolRunn...
Name
Number
ProtocolType
StimReq
StimulusLocation
XmlText
Methods
Clone
LoadProtocol (...
OnPropertyCha...
ProtocolLoader...
Events
PropertyChang...
MonthDayYearT...
Class
Methods
Convert
ConvertBack
EntryPoint
Class
Methods
Main
List<T>
Generic Class
Properties
Capacity
Count
this
Methods
Add
AddRange
AsReadOnly
BinarySearch (+...
Clear
Contains
ConvertAll<TO...
CopyTo (+ 2 ov...
Exists
Find
FindAll
FindIndex (+ 2...
FindLast
FindLastIndex (...
ForEach
GetEnumerator
GetRange
IndexOf (+ 2 ov...
Insert
InsertRange
LastIndexOf (+...
List (+ 2 overlo...
Remove
RemoveAll
RemoveAt
RemoveRange
Reverse (+ 1 ov...
Sort (+ 3 overlo...
ToArray
TrimExcess
TrueForAll
Nested Types
Battery
Class
List<ProtocolLoader>
Fields
_CurrentProtoc...
_IsRealBattery
hasher
Properties
BatteryFileName
CurrentProtoco...
IsRealBattery
MD5Sum
Name
Methods
AddComments...
Battery (+ 1 ov...
Validate

15


ProtocolRespon...
Class
Fields
DefaultRespons...
Response
Timer
UI
Properties
Feedback
Methods
~ProtocolResp...
FlashUI
GetResponse (...
GetResponseAs...
PauseForClick (...
ProtocolRespo...
Events
GotResponse
DigitSelectorRe...
Class
ProtocolResponder
Methods
DigitSelectorRe...
MouseResponder
Class
ProtocolResponder
Properties
CenterMouseO...
Methods
CenterCursorO...
Clicked
ConnectEventH...
MouseRespond...
UI_MouseDown
ButtonResponder
Class
ProtocolResponder
Fields
checkMark
Methods
ButtonRespond...
HardwareRespo...
Class
MouseResponder
Methods
GetResponse
HardwareResp...
UI_MouseDown
MouseAndKeyb...
Class
MouseResponder
Properties
Keys
Methods
ConnectEventH...
MouseAndKey...
AsyncMouseRes...
Class
MouseResponder
Methods
AsyncMouseRe...
FlashUI

16

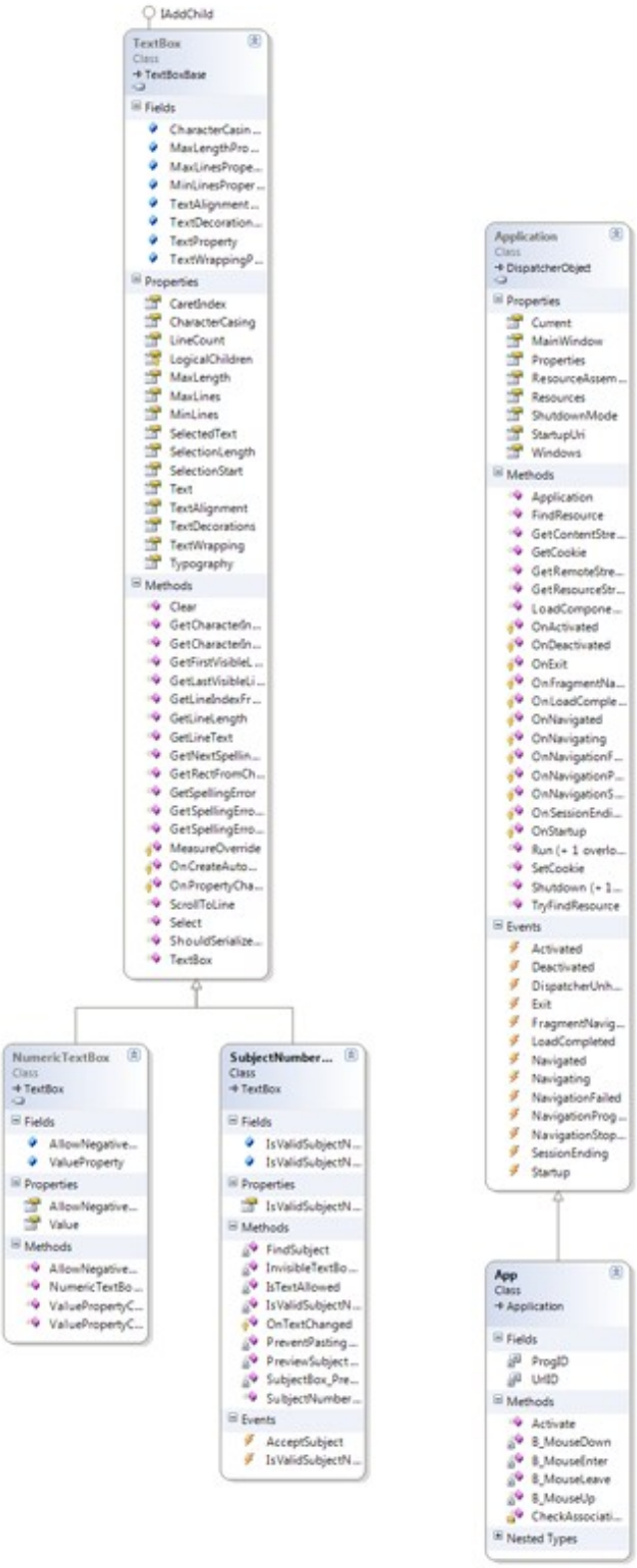
IAddChild
TextBox
Class
TextBoxBase
Fields
CharacterCasin...
MaxLengthPro...
MaxLinesPrope...
MinLinesProper...
TextAlignment...
TextDecoration...
TextProperty
TextWrappingP...
Properties
CaretIndex
CharacterCasing
LineCount
LogicalChildren
MaxLength
MaxLines
MinLines
SelectedText
SelectionLength
SelectionStart
Text
TextAlignment
TextDecorations
TextWrapping
Typography
Methods
Clear
GetCharacterIn...
GetCharacterIn...
GetFirstVisibleL...
GetLastVisibleLi...
GetLineIndexFr...
GetLineLength
GetLineText
GetNextSpellin...
GetRectFromCh...
GetSpellingError
GetSpellingErro...
GetSpellingErro...
MeasureOverride
OnCreateAuto...
OnPropertyCha...
ScrollToLine
Select
ShouldSerialize...
TextBox
Application
Class
DispatcherObject
Properties
Current
MainWindow
Properties
ResourceAssem...
Resources
ShutdownMode
StartupUri
Windows
Methods
Application
FindResource
GetContentStre...
GetCookie
GetRemoteStre...
GetResourceStr...
LoadCompone...
OnActivated
OnDeactivated
OnExit
OnFragmentNa...
OnLoadComple...
OnNavigated
OnNavigating
OnNavigationF...
OnNavigationP...
OnNavigationS...
OnSessionEndi...
OnStartup
Run (+ 1 overlo...
SetCookie
Shutdown (+ 1...
TryFindResource
Events
Activated
Deactivated
DispatcherUnh...
Exit
FragmentNavig...
LoadCompleted
Navigated
Navigating
NavigationFailed
NavigationProg...
NavigationStop...
SessionEnding
Startup
NumericTextBox
Class
TextBox
Fields
AllowNegative...
ValueProperty
Properties
AllowNegative...
Value
Methods
AllowNegative...
NumericTextBo...
ValuePropertyC...
ValuePropertyC...
SubjectNumber...
Class
TextBox
Fields
IsValidSubjectN...
IsValidSubjectN...
Properties
IsValidSubjectN...
Methods
FindSubject
InvisibleTextBo...
IsTextAllowed
IsValidSubjectN...
OnTextChanged
PreventPasting...
PreviewSubject...
SubjectBox_Pre...
SubjectNumber...
Events
AcceptSubject
IsValidSubjectN...
App
Class
Application
Fields
ProgID
UMID
Methods
Activate
B_MouseDown
B_MouseEnter
B_MouseLeave
B_MouseUp
CheckAssociati...
Nested Types

17


INotifyPropertyChanged
ApplicationSetting...
Abstract Class
SettingsBase
Properties
Context
Properties
PropertyValues
Providers
SettingsKey
this
Methods
ApplicationSett...
GetPreviousVer...
OnPropertyCha...
OnSettingChan...
OnSettingsLoa...
OnSettingsSavi...
Reload
Reset
Save
Upgrade
Events
PropertyChang...
SettingChanging
SettingsLoaded
SettingsSaving
Settings
Sealed Class
ApplicationSettingsBa...
Fields
defaultInstance
Properties
DataFolder
Default
Methods
SettingChangin...
Settings
SettingsSaving...
ProtocolBase
Abstract Class
Fields
_handler
Properties
IsPaused
RunThread
Methods
Abort
Continue
Initialize (+ 1 o...
ProtocolBase
Return
Run
Save
Events
ProtocolFinished
StandardProtoc...
Class
ProtocolBase
Fields
AdaptingColor
BlankStimulus
random
Stimuli
TestColor
Timer
Vars
Properties
BatteryMD5Sum
DataFolder
PrimaryStimula...
ProtocolName
ProtocolNumber
Responder
Staircases
Stimulators
TheSubject
TrainingStairca...
UI
Methods
~StandardProt...
Cleanup
DeliverAdjacent...
DeliverBasicAp...
DeliverBasicBlo...
DeliverBasicCo...
DeliverBasicSti...
DeliverBasicSti...
DeliverBasicSti...
DeliverQuadSit...
DeliverQuadSit...
DeliverQuadSit...
DeliverQuadSit...
DeliverReverse...
DeliverReverse...
DeliverSequenti...
DeliverSequenti...
DeliverSequenti...
DeliverStimuli ...
DeliverStimuli ...
DeliverStimuli ...
Initialize
InitializeUI
LoadBattery
LoadDefaults
PrimaryStimula...
Run
Run_CleanUpB...
Run_ExecuteNe...
Run_ExecuteNe...
Run_Interactive...
Run_Main_Setup
Run_RegularTra...
Run_SaveDataF...
Run_WaitTil
Save
SetupStaircases
SetupTrainingS...
StandardProtoc...
LinearStaircase
Class
Properties
CompletedTrials
Count
CurrentTrial
Initialized
IsCompleted
Name
Methods
DeSerialize
GetFinalStaircase
IncrementIndex
Initialize
LinearStaircase
NextStaircase
Save
Serialize
Events
Completed
IStaircaseCombo
ParallelStaircase
Class
Properties
CompletedTrials
Count
CurrentTrial
IsCompleted
Methods
DeSerialize
Initialize
NextStaircase
ParallelStaircase
Save
Serialize
Events
Completed

APPENDIX 4.3: SAMPLE XML PROTOCOL BATTERY

```
<Battery>
   <Protocol Name="Simple" Namespace="CorticalMetrics.Protocols.RT"
AssemblyLocation="RT.dll" Comments="">
      <ProtocolStandardVariables xmlns:xsi="http://www.w3.org/2001/XMLSchema-
instance" xmlns:xsd="http://www.w3.org/2001/XMLSchema" id="vars">
         <Comments />
         <LeadLagTime>0</LeadLagTime>
         <IntervalBetweenAdaptAndTest>0</IntervalBetweenAdaptAndTest>
         <ITI>3000</ITI>
         <NumTrials>20</NumTrials>
         <Bias>-1</Bias>
         <StepSize>0</StepSize>
         <MinVal>0</MinVal>
         <MaxVal>800</MaxVal>
         <StartInterprobeDistance>0</StartInterprobeDistance>
         <HeatPadTemp>0</HeatPadTemp>
         <TrainingTrials>1</TrainingTrials>
         <StimControlMode>Position</StimControlMode>
         <StimulusLocation>UL-D2,D3</StimulusLocation>
         <HandUsed>L</HandUsed>
         <MalingeringTrials>0</MalingeringTrials>
      </ProtocolStandardVariables>
      <Stimulus xmlns:xsi="http://www.w3.org/2001/XMLSchema-instance"
xmlns:xsd="http://www.w3.org/2001/XMLSchema" id="Stim1">
         <Amplitude>300</Amplitude>
         <Frequency>25</Frequency>
         <Duration>40</Duration>
         <Phase>0</Phase>
         <Indent>500</Indent>
         <IndentToStim>0</IndentToStim>
         <StartTemp>0</StartTemp>
         <Diameter>3</Diameter>
         <Shape>Circular</Shape>
      </Stimulus>
      <Stimulus xmlns:xsi="http://www.w3.org/2001/XMLSchema-instance"
xmlns:xsd="http://www.w3.org/2001/XMLSchema" id="Stim2">
         <Amplitude>0</Amplitude>
         <Frequency>25</Frequency>
         <Duration>40</Duration>
         <Phase>0</Phase>
         <Indent>500</Indent>
         <IndentToStim>0</IndentToStim>
         <StartTemp>0</StartTemp>
         <Diameter>3</Diameter>
         <Shape>Circular</Shape>
      </Stimulus>
   </Protocol>
```

```
   <Protocol Name="Dual_Site" Namespace="Amplitude"
AssemblyLocation="Amplitude.dll" Comments="">
      <ProtocolStandardVariables xmlns:xsi="http://www.w3.org/2001/XMLSchema-
instance" xmlns:xsd="http://www.w3.org/2001/XMLSchema" id="vars">
         <Comments />
         <LeadLagTime>0</LeadLagTime>
         <IntervalBetweenAdaptAndTest>0</IntervalBetweenAdaptAndTest>
         <ITI>5000</ITI>
         <NumTrials>24</NumTrials>
         <Bias>2</Bias>
         <StepSize>1</StepSize>
         <MinVal>1</MinVal>
         <MaxVal>2000</MaxVal>
         <StartInterprobeDistance>32</StartInterprobeDistance>
         <HeatPadTemp>0</HeatPadTemp>
         <TrainingTrials>3</TrainingTrials>
         <StimControlMode>Position</StimControlMode>
         <StimulusLocation>UL-D2,D3</StimulusLocation>
         <HandUsed>L</HandUsed>
      </ProtocolStandardVariables>
      <Stimulus xmlns:xsi="http://www.w3.org/2001/XMLSchema-instance"
xmlns:xsd="http://www.w3.org/2001/XMLSchema" id="Stim1">
         <Amplitude>0</Amplitude>
         <Frequency>33</Frequency>
         <Duration>1000</Duration>
         <Phase>0</Phase>
         <Indent>500</Indent>
         <IndentToStim>0</IndentToStim>
         <StartTemp>0</StartTemp>
         <Diameter>3</Diameter>
         <Shape>Circular</Shape>
      </Stimulus>
      <Stimulus xmlns:xsi="http://www.w3.org/2001/XMLSchema-instance"
xmlns:xsd="http://www.w3.org/2001/XMLSchema" id="Stim2">
         <Amplitude>20</Amplitude>
         <Frequency>33</Frequency>
         <Duration>1000</Duration>
         <Phase>0</Phase>
         <Indent>500</Indent>
         <IndentToStim>0</IndentToStim>
         <StartTemp>0</StartTemp>
         <Diameter>3</Diameter>
         <Shape>Circular</Shape>
      </Stimulus>
   </Protocol>
   <Protocol Name="Dual_Site_Sequential_DS"
Namespace="CorticalMetrics.Protocols.Duration"
AssemblyLocation="Duration.dll" Comments="">
```

```
      <ProtocolStandardVariables xmlns:xsi="http://www.w3.org/2001/XMLSchema-
instance" xmlns:xsd="http://www.w3.org/2001/XMLSchema" id="vars">
         <Comments />
         <LeadLagTime>500</LeadLagTime>
         <IntervalBetweenAdaptAndTest>0</IntervalBetweenAdaptAndTest>
         <ITI>5000</ITI>
         <NumTrials>20</NumTrials>
         <Bias>2</Bias>
         <StepSize>25</StepSize>
         <MinVal>525</MinVal>
         <MaxVal>1000</MaxVal>
         <StartInterprobeDistance>32</StartInterprobeDistance>
         <HeatPadTemp>0</HeatPadTemp>
         <TrainingTrials>3</TrainingTrials>
         <StimControlMode>Position</StimControlMode>
         <StimulusLocation>UL-D2,D3</StimulusLocation>
         <HandUsed>L</HandUsed>
         <MalingeringTrials>0</MalingeringTrials>
      </ProtocolStandardVariables>
      <Stimulus xmlns:xsi="http://www.w3.org/2001/XMLSchema-instance"
xmlns:xsd="http://www.w3.org/2001/XMLSchema" id="Stim1">
         <Amplitude>400</Amplitude>
         <Frequency>40</Frequency>
         <Duration>500</Duration>
         <Phase>0</Phase>
         <Indent>500</Indent>
         <IndentToStim>0</IndentToStim>
         <StartTemp>0</StartTemp>
         <Diameter>3</Diameter>
         <Shape>Circular</Shape>
      </Stimulus>
      <Stimulus xmlns:xsi="http://www.w3.org/2001/XMLSchema-instance"
xmlns:xsd="http://www.w3.org/2001/XMLSchema" id="Stim2">
         <Amplitude>300</Amplitude>
         <Frequency>40</Frequency>
         <Duration>750</Duration>
         <Phase>0</Phase>
         <Indent>500</Indent>
         <IndentToStim>0</IndentToStim>
         <StartTemp>0</StartTemp>
         <Diameter>3</Diameter>
         <Shape>Circular</Shape>
      </Stimulus>
   </Protocol>
   <Protocol Name="Data_Report" Namespace="CorticalMetrics.Protocols.Surveys"
AssemblyLocation="Surveys.dll" Comments="">
   </Protocol>
</Battery>
```

REFERENCES

Baron-Cohen S, Wheelwright S, Skinner R, Martin J, Clubley E (2001). "The Autism-Spectrum Quotient (AQ): evidence from Asperger syndrome/high-functioning autism, males and females, scientists and mathematicians" (PDF). J Autism Dev Disord 31 (1): 5–17. doi:10.1023/A:1005653411471. PMID 11439754. Retrieved 2008-08-28

Boll TJ. Right and left cerebral hemisphere damage and tactile perception: Performance of the ipsilateral and contralateral sides of the body. *Neuropsychologia* 12:235-238, 1974.

Briggs RW, Dy-Liacco I, Malcolm MP, Lee H, Peck KK, Gopinath KS, Himes NC, Soltysik DA, Browne P, Tran-Son-Tay Roger. A pneumatic vibrotactile stimulation device for fMRI. *Magnetic Resonance in Medicine* 51:640-643, 2004.

Chen LM, Friedman RM, Row AW. Optical Imaging of a Tactile Illusion in Area 3b of the Primary Somatosensory Cortex. *Science* 302: 881-885, 2003.

Chen LM, Friedman RM, Row AW. Optical Imaging of Digit Topography in Individual Awake and Anesthetized Squirrel Monkeys. *Exp Brain Res* 196: 393-401, 2009.

Chen LM, Turner GH, Friedman RM, Zhang N, Gore JC, Roe AW, Avison MJ. High-Resolution Maps of Real and Illusory Tactile Activation in Primary Somatosensory Cortex in Individual Monkeys with Functional Magnetic Resonance Imaging and Optical Imaging. *J Neurosci* 27(34): 9181-9191, 2007.

Chubbuck JG. Small-motion biological stimulator. *APL Tech Digest* pp. 18-23, 1966.

Codd, E.F. (June 1970). "A Relational Model of Data for Large Shared Data Banks". Communications of the ACM 13 (6): 377–387. doi:10.1145/362384.362685.

Codd, E.F. "Further Normalization of the Data Base Relational Model". (Presented at Courant Computer Science Symposia Series 6, "Data Base Systems", New York City, May 24–25, 1971.) IBM Research Report RJ909 (August 31, 1971). Republished in Randall J. Rustin (ed.), Data Base Systems: Courant Computer Science Symposia Series 6. Prentice-Hall, 1972.

Cornsweet TN. The staircase-method in psychophysics. *Am J Psychol* 75:485-491, 1962.

Craner SL, Ray RH. Somatosensory cortex of the neonatal pig: I. Topographic organization of the primary somatosensory cortex (SI). J Comp Neurol (1991).

Dennis RG, Kosnik PE. Mesenchymal cell culture: instrumentation and methods for evaluating engineered muscle. In *Methods in Tissue Engineering* ed. Atala A & Lanza R, pp. 307-316, 2002.

Di Pierro M. Web2py Full-Stack Web Framework, 4th Edition. Experts4Solutions, 2011. Print.

Elise Titia Gieling, Rebecca Elizabeth Nordquist, Franz Josef van der Staay. *Assessing learning and memory in pigs*. Angimal Cognition (2011).

Folger SE, Tannan V, Zhang Z, Holden JK, Tommerdahl M. Effects of N-methyl-D-aspartate receptor antagonist dextromethorphan on vibrotactile adaptation. *BMC Neurosci* 16(9): 87, 2008.

Francis ST, Kelly EF, Bowtell R, Dunseath WJR, Folger SE, McGlone F. fMRI of the Responses to Vibratory Stimulation of Digit Tips. *NeuroImage* 11:188-202, 2000.

Francisco E, Tannan V, Zhang Z, Holden J, Tommerdahl M. Vibrotactile amplitude discrimination capacity parallels magnitude changes in somatosensory cortex and follows Weber's Law. *Exp Brain Res* 191(1): 49-56, 2008.

Francisco E, Holden J, Zhang Z, Favorov O, Tommerdahl M. Rate dependency of vibrotactile stimulus modulation. *Brain Res* 1415:76-83, 2011.

Friedman RM, Chen LM, Row AW. Responses of Areas 3b and 1 in Anesthetized Squirrel Monkeys to Single- and Dual-Site Stimulation of the Digits. *J Neurophysiol* 100: 3185-3196, 2008.

Gamma, E., Helm, R., Johnson, R.,, Vlissides, J. M. Design Patterns: Elements of Reusable Object-Oriented Software. Addison-Wesley Professional. ISBN: 0201633612 1994

Goble AK, Hollins M. Vibrotactile adaptation enhances amplitude discrimination. *J Acoust Soc Am* 93(1):418-424, 1993.

Golaszewski SM, Zschienger F, Siedentopf CM, Unterrainer J, Sweeney RA, Willhelm E, Lechner-Steinleitner S, Mottaghy FM, Felber S. A new pneumatic vibrator for functional magnetic resonance imaging of the human sensorimotor cortex. *Neuroscience Letters* 324:125-128, 2002.

Häger-Ross C, Schieber MH. Quantifying the Independence of Human Finger Movements: Comparisons of Digits, Hands, and Movement Frequencies. *J Neurosci* 20(22): 8542-8550, 2000.

Harrington GS, Wright CT, Downs JH III. A new vibrotactile stimulator for functional MRI. *Human Brain Mapping* 10:140-145, 2000.

Hegner YL, Lee Y, Grodd W, Braun C. Comparing Tactile Pattern and Vibrotactile Frequency Discrimination: A Human fMRI Study. *Journal of Neurophysiology* 103:3115-3122, 2010

Holden JK, Francisco EM, Zhang Z, Baric C, Tommerdahl M. An undergraduate laboratory exercise to study Weber's Law. *J Undergrad Neurosci Edu* 9(2):A71-A74.

Juliano SL, Whitsel BL, Tommerdahl M, Cheema SS. Determinants of patchy metabolic labeling in the somatosensory cortex of cats: a possible role for intrinsic inhibitory circuitry. *J Neurosci* 9(1):1-12, 1989.

LaMotte RH, Mountcastle VB. Capacities of humans and monkeys to discriminate vibratory stimuli of different frequency and amplitude: a correlation between neural events and psychological measurements. *J Neurophysiol* 38(3):539-559, 1975.

Mountcastle VB, Talbot WH, Sakata H, Hyvärinen J. Cortical neuronal mechanisms in flutter-vibration studied in unanesthetized monkeys. Neuronal periodicity and frequency discrimination. *J Neurophysiol* 32(3):452-484, 1969.

Nelson TS, Suhr CL, Lai A, Halliday AJ, Freestone DR, McLean KJ, Burkitt AN, Cook MJ. Exploring the tolerability of spatiotemporally complex electrical stimulation paradigms. *Epilepsy Res* 2011.

Reitan RM and Wolfson D. The Halstead-Reitan neuropsychological test battery: Theory and clinical interpretation (2nd ed.). Tuscon AZ: Neuropsychology Press.

Sauleau P., Lapouble E., Val-Laillet D. and Malbert C-H. The pig model in brain imaging and neurosurgery. *Animal* 2009.

Schach, Stephen. Object-Oriented and Classical Software Engineering, Seventh Edition. McGraw-Hill. ISBN 0-07-319126-4 2006.

Slobounov S, Johnston J, Chiang H, Ray WJ. Motor-related Cortical Potentials Accompanying Enslaving Effect In Single Versos Combination of Fingers Force Production Tasks. *Clinical Neurophysiology* 113: 1444-1452, 2002.

Swindle Michael M., DVM. *Porcine Integumentary System Models: Part 1 – Dermal Toxicology* 2008.

Tannan V, Dennis R, Tommerdahl M. A novel device for delivering two-site vibrotactile stimuli to the skin. *J Neurosci Methods* 147(2): 75-81, 2005a.

Tannan V, Dennis RG, Tommerdahl M. Stimulus-dependent effects on tactile spatial acuity. *Behav Brain Funct* 1: 18, 2005b.

Tannan V, Dennis RG, Zhang Z, Tommerdahl M. A portable tactile sensory diagnostic device. *J Neurosci Methods* 164(1): 131-138, 2007a.

Tannan V, Holden JK, Zhang Z, Baranek GT, Tommerdahl MA. Perceptual metrics of individuals with autism provide evidence for disinhibition. *Autism Res* 1(4): 223-230, 2008.

Tannan V, Simons S, Dennis RG, Tommerdahl M. Effects of adaptation on the capacity to differentiate simultaneously delivered dual-site vibrotactile stimuli. *Brain Res* 1186: 164-170, 2007b.

Tannan V, Whitsel BL, Tommerdahl MA. Vibrotactile adaptation enhances spatial localization. *Brain Res* 1102(1): 109-116, 2006.

Tommerdahl M, Delemos KA, Favorov OV, Metz CB, Vierck CJ Jr, Whitsel BL. Response of anterior parietal cortex to different modes of same-site skin stimulation. *J Neurophysiol* 80(6):3272-3283, 1998.

Tommerdahl M, Favorov OV, Whitsel BL. Dynamic Representations of the Somatosensory Cortex. *Neuroscience and Biobehavioral Reviews* 34: 160-170, 2010.

Tommerdahl M, Favorov OV, Whitsel BL. Effects of High-Frequency Skin Stimulation on SI Cortex: Mechanisms and Functional Implication. *Somatosensory and Motor Research* 22(3): 151-160, 2005.

Tommerdahl M, Favorov O, Whitsel BL. Optical imaging of intrinsic signals in somatosensory cortex. *Behav Brain Res* 135(1-2):83-91, 2002.

Tommerdahl M, Favorov O, Whitsel BL, Nakhle B, Gonchar YA. Minicolumnar activation patterns in cat and monkey SI cortex. *Cereb Cortex* 3(5):399-411, 1993.

Tommerdahl M, Simons SB, Chiu JS, Favorov O, Whitsel BL. Ipsilateral input modifies the primary somatosensory cortex response to contralateral skin flutter. *J Neurosci* 26(22): 5970-5977, 2006.

Tommerdahl M, Tannan V Cascio CJ, Baranek GT, Whitsel BL. Vibrotactile adaptation fails to enhance spatial localization in adults with autism. *Brain Res* 1154:116-123, 2007a.

Tommerdahl M, Tannan V, Holden JK, Baranek GT. Absence of stimulus-driven synchronization effects on sensory perception in autism: Evidence for local underconnectivity? *Behav Brain Funct* 24(4): 19, 2008.

Tommerdahl M, Tannan V, Zachek M, Holden JK, Favorov OV. Effects of stimulus-driven synchronization on sensory perception. *Behav Brain Funct* 4(3): 61, 2007b.

Vierck CJ Jr, Jones MB. Influences of low and high frequency oscillation upon spatio-tactile resolution. *Physiol Behav* 5(12):1431-1435, 1970.

Zhang Z, Tannan V, Holden JK, Dennis RG, Tommerdahl M. A quantitative method for determining spatial discriminative capacity. *Biomed Eng Online* 10(7):12, 2008.

Zhang Z, Francisco EM, Holden JK, Dennis RG, Tommerdahl M. The impact of non-noxious heat on tactile information processing. *Brain Res* 1302:97-105, 2009.

Zhang Z, Zolnoun DA, Francisco EM, Holden JK, Dennis RG, Tommerdahl M. Altered central sensitization in subgroups of women with vulvodynia. *Clin J Pain* 2011.